DR·0690·4

Energy

CONSERVATION

THERMOPHYSICAL PROPERTIES OF WORKING FLUIDS
FOR BINARY GEOTHERMAL CYCLES

Final Report

By
D. E. Diller   J. M. H. Levelt Sengers
J. S. Gallagher   J. V. Sengers
B. Kamgar-Parsi   L. J. Van Poolen
G. Morrison   M. Waxman

July 1984

Technical Information Center
Office of Scientific and Technical Information
United States Department of Energy

DISCLAIMER

DISCLAIMER

Portions of this document may be illegible in electronic image products. Images are produced from the best available original document.

DISCLAIMER

THERMOPHYSICAL PROPERTIES OF WORKING FLUIDS
FOR BINARY GEOTHERMAL CYCLES

By
D. E. Diller
J. S. Gallagher
B. Kamgar-Parsi
G. Morrison
J. M. H. Levelt Sengers
J. V. Sengers
L. J. Van Poolen
M. Waxman

Final Report
for the Division of Geothermal and Hydropower Technology
Office of Renewable Technology
U. S. Department of Energy

July 1984

Chemical Engineering Science Division 773
National Bureau of Standards
Boulder, CO 80303

Thermophysics Division 774
National Bureau of Standards
Gaithersburg, MD 20899

Institute for Physical Sciences and Technology
University of Maryland
College Park, MD 20742

Table of Contents

Tables

Introduction

As an alternative to electric power generation by non-renewable energy sources such as gas, oil and coal, geothermal brines can be used as heat sources in power cycles.[1] In one design, the dry steam flashed from the brine is expanded in a turbine. Since geothermal temperatures are much lower than those used in conventional steam power generation, the use of a working fluid with a critical temperature much lower than that of steam has been advocated. Pure isobutane was the first choice of working fluid. By using a mixture of isobutane and isopentane, however, two advantages are obtained: the location of the critical point can be optimized by modifying the composition; and the performance of the heat exchanger is improved because the mixture, contrary to the pure fluid, undergoes the isobaric phase transition from liquid density to subcritical density over a range of temperatures, rather than abruptly. For these reasons, the demonstration project which is being constructed under sponsorship of the Department of Energy will use a 90 mol % isobutane - 10 mol % isopentane mixture as a working fluid.

In the design of the power cycle, it is necessary to have information on the thermodynamic and transport properties of the working fluid. For the past six years, groups at the National Bureau of Standards have worked at obtaining the data base, validating existing data and models and developing correlative and predictive methods for establishing these property values. This report contains the data obtained under this contract, their evaluation, and the predictive methods, previously existing ones as well as those developed for this project. The report consists of three parts, two referring to the thermodynamic, the third to the transport properties. The approaches used in the two cases are somewhat different. In the case of the thermodynamic properties, no predictive methods were available even for pure isobutane, let alone for

1

the mixtures. Thus, in the early stages of the work, the vapor pressure
and several PV isotherms of supercritical and liquid isobutane were
measured.[2,3,4] This enabled NBS scientists to select the reliable data
from the body of data available in the literature,[5,6] On the basis of these
validated data, a thermodynamic surface was constructed. This surface was
not accurate in the critical region. On the basis of the Wilson-Kadanoff
renormalization group theory, a separate nonclassical (scaled) surface was
constructed for the critical region.[7]

For the isobutane-isopentane mixtures, the first step was to obtain
(P,x,T) data for the critical line. In the process, the critical point of
pure isopentane, and vapor pressure data between 370 K and the critical point
(408 K) were measured. In addition, the pressures, densities and compositions
of coexisting phases of mixtures of approximately 50 mol % isobutane -
50 mol % isopentane were measured in the range of 290-325 K. Within the
framework of another contract, a global thermodynamic surface was developed
on the basis of the principle of generalized corresponding states. In
part II of this report, the data for pure isopentane and for the critical
line are used to develop a nonclassical (scaled) thermodynamic surface
for the mixtures. This surface was intended to be valid within a range
of approximately 3 K below to 30 K above the critical line. We will
compare the scaled surface for the mixture with the global surface
reported elsewhere.[8,9] Unfortunately, the agreement is not good. Our
conclusion is that the scaled surface needs further basic work.

The work on the transport properties has been developed from a
different perspective. Predictive techniques for the transport properties
of hydrocarbon fluids were available at the onset of this project in the
form of the program TRAPP developed by NBS scientists[10,11] on the basis of

2

generalized corresponding states. The experimental program on transport properties was therefore directed at validation of the TRAPP program for pure fluids and mixtures, over as large a range of reduced temperatures and pressures as experimentally feasible. Since the available viscometer has an upper temperature limit of 320 K, initially cryogenic fluids[12-17] and some of their mixtures[18-20] such as nitrogen, methane and ethane were studied. This work led to the conclusion that the program TRAPP predicts viscosities correctly on the $\pm$ 5% level for densities smaller than $2\rho_c$.

In the second half of the work, however, experimental studies were done of the two isomers normal butane and isobutane.[21] It was then found that there is a rather substantial isomeric effect in the viscosities of the liquid that is not well predicted by the program TRAPP. An alternative formulation of the viscosity of liquid isobutane is proposed. This study of the transport properties of hydrocarbons has enabled us to identify the ranges of experimental parameters in which the results of the program TRAPP can be used with confidence.

In the first two parts of this report, we will present the experimental thermodynamic data obtained under this contract, and give the results of the correlations developed with estimates of their reliability. In the third part, we will do similarly for the transport properties, and compare with the prediction of the program TRAPP. In Appendix A, we give a complete listing of the publications that have resulted from this project.

Thermodynamic Properties of Isobutane and Isobutane-Isopentane Mixtures

1. Experimental data obtained under this contract

1.1 Summary of Burnett PVT data for isobutane

In a high-quality Burnett PVT apparatus, expansions were performed along two isotherms in the supercritical fluid and along two isotherms in the subcritical vapor for a 99.98% pure sample of isobutane. In addition, the vapor pressure of isobutane was measured from 298.15 to 398.15 K. All results have been published, with an assessment of the reliability of the data.[2,3] The supercritical PVT data are listed in Table I1, the virial coefficients at the four temperatures in Table I2, and the vapor pressure in Table I3. The authors estimate the inaccuracy of pressures above 0.5 MPa as 0.01%. The inaccuracy of densities and compressibility factors is at most an order of magnitude larger.

1.2 Critical-point and critical-line data on isobutane, isopentane and their mixtures

1.2.1 Visual Cell

For observation of the meniscus disappearance in samples of isobutane, isopentane and their mixtures, a simple optical cell was constructed (Fig. I1). It consists of a stainless-steel-316 ring, of inner diameter 2.54 cm, thickness 1.27 cm, sandwiched between two circular sapphire windows (of diameter 5 cm, thickness 3 mm) by means of an aluminum clamp. Tin foil of 0.25 mm thickness serves as a gasket. This way, a disk-shaped cell of nominally 6.5 cm^3 volume is formed. The dimensions of the ring were calibrated at 20 °C by the NBS Metrology Division. From the calibration, the volume of the cell at 20 °C was calculated to be 6.4484 cm^3, with an uncertainty of 0.1%; the thickness

4

of the tin foil gasket has been taken into account. The cell contains a stirrer, a soft-magnetic-steel rod which is moved around by means of a hand-operated external magnet. The volume of the stirrer is 126 mm^3. One end of a capillary of 1.6 mm outer diameter, 0.45 mm inner diameter and 8 cm length is welded into the ring. The other end is sealed off by means of a miniature pressure valve. The combined volume in line and valve is 22 mm^3, as calculated from the dimensions. The coefficients of thermal expansion of the steel ring, which determines the cell volume at temperatures other than 20 °C, is assumed to be 16.5 x 10^{-6} per K in the range of 20-200 °C. This conclusion was reached on the basis of thermal expansion data for stainless steel 304 in Ref. 22, and the observation, in Ref. 23, that the stainless steels 304 and 316 have identical expansion coefficients below 300 K.

The assembled cell and valve have a mass of just over 400 g. The sample mass, typically of the order of 1.5 g, is determined by weighings of the empty and the filled cell on a 1-kg balance with resolution of 0.5 mg.

The cell is connected to a manifold that contains a miniature Sensotech* strain-gage pressure transducer and another valve (Fig. I 1). Sample gas vented from the cell is captured above water in an inverted graduated cylinder. The pressure transducer was claimed by the manufacturer to be precise to 0.1% in a temperature range up to 200 °C. The arrangement of Fig. 1 permits in-situ calibration of the pressure transducer with respect to a dead-weight gage. We found the transducer performance satisfactory at room temperature; pressure measurements at temperatures above 130 °C, however, were hampered by strong drifts of the transducer, often as much as 10 kPa (0.1 bar) per day; these measurements are therefore not as reliable as we had hoped them to be on the basis of the manufacturer's claim. In the measurements on pure isopentane, however, we mounted the pressure transducer outside the bath, so that these pressures have better reliability than those of the mixtures.

The measurement procedure is to weigh in the required amount of isopentane, and then put in the matching amount of isobutane by means of a volume pump, so as to obtain a mixture of the desired composition at an overall fill density 5-10% above the estimated critical value. The amounts of isobutane and isopentane are obtained by weighing. The cell is then hooked up to the manifold and placed inside a commercial "visibility bath" filled with a low-vapor-pressure silicone oil; the temperature of the bath is controlled to a few hundredths K. The mixture is heated until the meniscus disappears from the cell at the top. The cell is then heated several degrees while the line and pressure transducer sections are evacuated. The fluid is expanded into the pressure transducer section. Care is taken that the mixture does not phase-separate in the cell. A full expansion corresponds with about 5% decrease in density. It is not necessary to do a complete expansion, although this was done most of the time. With the cell valve open, the fluid is now cooled in steps, and the pressure and temperature measured, until a dark brown color in the cell betrays the closeness of a phase separation. The cell valve is then closed and the temperature lowered until the meniscus appears. The meniscus level, at first appearance, and after vigorous stirring, is read with a cathetometer. It will generally be in the upper part of the cell. The cell is then heated until well into the one-phase region, while the fluid in the transducer is expanded into the inverted graduated cylinder (approximately 20 cm^3 at room temperature). After the vent valve is closed, the sequence of pressure measurements and meniscus level determination is repeated. The critical point temperature and density are obtained by interpolating in the meniscus level measurements for meniscus disappearance at mid-level in the cell (after allowances for the capillary, valve and stirrer volumes are made). The critical pressure is obtained by extrapolating the isochoric pressures to the transition points, and interpolating between isochores. In several instances we stopped the

6

sequence when the meniscus disappeared at mid-level, and immediately, in situ, calibrated the transducer with respect to a calibrated dead-weight gage. This alleviated somewhat the problems that were caused by the strong drift of the pressure transducer. The barometric pressure is read on an aneroid gage with a resolution of 25 μm of mercury.

After all measurements are completed, the cell is removed, cleaned and weighed, after which the remaining sample is blown off and the empty cell weighed again. The amounts released from the cell during the measurements are calculated from the gasometry data, corrected for gas nonideality. Proof of a successful series of measurements is that the gasometry data add up to the weight loss observed. We have rejected those runs in which the mismatch between the gasometry and weight data exceeded 15 mg. (For those runs we retained, the agreement was usually an order better than that.) Therefore, no uncertainty larger than 1% in the reported density results.

The data obtained with this apparatus are summarized in Table I 4 (isochoric PρT data), Table I 5 (critical-line data), Table I 6 (vapor pressure of pure isopentane) and Table I 7 (dew-bubble data). We estimate the reliability of the data to be on the level of 20 mK in temperature, 4 kPa in pressure, 1% in density and 0..001 in composition.

The isopentane used in this work was Phillips* research grade of 99.99+ mol percent claimed purity, the isobutane was Phillips* research grade, claimed to be at least 99.9% pure. The isobutane liquid was analyzed by chromatography after the measurements of the isobutane vapor pressure and found to contain 30 ppm of nitrogen and 300 ppm of propane. The n-butane content could not be determined.

The isopentane was kept at atmospheric pressure and must therefore have contained some dissolved air. When introducing it as the first component into the visual cell, we always overfilled and blew off some vapor by mild heating of the cell, thus eliminating most of the volatiles.

7

1.3 VLE data

A schematic of the VLE cell and manifold is given in Fig. I 2. The pressure cell is a sapphire tube; stainless-steel plugs inserted in the tube at both ends seal it by means of O-rings.[24] Samples are introduced from a thermal compressor which is removable and is filled from a gas buret; the amounts of the components of a mixture are determined by weighing. The compositions thus obtained are reliable to $\pm$ 0.0002 in mole fraction.[25] Mercury fills a calibrated injector pump, the capillaries and part of the sample cell (Fig. I 2). It is used to displace the sample from the thermal compressor into the cell, to serve as a pressure-transmitting medium and to fill all noxious volumes, so that the mixture sample is strictly confined to the sapphire tube. The bore of the sapphire tube was calibrated over its length by means of triple-distilled mercury; that of the injector pump was similarly calibrated by means of decane, the density of which was determined by pycnometry. The pump is calibrated to $\pm$ 2 mm^3. The pressure is measured by means of a Validyne* pressure transducer, kept at ambient temperature and calibrated with respect to a dead-weight tester. The transducer is filled with mercury in order to eliminate noxious volumes. Pressures are measured to 0.1% and head corrections are made. The barometric pressure is read on an aneroid gage with a resolution of 25 μm of mercury. The system is immersed in a stirred water bath, controlled to better than 1 mK. The temperature is read on a quartz thermometer calibrated with respect to a standard platinum resistance thermometer. The temperature resolution is 0.3 mK, the accuracy 1 mK.

VLE measurements are obtained by measuring the meniscus levels of mercury and the vapor-liquid interface of a predetermined amount of mixture prepared gravimetrically, at measured values of pressure and temperature.

8

At fixed P and T, the compositions and densities of coexisting phases are nonvariants. By introducing at least two samples of different known compositions, the densities of the coexisting phases can be calculated from the observed phase volumes and the known total mass.[26] In this way, the liquid densities listed in Table I 8 were obtained. In this temperature range, the vapor densities are too low to be obtained with any accuracy by this method.

The VLE data have been proven highly useful in the construction of a thermodynamic surface, which is under way under a different contract.

2. Thermodynamic surfaces for isobutane and for isobutane-isopentane mixtures

2.1 Global thermodynamic surface for isobutane

On the basis of validated PVT data for isobutane, a thermodynamic surface was constructed that spans the range of 250–600 K at pressures from 0.1 to 40 MPa. The surface, and a comparison with data, are described in detail in two publications by Waxman and Gallagher.[2,3] At given pressure and temperature, the surface will give densities that are, in general, reliable to approximately 0.1%. The reliability deteriorates near the critical point. The surface was not constrained to the physical critical point because such constraint usually leads to a deterioration in other areas, such as in the supercritical region. In a small region around the critical point, defined by

$$0.985 < T_c/T < 1.015$$

$$\text{and } 0.7 < \rho_c/\rho < 1.3$$

the surface should not be used. In this report, we will give the equations defining the surface in a dimensionless form (Refs. 2 and 3 are dimensional). The Helmholtz function in this form can be expressed as

$$\overline{A} = \overline{A}_0(\overline{T}) + \overline{A}_1(\overline{V},\overline{T}) + \overline{A}_2(\overline{V},\overline{T}) + \overline{A}_3(\overline{V},\overline{T}), \qquad \text{I(1)}$$

where $\overline{A}_0$ is the ideal gas contribution, written in the form:

9

$$\overline{A}_o = (A_{00} + A_{01}\overline{T})\, \ln\overline{T} + \sum_{i=2}^{8} A_{0i}\overline{T}^{(i-4)} + A_{09}\overline{T}\ln(e^{x_o/\overline{T}}-1); \qquad I(2)$$

$\overline{A}$, $\overline{V}$ and $\overline{T}$ are the dimensionless Helmholtz free energy, volume and temperature, to be defined shortly. $A_{00} - A_{09}$ and x_o are dimensionless constants listed in Table I9. $\overline{A}_1$ is the "hard sphere" contribution, of the form

$$\overline{A}_1 = A_{10}\overline{T}\left[\ln\frac{1}{\overline{V}(1-y)} + \frac{3}{2(1-y)^2} - 4y\right]; \qquad I(3)$$

y is given by

$$y = b\,\rho/4 = \overline{b}/4\overline{V}, \qquad I(4)$$

where b is an equivalent hard-sphere volume, itself a function of temperature. The representation of y as a function of temperature is

$$y = \frac{1}{\overline{V}}\left[y_0 + y_1\,\ln\overline{T} + \frac{y_2}{\overline{T}^4} + \frac{y_3}{\overline{T}^8}\right], \qquad I(5)$$

The dimensionless constants $y_0 - y_3$ are listed in Table I 9.

A_2 is the "second virial" contribution, of the form

$$\overline{A}_2 = \frac{\overline{T}}{\overline{V}}\left[A_{20} + \frac{A_{21}}{\overline{T}} + \frac{A_{22}}{\overline{T}^3} + \frac{A_{23}}{\overline{T}^5} + \frac{A_{24}}{\overline{T}^{10}}\right]; \qquad I(6)$$

the dimensionless constants $A_{20} - A_{24}$ are given in Table I 9. Finally, the free energy contains a "residual" term A_3. It is obtained by fitting a function of the form

$$\overline{A}_3 = \sum_i \sum_j B_{ij} z^{i+1}\left(\frac{1}{\overline{T}}\right)^j, \text{ with } z = 1-e^{-z_o/\overline{V}}, \qquad I(7)$$

to the differences between experimental data and calculated values based on the sum of $\overline{A}_o$, $\overline{A}_1$, and $\overline{A}_2$. The dimensionless constants B_{ij} and z_o are given in Table I 9.

The dimensionless quantities are defined as follows:

$$\bar{T} = T/T^*,$$ I(8)

$$\bar{V} = V/V^*,$$

$$\bar{P} = P/P^*,$$

$$\bar{A} = A/A^{**},$$

$$\bar{S} = S/S^{**},$$

where T^*, V^*, P^* are dimensioned reference values listed in Table I 9, and

A^{**}, S^{**} dimensioned reduction factors for free energy and entropy, resp.,

derived from V^*, T^* and P^*. Also required is the reduced gas constant

$$R^{**} = R/S^{**}.$$ I(9)

The other thermodynamic functions can be obtained from combinations of the

derivatives of $\bar{A}$ with respect to $\bar{V}$ and $\bar{T}$ in the usual way, for instance:

$$\bar{P} = - \left(\frac{\partial \bar{A}}{\partial \bar{V}}\right)_{\bar{T}} ,$$ I(10)

$$\bar{S} = - \left(\frac{\partial \bar{A}}{\partial \bar{T}}\right)_{\bar{V}}$$ I(11)

and

$$\bar{S} = \bar{A} + \bar{P}\bar{V} .$$ I(12)

2.2 Global thermodynamic surface for isobutane-isopentane mixtures

A global thermodynamic surface for isobutane-isopentane mixtures,

based on the global surface for isobutane, described in Sec. 2.1, as a

reference, and on a generalized principle of corresponding states, is

being developed under a different contract.[9] The principal equations and

preliminary results are summarized here.

11

The first step in the process is to construct a thermodynamic surface for isopentane based on that of isobutane as a reference. We define the ratios

$$f° = \overline{T}_5{}^c / \overline{T}_4{}^c ,$$

$$h° = \overline{V}_5{}^c / \overline{V}_4{}^c , \qquad\qquad I(13)$$

$$g° = \overline{P}_5{}^c / \overline{P}_4{}^c ,$$

where the subscript 5 refers to isopentane, the subscript 4 to isobutane, and the superscript c indicates a critical-point value, while the symbol V indicates a molar volume. The properties of isopentane are made dimensionless by means of the same reference constants as those of isobutane (Table I 9). By our choice of reference constants, $\overline{T}_4{}^c$, $\overline{P}_4{}^c$ and $\overline{V}_4{}^c$ happen to be unity.

The principle of corresponding states postulates for the compressibility factor $Z = PV/RT$:

$$Z_5 \ (\overline{V}_5, \overline{T}_5) = Z_4 \ (\overline{V}_4 = \overline{V}_5/h°, \ \overline{T}_4 = \overline{T}_5/f°)$$

and for the configurational Helmholtz free energy A^{cf}:

$$\overline{A}_5{}^{cf} \ (\overline{V}_5, \overline{T}_5) = f° \ \overline{A}_4{}^{cf} \ (\overline{V}_4 = \overline{V}_5/h°, \ \overline{T}_4 = \overline{T}_5/f°) - R**T_5 \ \ln h° \qquad I(14)$$

for all values of V, T. It implies that

$$f° = h° \ g° . \qquad\qquad I(15)$$

Since no two substances obey the principle of corresponding states accurately, Rowlinson et al.[27] and Leland et al[28,29] proposed to generalize the principle by the use of two functions, $\theta(\overline{V},\overline{T})$ and $\phi(\overline{V},\overline{T})$ that ensure an exact mapping of Z and A^{cf} from one substance to the other.

12

We define these functions by means of

$$f = (\overline{T}_5{}^c/\overline{T}_4{}^c) \; \theta(\overline{V}_4, \overline{T}_4)$$

and

$$g = (\overline{P}_5{}^c/\overline{P}_4{}^c) \; \theta(\overline{V}_4, \overline{T}_4)/\phi(\overline{V}_4, \overline{T}_4) \; , \qquad \text{I(16)}$$

in such a way that

$$Z_5(\overline{V}_5, \; \overline{T}_5) = Z_4(\overline{V}_4 = \overline{V}_5/h, \; \overline{T}_4 = \overline{T}_5/f) \; ,$$

$$\overline{A}_5{}^{cf}(\overline{V}_5, \; \overline{T}_5) = f \; \overline{A}_4{}^{cf}(\overline{V}_4 = \overline{V}_5/h, \; \overline{T}_4 = \overline{T}_5/f) - R^{**}T_5 \; \ln h \; , \qquad \text{I(17)}$$

with h given by

$$h = f/g = (\overline{V}_5{}^c/\overline{V}_4{}^c)(\overline{Z}_4{}^c/\overline{Z}_5{}^c) \; \phi(\overline{V}_4, \overline{T}_4) \; . \qquad \text{I(18)}$$

We have used the experimental data available for the vapor pressure of isopentane (Table I 6) and for coexisting vapor and liquid densities determined by Young[30] at the turn of the century to calculate point values of $\theta(\overline{V}_4, \overline{T}_4)$ and $\phi(\overline{V}_4, \overline{T}_4)$. We have represented θ and ϕ as simple functions of density and temperature:

$$\theta = a_1 + a_2(\overline{\rho}_4 - 1) + a_3(\overline{T}_4 - 1)$$

and

$$\rho = b_1 + b_2(\overline{\rho}_4 - 1) + b_3(\overline{T}_4 - 1) \; . \qquad \text{I(19)}$$

The values of the constants $a_1 - b_3$ are given in Table I 10. The constants a_1, b_1 have been set equal to unity because their fitted values did not depart significantly from unity.

The thermodynamic surface of isopentane is completely defined by: the reference Helmholtz function for isobutane (Table I 9); the ideal-gas Helmholtz function for isopentane, obtained by interpolation in the table of Scott[31]; the shape factors θ and ϕ characterized by the constants listed in Table I 10; and the critical constants of isobutane and isopentane listed

13

in Table I 11. Since the critical temperature of the global isobutane surface
is about 2 K above the physical critical point, a similar offset will occur in
the isopentane surface.

The next step is the development of a thermodynamic surface for the
mixtures of isobutane and isopentane. This is achieved by again invoking the
principle of corresponding states. For a mixture of composition x, molar
volume V_x and temperature T_x we obtain the molar configurational Helmholtz
free energy from that of isobutane by the relations

$$Z_x(\overline{V}_x, \overline{T}_x) = Z_4(\overline{V}_4 = \overline{V}_x/h_x, \overline{T}_4 = \overline{T}_x/f_x)$$

and

$$\overline{A}_x^{cf}(\overline{V}_x, \overline{T}_x) = f_x \overline{A}_x^{cf}(\overline{V}_4 = \overline{V}_x/h, \overline{T}_4 = \overline{T}_x/f_x) - R**\overline{T}_x \ln h_x . \qquad I(20)$$

Here h_x, f_x are defined by

$$h_x = (V_x^c/V_4^c) [1 + x\{\theta(\overline{V}_4, \overline{T}_4) - 1\}]$$

and

$$f_x = (T_x^c/T_4^c)[1 + x\{\theta(\overline{V}_4, \overline{T}_4) - 1\}]. \qquad I(21)$$

Left to be defined are the pseudocritical constants V_x^c, T_x^c in I(21). We
have used the following Van-der-Waals-type mixing rules

$$V_x^c = (1-x)^2 V_4^c + 2x(1-x)V_{45}^c + x^2 V_5^{c'},$$

$$T_x^c = (1-x)^2 T_4^c + 2x(1-x)T_{45}^c + x^2 T_5^c, \qquad I(22)$$

with the combining rules

$$V_{45}{}^c = k \; [\frac{(V_4{}^c)^{1/3} + (V_5{}^{c'})^{1/3}}{2}]^3 \qquad\qquad I(23)$$

and
$$T_{45}{}^c = \ell \; [T_4{}^c \; T_5{}^c]^{1/2} \; , \qquad\qquad I(24)$$

where
$$V_5{}^{c'} = V_5{}^c \; Z_4{}^c / Z_5{}^c \; . \qquad\qquad I(25)$$

The guides in establishing the parameter values of k and ℓ are the experimental data on the critical line and vapor-liquid equilibria. Obtaining the location of the real critical line from the surface defined by I(2) - I(25) is not trivial. We developed a search method that locates the zero of $(\partial^2 G/\partial x^2)_{PT}$ as the critical line is approached from the one-phase region. Since the critical temperatures of the global surfaces for isobutane and isopentane are about 2 K higher than the physical values, we required for the critical line of the mixture surface that it be displaced by a similar amount from the measured values. The parameters k and ℓ were optimized by this procedure (Table I 12).

The global surface so defined for the mixture was used in the comparisons with the critical-region surface developed within the framework of this contract (Part II).

2.3 A scaled thermodynamic surface for the critical region of isobutane

The global thermodynamic surface that we developed for isobutane is inaccurate in the immediate vicinity of the critical point. In a region of the size

$$401.8 \; K \leq T \leq 414 \; K$$

and
$$173.4 \leq \rho \leq 322 \; kg/m^3 \qquad\qquad I(26)$$

this surface should not be used. The modern theory of critical phenomena has provided us with the tools to describe the critical region of fluids. The

principle of critical-point universality implies that the critical anomalies of all fluids and fluid mixtures can be described by the same scaled thermodynamic potential save for two arbitrary scaling constants.[32,33] The renormalization-group approach initiated by Kadanoff[34] and formalized by Wilson[35] predicts the critical exponents and amplitude ratios of the scaled potential, and the form of the corrections to scaling[36]. This potential has been applied to a number of fluids,[37] so that a brief summary may suffice here. For some of the details, we refer to Part II of this report.

The scaled thermodynamic surface is a relationship between the intensive thermodynamic variables pressure P, chemical potential μ and temperature T. We use the reduced variables

$$\tilde{P} = \frac{\bar{P}}{T} \,,$$

$$\tilde{\mu} = \frac{\bar{\mu}}{T} = \frac{\mu \rho^\star}{P^\star} \frac{1}{T} \,, \qquad\qquad I(27)$$

$$\tilde{T} = -\frac{1}{T} \,,$$

where the "starred" and "barred" variables are those defined in Sec. 2.1.

The fundamental equation yields the thermodynamic potential $\tilde{P}$ as a function of $\tilde{\mu}$ and $\tilde{T}$ and has the form

$$\tilde{P} = \tilde{P}_o\,(\tilde{T}) + \Delta\tilde{\mu} + \tilde{P}_{11}\,\Delta\tilde{\mu}\,\Delta\tilde{T} + \Delta\tilde{P} \qquad\qquad I(28)$$

with
$$\Delta\tilde{T} = \tilde{T} + 1 \,,$$

$$\Delta\tilde{\mu} = \tilde{\mu} - \tilde{\mu}_o(\tilde{T}) \,. \qquad\qquad I(29)$$

The functions $\tilde{P}_o\,(\tilde{T})$ and $\tilde{\mu}\,(\tilde{T})$ are represented by truncated Taylor series expansions

$$\tilde{\mu}_o\,(\tilde{T}) = \tilde{\mu}_c + \sum_{j=1}^{3} \tilde{\mu}_j\,(\Delta\tilde{T})^j$$

and
$$\tilde{P}_0(\tilde{T}) = 1 + \sum_{j=1}^{2} \tilde{P}_j(\Delta\tilde{T})^j \ . \qquad\qquad I(30)$$

The singular part $\Delta\tilde{P}$ in I(28) is related to $\Delta\tilde{\mu}$ and $\Delta\tilde{T}$ by means of two auxiliary (parametric) variables r and θ

$$\Delta\tilde{\mu} = r^{\beta\delta}a\theta(1-\theta^2) \ ,$$

$$\Delta\tilde{T} = r(1-b^2\theta^2) - c\Delta\tilde{\mu} \ ,$$

$$\Delta\tilde{P} = r^{\beta(\delta+1)} ak_0 p_0(\theta) + r^{\beta(\delta+1)+\Delta_1} ak_1 p_1(\theta) \ . \qquad\qquad I(31)$$

Here β, δ and Δ_1 are universal critical exponents, b^2 a universal parameter and a, c, k_0 and k_1 are constants that differ from substance to substance. The functions $p_0(\theta)$ and $p_1(\theta)$ are universal quadratic polynomials in θ^2 given elsewhere.[33,37] The parameters of the revised and extended scaled potential $\tilde{P}$ are listed in Table I 13. Most of the parameters were determined by a fit to Beattie's critical-region PVT data, supplemented by data points generated from the global surface in the region where the latter is still valid, but within the range of validity of the scaled equation. The expansion coefficients $\tilde{\mu}_2$ and $\tilde{\mu}_3$ of the chemical potential were obtained by fitting to c_v data generated from the global surface in the same range. The coefficients $\tilde{\mu}_c$ and $\tilde{\mu}_1$ were obtained by setting the energy and entropy of the critical-region surface equal to those of the global surface at the reference point of 438 K in temperature and 205 kg/m^3 in density.

Detailed information on this surface and tables of thermodynamic properties generated from it can be found in Ref. 7.

The critical-region surface matches with the global surface in the supercritical region very well. There are some problems in the subcritical region near the saturation boundary. There are very few reliable data in that

region; also the ranges of validity of the global and the critical surface do not overlap below T_c.

Part II

A Scaled Fundamental Equation for Mixtures of Isobutane

and Isopentane near the Gas-Liquid Critical Line

1. Introduction

In Part I, Sec. 2.3 of this report we discussed how the thermodynamic behavior of a pure fluid near a critical point is represented by a non-classical scaled potential. In this part of the report, we explore the application of the scaling laws to fluid mixtures. In principle, this is straightforward: critical-point universality implies that the properties of all systems in the class of Ising-like system scale in the same way. This class encompasses not only fluids and fluid mixtures, but also many other systems, such as uniaxial ferromagnets passing through their Curie point and binary alloys undergoing an order-disorder phase transition. The generalization from one-component to two-component fluid mixtures was made by Griffiths and Wheeler[38], who pointed out that the mixture, at constant activity, scales like the pure fluid. Leung and Griffiths[39] subsequently developed a model based on this principle, and applied it to the mixture of ^{3}helium and ^{4}helium. Other applications followed, such as those of Moldover coworkers[40,41] to mixtures of carbon dioxide and hydrocarbons, and those of Chang and Doiron[42] for carbon dioxide - ethane mixtures. In order to apply the Leung-Griffiths model, we have to begin with constructing simple scaled equations for isobutane and isopentane. The scaled equation constructed in · Sec. 2.3 contains contributions from liquid-vapor asymmetry and corrections to scaling; the Leung-Griffiths model, however, cannot handle these refinements. Thus, for isobutane and isopentane, simple scaled potentials have to be

developed that treat liquid and vapor in a symmetric fashion; corrections to scaling are taken into account in an approximate fashion by having the leading critical exponents assume average values that depart somewhat from their true asymptotic values. In Sec. 2 of this part of the report, we develop these thermodynamic potentials for the pure fluids. In Sec. 3, we develop the Leung-Griffiths model and in Sec. 4 we compare the model with experimental data.

Since this part of the report was developed independently from the first part, there are some redundancies and some minor changes in notation that have not been eliminated for the sake of clarity and independent readability of this part of the report.

2. Scaled fundamental equation for one-component fluids

2.1 Critical power laws

Let T be the temperature, ρ the density, P the pressure, V the volume, μ the chemical potential per mole, A the Helmholtz free energy, S the entropy, H the enthalpy, C_v the heat capacity at constant volume, C_p the heat capacity at constant pressure and $K_T \equiv \rho^{-1}(\partial\rho/\partial P)_T$ the isothermal compressibility. In practice we find it convenient to introduce a symmetrized compressibility defined as

$$\chi_T \equiv \left(\frac{\partial\rho}{\partial\mu}\right)_T = \rho^2 K_T \quad . \qquad\qquad \text{II(1)}$$

The thermodynamic properties are made dimensionless by expressing them in terms of the critical temperature T_c, the critical density ρ_c and the critical pressure P_c.

$$\hat{T} = -\frac{T_c}{T} \ , \ \hat{\rho} = \frac{\rho}{\rho_c} \ , \ \hat{P} = \frac{P}{T} \cdot \frac{T_c}{P_c} \ ,$$

$$\hat{\mu} = \frac{\mu}{T} \cdot \frac{\rho_c T_c}{P_c} \ , \ \hat{U} = \frac{U}{V} \cdot \frac{1}{P_c} \ , \ \hat{A} = \frac{A}{VT} \cdot \frac{T_c}{P_c} \ ,$$

$$\hat{S} = \frac{S}{V} \cdot \frac{T_c}{P_c} \ , \ \hat{H} = \frac{H}{VT} \cdot \frac{T_c}{P_c} \ , \ \hat{\chi}_T = \left(\frac{\partial\hat{\rho}}{\partial\hat{\mu}}\right)_T \ , \qquad \text{II(2)}$$

$$\hat{C}_v = \frac{C_v}{V} \cdot \frac{T_c}{P_c} \ , \ \hat{C}_p = \frac{C_p}{V} \cdot \frac{T_c}{P_c} \quad .$$

21

Note that the reduced extensive properties $\hat{A}$, $\hat{U}$, $\hat{H}$, $\hat{S}$, $\hat{C}_p$, $\hat{C}_v$ are all taken per unit volume rather than per unit mass. The reason is that the singular part of the extensive thermodynamic properties per unit volume appear to be an approximately symmetric or antisymmetric function of $\rho - \rho_c$ as shown in earlier papers[43,44]. As a consequence χ_T is also a symmetric function of $\rho - \rho_c$, while the compressibility $K_T = \chi_T/\rho^2$ is not. In addition we introduce the reduced differences

$$\Delta\hat{T} = \hat{T} + 1 \ , \qquad\qquad\qquad II(3a)$$

$$\Delta\hat{\rho} = \hat{\rho} - 1 \ , \qquad\qquad\qquad II(3b)$$

$$\Delta\hat{\mu} = \hat{\mu} - \hat{\mu}(\rho_c, T) \ . \qquad\qquad II(3c)$$

To represent the singular thermodynamic behavior of fluids in the vicinity of the critical point, we first define critical power laws. The exponents of these power laws depend on the property considered and on the path along which the critical point is approached. The most important critical power laws are

$$\hat{C}_v = \frac{A}{\alpha}\,|\Delta\hat{T}|^{-\alpha} \qquad (\Delta\hat{\rho} = 0, \ \Delta\hat{T} > 0) \ , \qquad II(4a)$$

$$\Delta\hat{\rho} = \pm\,B|\Delta\hat{T}|^{\beta} \qquad (\text{coexistence boundary}) \ , \qquad II(4b)$$

$$\tilde{\chi}_T = \Gamma|\Delta\hat{T}|^{-\gamma} \qquad (\Delta\hat{\rho} = 0, \ \Delta\hat{T} > 0) \ , \qquad II(4c)$$

$$\Delta\hat{\mu} = \pm\,D|\Delta\hat{\rho}|^{\delta} \qquad (\Delta\hat{T} = 0) \ . \qquad II(4d)$$

22

The critical exponents α, β, γ, δ are related by the exponent relations[44]

$$\beta(\delta+1) = 2-\alpha \quad , \quad \beta(\delta-1) = \gamma \quad . \qquad \text{II(5)}$$

The values of the critical exponents are universal, i.e., they are the same for all systems belonging to the same universality class. Theory predicts that fluids near the gas-liquid critical point belong to the universality class of 3-dimensional Ising-like systems[32]. The exponents for this universality class are currently known with considerable accuracy[45,46]. It is noted that the critical power laws defined by II(4) are the leading terms of expansions around the critical point[33,47].

2.2 Linear-model fundamental equation

As our fundamental equation we consider the potential $\tilde{P}$ as a function of $\hat{T}$ and $\hat{\mu}$. This potential satisfies the differential equation

$$d\tilde{P} = \hat{U}d\hat{T} + \hat{\rho}d\hat{\mu} \quad . \qquad \text{II(6)}$$

To formulate a scaled fundamental equation for the thermodynamic properties of fluids near the critical point two procedures are currently available. The oldest approach is to formulate a simple scaled equation that incorporates the critical power laws defined in II(4) without nonanalytic corrections to the power laws. We have found that this approach yields a reasonably accurate representation of the thermodynamic properties of fluids in the critical region, but with effective values[44] for the critical exponents that differ slightly from the theoretical values[45,46] calculated for the universality class of Ising-like systems. A more rigorous approach is to formulate

23

a revised and extended scaled fundamental equation that incorporates the most important correction terms to the asymptotic critical power laws[33,37]. This revised and extended scaled fundamental equation has been shown to yield a good representation of the thermodynamic properties of various fluids in the critical region[37] including isobutane[7]. The Leung-Griffiths model[39] is a generalization of the simple scaled fundamental equation to mixtures. A generalization of the revised and extended scaled fundamental equation to mixtures is not yet available. Before we are able to apply the Leung-Griffiths model to isobutane-isopentane mixtures, we first need to represent the thermodynamic properties of the individual components near their critical points in terms of a simple scaled fundamental equation.

The potential $\hat{P}$ is written as the sum of a regular part $\hat{P}_r$ and a scaled part $\hat{P}_s$

$$\hat{P} = \hat{P}_r(\Delta\hat{T}, \Delta\hat{\mu}) + \hat{P}_s(\Delta\hat{T}, \Delta\hat{\mu}) \quad . \qquad\qquad II(7)$$

The functions $\hat{P}_r(\Delta\hat{T}, \Delta\hat{\mu})$ in II(7) and $\hat{\mu}(\rho_c, T) \equiv \hat{\mu}_o(\Delta\hat{T})$ in II(3c) are analytic functions that can be approximated by truncated Taylor-series expansions:

$$\hat{\mu}(\rho_c, T) = \hat{\mu}_o(\Delta\hat{T}) = \hat{\mu}_c + \sum_{i=1}^{3} \hat{\mu}_i (\Delta\hat{T})^i \quad , \qquad\qquad II(8)$$

$$\hat{P}_r(\Delta\hat{T}, \Delta\hat{\mu}) = \hat{P}_o(\Delta\hat{T}) + \Delta\hat{\mu} = 1 + \sum_{i=1}^{3} \hat{P}_i (\Delta\hat{T})^i + \Delta\hat{\mu} \quad . \qquad II(9)$$

24

In order to specify the scaled part $\hat{P}_s$ of the potential one introduces a new set of variables r and θ in the one-phase region that are related to the physical variables $\Delta\hat{T}$ and $\Delta\hat{\mu}$ by the transformation

$$\Delta\hat{T} = r(1-b^2\theta^2) \ , \qquad\qquad II(10a)$$

$$\Delta\hat{\mu} = ar^{\beta\delta}\theta(1-\theta^2) \ , \qquad\qquad II(10b)$$

where a and b are constants. This transformation is chosen such that $\theta = 0$ corresponds to the critical isochore $\Delta\hat{\rho} = 0$ above the critical temperature, $\theta = \pm 1/b$ to the critical isotherm $\Delta\hat{T} = 0$ and $\theta = \pm 1$ to the two branches of the coexistence curve. In the linear-model scaled equation adopted here, the constant b in the transformation equation II(10a) is related to the critical exponents by[44]

$$b^2 = \frac{\delta-3}{(\delta-1)(1-2\beta)} \ . \qquad\qquad II(11)$$

In terms of the parametric variables the scaled part $\hat{P}_s$ of the potential is given by

$$\hat{P}_s = akr^{\beta(\delta+1)}\left(p_o+p_2\theta^2+p_4\theta^4\right) \qquad\qquad II(12)$$

with

25

$$P_0 = \frac{\beta\delta - 3\beta - b^2\alpha\gamma}{2b^4(2-\alpha)(1-\alpha)\alpha} \quad . \qquad\qquad \text{II(13a)}$$

$$P_2 = -\frac{\beta\delta - 3\beta - b^2\alpha(2\beta\delta - 1)}{2b^2(1-\alpha)\alpha} \quad , \qquad\qquad \text{II(13b)}$$

$$P_4 = \frac{2\beta\delta - 3}{2\alpha} \quad . \qquad\qquad \text{II(13c)}$$

With the potential $\hat{P}$ specified by II(7), II(9) and II(12) all thermodynamics properties can be derived with the aid of the differential relation II(6). Specifically one obtains for the density the simple relation

$$\Delta\hat{\rho} = kr^\beta\theta \quad . \qquad\qquad \text{II(14)}$$

The simple scaled fundamental equation adopted here is known as the "linear model" because of the linear relationship between $\Delta\hat{\rho}$ and θ. A complete list of the relevant linear model equations is presented in Appendix B.

The amplitudes A, B, Γ, D of the critical power laws defined in II(4) are related to the linear-model fundamental equation by[44]

$$A = ak(2-\alpha)(1-\alpha)P_0 \quad , \qquad\qquad \text{II(15a)}$$

$$B = k/(b^2-1)^\beta \quad , \qquad\qquad \text{II(15b)}$$

$$\Gamma = k/a \quad , \qquad\qquad \text{II(15c)}$$

$$D = a(b^2-1)b^{\delta-3}/k^\delta \quad . \qquad\qquad \text{II(15d)}$$

26

In summary, the linear-model fundamental equation contains the following parameters: the two critical exponents β and δ, the two parameters a and k which together with the exponents β and δ specify the amplitudes of the critical power laws, the critical parameters T_c, ρ_c, P_c, three pressure background parameters $\hat{P}_1$, $\hat{P}_2$, $\hat{P}_3$ and four caloric background parameters $\hat{\mu}_c$, $\hat{\mu}_1$, $\hat{\mu}_2$ and $\hat{\mu}_3$. The parameters $\hat{\mu}_c$ and $\hat{\mu}_1$ specify the reference points of energy and entropy. In this report we adopt the convention that the energy $\hat{U}$ and the entropy $\hat{S}$ of isobutane and of isopentane are taken to be zero at their respective critical points. This condition implies

$$\hat{\mu}_c = 1 \quad ,$$
II(16a)

$$\hat{\mu}_1 = \hat{P}_1 \quad .$$
II(16b)

In our previous work we have found that the simple linear-model fundamental equation can be used in a range around the critical point approximately specified by[44].

$$0.0005 < |\Delta \hat{T}| < 0.03 \quad , \quad |\Delta \hat{\rho}| < 0.25 \quad ,$$
II(17)

if for the critical exponents the following effective universal values are used

$$\beta = 0.355 \quad , \quad \delta = 4.352 \quad , \quad \alpha = 0.100 \quad , \quad \gamma = 1.190$$
II(18)

and with b^2 as determined from II(11)

$$b^2 = 1.3909 \quad .$$
II(19)

27

2.3 Determinaton of parameters for isobutane

The scaled fundamental equation presented here for isobutane is valid in the range

$$407.6 \text{ K} < T < 420.1 \text{ K} \quad ,$$

II(20)

$$169 \text{ kg/m}^3 < \rho < 282 \text{ kg/m}^3 \quad .$$

The critical temperature and the critical density of isobutane have been determined experimentally as[5,6,7] (c.f. Table I 11)

$$T_c^{(4)} = 407.84 \text{ K} \quad ,$$

II(21)

$$\rho_c^{(4)} = 225.5 \text{ kg/m}^3 = 3.8796 \text{ mol/dm}^3 \quad .$$

In this part of the report we adopt the convention that quantities with a superscript (4) refer to pure isobutane and those with a superscript (5) to pure isopentane.

The critical pressure P_c and the parameters a, k, $\hat{P}_1$, $\hat{P}_2$, and $\hat{P}_3$ can be determined by fitting the linear-model equation to experimental equation-of-state data. The primary experimental data available for this purpose are the data reported by Beattie et al.[48,49] Unfortunately the experimental data of Beattie et al. cover only a small portion of the range specified by II(20). Specifically, we have 174 data points restricted to temperatures between 407.764 K and 408.314 K and densities between 180.5 kg/m^3 and 270.2 kg/m^3. To

28

cover the entire range specified in II(20), we supplemented the experimental data with pressure data calculated from the revised and extended scaled equation earlier constructed for isobutane by Levelt Sengers et al.[7] Specifically, we calculated 24 data points spaced by 5 kg/m^3 intervals in the density range 168 kg/m^3 < ρ < 283 kg/m^3 at each of the following temperatures: 412 K, 414 K, 416 K, 418 K and 420 K. We thus obtained 120 calculated data points supplementing the 174 experimental data of Beattie et al. We assigned to the experimental and to the calculated data points the error estimates of Beattie et al., namely

$$\sigma_P = 10^{-4} \text{ MPa} , \quad \sigma_T = 0.005 \text{ K} , \quad \sigma_\rho = 0.058 \text{ kg/m}^3 . \qquad \text{II(22)}$$

It was found that the linear-model equation represents these data with a reduced chi-square of 1.84. The parameter values deduced from the fit are given in Table II 1.

The parameters $\hat{\mu}_c$ and $\hat{\mu}_1$ were selected in accordance with II(16). The parameters $\hat{\mu}_2$ and $\hat{\mu}_3$ can be determined from experimental specific heat data. In the absence of experimental specific heat data for isobutane in the critical region, we resorted again to the revised and extended scaled equation for isobutane from which we generated calculated data for the specific heat at constant volume. A total of 168 points, at seven temperatures at 2 K intervals between 408 K and 420 K and at 5 kg/m^3 density intervals in the range from 168 kg/m^3 to 283 kg/m^3, were used in the fit to determine $\hat{\mu}_2$ and $\hat{\mu}_3$; the values thus obtained for these parameters are given in Table II 1. The differences between C_v values calculated from the simple scaled equation presented here and

those calculated from the original revised and extended scaled equation are about 3% very close to the critical point and are well within 1% at the edges of the range specified by II(20). The differences between C_p values calculated from the simple scaled equation and those calculated from the revised and extended scaled equation, are generally about 3% in the range II(20), but very close to the critical point, specifically on the isotherm at 408 K, the differences become as large as 20%.

2.4   Determination of parameters for isopentane

The scaled fundamental equation presented here for isopentane is valid in the range

$$460.3 \text{ K} \leqslant T \leqslant 474.3 \text{ K} \quad ,$$

II(23)

$$177 \text{ kg/m}^3 \leqslant \rho \leqslant 294 \text{ kg/m}^3 \quad .$$

The critical-point parameters of isopentane are (c.f. Table I 11):

$$T_c^{(5)} = 460.51 \text{ K} \quad ,$$

$$\rho_c^{(5)} = 235.57 \text{ kg/m}^3 = 3.265 \text{ mol/dm}^3 \quad , \qquad \text{II(24)}$$

$$P_c^{(5)} = 3.371 \text{ MPa} \quad .$$

In the absence of experimental PVT data for isopentane in the critical region, we cannot determine the parameters a and k in the scaling functions from experimental data directly although the product ak can be inferred from vapor pressure data. Instead we assume that the singular parts of the potentials of isobutane and isopentane satisfy corresponding states which implies a and k to be the same for isobutane and isopentane. Previous work has shown this assumption to be valid when the thermodynamic properties of D_2O in the critical regiona are compared with those of H_2O in the critical region, even though these fluids themselves do not satisfy corresponding states[50].

We determine the pressure background parameters $\hat{P}_1$, $\hat{P}_2$, $\hat{P}_3$ from experimental vapor-pressure data given in Table I 6. The vapor-pressure data are represented by the simple scaled equation

$$\hat{P} = 1 + \hat{P}_1 \Delta\hat{T} + \hat{P}_\alpha \left|\Delta\hat{T}\right|^{\beta(\delta+1)} + \hat{P}_2(\Delta\hat{T})^2 + \hat{P}_3(\Delta\hat{T})^3 \quad , \qquad II(25)$$

where the coefficient $\hat{P}_\alpha$ of the nonanalytic term is (c.f.(B.20) in Appendix B)

$$\hat{P}_\alpha = \frac{ak(p_0 + p_2 + p_4)}{(1-b^2)^{\beta(\delta+1)}} \quad . \qquad II(26)$$

With the previously adopted values of b^2, a and k we find $\hat{P}_\alpha = 30.2137$. With estimated experimental errors

$$\sigma_T = 0.01 \text{ K} , \quad \sigma_P = 0.003 \text{ MPa} \quad , \qquad II(27)$$

31

the vapor-pressure equation II(25) reproduces the experimental data with a chi-square of 0.52 and with coefficients

$$\hat{P}_1^{(5)} = 6.1720 , \quad \hat{P}_2^{(5)} = 18.0281 , \quad \hat{P}_3^{(5)} = 19.4960 . \qquad \text{II(28)}$$

A detailed comparison between the experimental and calculated vapor pressures is presented in Table I 6.

In order to determine the caloric background parameters $\hat{\mu}_2$ and $\hat{\mu}_3$ we need estimates for the specific heat. Again experimental information for the specific heat of isopentane in the critical region is not available. As an alternative we decompose the specific C_v into the ideal-gas specific heat $C_{v,id}$ and an excess specific heat $\Delta C_v = C_v - C_{v,id}$

$$C_v = \Delta C_v + C_{v,id} , \qquad \text{II(29)}$$

and assume that the excess specific heat contributions $\Delta C_v^{(4)}$ and $\Delta C_v^{(5)}$ for isobutane and isopentane satisfy corresponding states. For isobutane the ideal-gas specific heat $C_{v,id}^{(4)}$ is calculated from the global thermodynamic surface of Waxman and Gallagher[3]. The excess specific heat $\Delta C_v^{(4)}$ for isobutane is then deduced as $C_v^{(4)} - C_{v,id}^{(4)}$ with $C_v^{(4)}$ again calculated from the revised and extended scaled equation of state for isobutane given in Part I. The excess specific heat $\Delta C_v^{(5)}\left(\dfrac{T}{T_c}(5), \dfrac{\rho}{\rho_c}(5)\right)$ for isopentane is then constructed from $\Delta C_v^{(4)}\left(\dfrac{T}{T_c}(4), \dfrac{\rho}{\rho_c}(4)\right)$ for isobutane as

$$\frac{\Delta C_v^{(5)}}{Z_c^{(5)}} = \frac{\Delta C_v^{(4)}}{Z_c^{(4)}} \qquad \text{II(30)}$$

with

$$Z_c^{(4)} = \frac{P_c^{(4)}}{R \rho_c^{(4)} T_c^{(4)}} \quad , \quad Z_c^{(5)} = \frac{P_c^{(5)}}{R \rho_c^{(5)} T_c^{(5)}} \quad . \qquad \text{II(31)}$$

Finally, the total specific heat $C_v^{(5)}$ of isopentane is obtained as the sum of the excess specific heat $\Delta C_v^{(5)}$ estimated on the basis of corresponding states and the ideal-gas specific heat $C_{v,id}^{(5)}$ of isopentane calculated from the generalized corresponding states surface described in Part I, Sec. 2.2. Having thus generated a set of C_v data for isopentane we fit the simple scaled equaton to these data to determine $\hat{\mu}_2$ and $\hat{\mu}_3$. The differences between the generated specific heat data and the values calculated from the simple scaled equation are at most 2.2% very near the critical point and within 1% in most of the range specified by II(23). The coefficients $\hat{\mu}_c$ and $\hat{\mu}_1$ again are fixed by the convention that the energy and entropy of isopentane are taken to be zero at the critical point.

The parameters for isopentane are all given in Table II 1.

3. Scaled fundamental equation for fluid mixtures

3.1 Reduced thermodynamic variables

The scaled fundamental equation for fluids as discussed in Part II, Sec. 2 can be generalized by a procedure proposed by Leung and Griffiths[39]. However, the equations used by Leung and Griffiths[39] as well as by others[40-42] are not

33

in dimensionless form unlike the scaled equations used in this report. This makes the equations inconvenient when one wants to change from one system of units to another. As a first step, therefore, we reformulate the equations of Leung and Griffiths so as to bring them into dimensionless form.

We treat pure isobutane as the reference fluid and we make the thermodynamic properties of the mixtures dimensionless with the aid of the critical-point parameters $T_c^{(4)}$, $\rho_c^{(4)}$ and $P_c^{(4)}$ of isobutane, which are the "starred" reference values listed in Table I 9. We thus define for the mixture

$$\hat{T} = -\frac{T_c^{(4)}}{T} \quad , \quad \hat{\rho} = \frac{\rho}{\rho_c^{(4)}} \quad , \quad \hat{P} = \frac{P}{T} \cdot \frac{T_c^{(4)}}{P_c^{(4)}} \quad , \quad \hat{U} = \frac{U}{V} \cdot \frac{1}{P_c^{(4)}} \quad . \quad \text{II(32)}$$

Let ρ_4 and ρ_5 be the molar densities and μ_4 and μ_5 the chemical potentials of isobutane and isopentane in the mixture. These quantities are similarly made dimensionless as

$$\hat{\rho}_4 = \frac{\rho_4}{\rho_c^{(4)}} \quad , \quad \hat{\rho}_5 = \frac{\rho_5}{\rho_c^{(4)}} \quad , \quad \quad \text{II(33)}$$

$$\hat{\mu}_4 = \frac{\mu_4}{T} \frac{\rho_c^{(4)} T_c^{(4)}}{P_c^{(4)}} \quad , \quad \hat{\mu}_5 = \frac{\mu_5}{T} \frac{\rho_c^{(4)} T_c^{(4)}}{P_c^{(4)}} \quad . \quad \quad \text{II(34)}$$

34

In this report we also consider the mole fraction x of isopentane in the mixtures which is related to the densities $\hat{\rho}_4$ and $\hat{\rho}_5$ by

$$x = \frac{\hat{\rho}_5}{\hat{\rho}} = \frac{\hat{\rho}_5}{\hat{\rho}_4 + \hat{\rho}_5} \quad . \qquad II(35)$$

As in the case of the one-component fluids we shall formulate a fundamental equation for the potential $\hat{P}$. This potential $\hat{P}$ satisfies the differential equation

$$d\hat{P} = \hat{\rho}_4 d\hat{\mu}_4 + \hat{\rho}_5 d\hat{\mu}_5 + \hat{U}d\hat{T} \quad . \qquad II(36)$$

Following Leung and Griffiths[39] we do not consider $\hat{P}$ as a function of $\hat{\mu}_4$, $\hat{\mu}_5$ and $\hat{T}$, but as a function of a new set of variables ζ, τ and h which are related to the original set of intensive variables by

$$\zeta = \frac{e^{\hat{\mu}_5}}{e^{\hat{\mu}_4} + e^{\hat{\mu}_5}} \quad , \qquad II(37)$$

$$\tau = \hat{T} - \hat{T}_c(\zeta) \quad , \qquad II(38)$$

$$h = \ln(e^{\hat{\mu}_4} + e^{\hat{\mu}_5}) - H(\zeta,\tau) \quad . \qquad II(39)$$

35

The variable ζ plays the role of an intensive composition variable such that $\zeta = 0$ corresponds to pure isobutane and $\zeta = 1$ to pure isopentane. The critical temperature $T_c(\zeta)$, the critical density $\rho_c(\zeta)$ and the critical pressure $P_c(\zeta)$ are now treated as functions of ζ rather than of the mole fraction x. The critical parameters of the mixture in dimensionless form are

$$\hat{T}_c(\zeta) = - \frac{T_c^{(4)}}{T_c(\zeta)} \quad , \quad \hat{\rho}_c(\zeta) = \frac{\rho_c(\zeta)}{\rho_c^{(4)}} \quad , \quad \hat{P}_c(\zeta) = \frac{P_c(\zeta)}{T_c(\zeta)} \cdot \frac{T_c^{(4)}}{P_c^{(4)}} \quad . \quad \text{II(40)}$$

The function $H(\zeta,\tau)$ represents the value of $\ln(e^{\tilde{\mu}_4} + e^{\tilde{\mu}_5})$ along the phase boundary. The variables τ and h are defined in such a way that in the limit $\zeta \to 0$ they reduce to the variables $\Delta\hat{T}$ and $\Delta\hat{\mu}$ for pure isobutane.

3.2 Scaled fundamental equation for the mixture

In analogy to II(7) we decompose the potential $\hat{P}$ again in a regular part $\hat{P}_r$ and a scaled part $\hat{P}_s$

$$\hat{P} = \hat{P}_r(\zeta,\tau,h) + \hat{P}_s(\zeta,\tau,h) \quad . \quad\quad\quad \text{II(41)}$$

The functions $P_r(\zeta,\tau,h)$ in II(41) and $H(\zeta,\tau)$ in II(39) are analytic functions that are represented by truncated Taylor series expansions in analogy to II(8) and II(9):

$$H(\zeta,\tau) = \sum_{i=0}^{3} H_i(\zeta)\tau^i \quad , \quad\quad\quad \text{II(42)}$$

36

$$\hat{P}_r(\zeta, \tau, h) = \sum_{1=0}^{3} \hat{P}_1(\zeta)\tau^1 + \hat{\rho}_c(\zeta)h \quad . \qquad \text{II(43)}$$

The singular part $\hat{P}_s$ is specified as

$$\hat{P}_s(\zeta, \tau, h) = q(\zeta)\Delta\hat{P}(\bar{\tau}, h) \qquad \text{II(44)}$$

with

$$\bar{\tau} = \ell(\zeta)\tau \quad . \qquad \text{II(45)}$$

The function $\Delta\hat{P}(\tau, h)$ is to be identified with the function $\Delta\hat{P}(\Delta\hat{T}, \Delta\hat{\mu})$ defined in Appendix B for one-component fluids. Specifically

$$\bar{\tau} = \ell(\zeta)\tau = r(1-b^2\theta^2) \quad , \qquad \text{II(46)}$$

$$h = ar^{\beta\delta}\theta(1-\theta^2) \quad , \qquad \text{II(47)}$$

$$\Delta\hat{P} = akr^{\beta(\delta+1)}(p_0 + p_2\theta^2 + p_4\theta^4) \quad . \qquad \text{II(48)}$$

The functions $\hat{T}_c(\zeta)$, $\hat{\rho}_c(\zeta)$, $\hat{P}_c(\zeta) = \hat{P}_0(\zeta)$, $\hat{P}_1(\zeta)$, $H_1(\zeta)$, $q(\zeta)$, $\ell(\zeta)$ are all analytic functions of the variable ζ and may be expanded in series of the form

$$f(\zeta) = f_0 + f_1\zeta + f_2\zeta(1-\zeta) + f_3\zeta^2(1-\zeta) + \ldots \quad . \qquad \text{II(49)}$$

37

We note that the coefficients a and k in II(47) and II(48) are, in principle, functions of the variable ζ. However, as discussed in Part II, Sec. 2.4 for our mixture $a = a^{(4)} = a^{(5)}$ and $k = k^{(4)} = k^{(5)}$ are taken as constants.

A list of equations for various thermodynamic properties implied by this fundamental equation is presented in Appendix C.

3.3 Determination of parameters for isobutane-isopentane mixtures

The equations presented in Part II, Sec. 3.2, specify the thermodynamic surface of the mixture in terms of the following constants ($j = 0, 1, 2, 3$):

$$\hat{T}_{cj}, \; \hat{\rho}_{cj}, \; \hat{P}_{ij}, \; H_{ij}, \; q_j, \; \ell_j \; .$$

In determining these constants we need to impose the conditions that the fundamental equation reproduce the fundamental equation for pure isobutane in the limit $\zeta \to 0$ and the one for pure isopentane in the limit $\zeta \to 1$. This condition implies the following relationships between the constants in the fundamental equation of the mixture and those in the fundamental equation of the pure components:

$$\hat{T}_{c0} = -1 \;, \qquad \hat{T}_{c1} = 1 - \frac{T_c^{(4)}}{T_c^{(5)}} \;, \qquad \qquad \text{II(50)}$$

$$\hat{\rho}_{c0} = 1 \;, \qquad \hat{\rho}_{c1} = \frac{\rho_c^{(5)}}{\rho_c^{(4)}} - 1 \;, \qquad \qquad \text{II(51)}$$

38

$$\hat{P}_{00} = 1 \quad , \qquad \hat{P}_{01} = \frac{P_c^{(5)}}{P_c^{(4)}} \frac{T_c^{(4)}}{T_c^{(5)}} - 1 \quad , \qquad \text{II(52)}$$

$$\hat{P}_{10} = \hat{P}_i^{(4)} \quad , \qquad \hat{P}_{i1} = \frac{P_c^{(5)}}{P_c^{(4)}} \left(\frac{T_c^{(5)}}{T_c^{(4)}} \right)^{i-1} \hat{P}_i^{(5)} - \hat{P}_i^{(4)} \quad , \qquad \text{II(53)}$$

$$H_{00} = \hat{\mu}_c^{(4)} \quad , \qquad H_{01} = \frac{Z_c^{(5)}}{Z_c^{(4)}} \hat{\mu}_c^{(5)} - \hat{\mu}_c^{(4)} \quad , \qquad \text{II(54)}$$

$$H_{10} = \hat{\mu}_i^{(4)} \quad , \qquad H_{i1} = \frac{Z_c^{(5)}}{Z_c^{(4)}} \left(\frac{T_c^{(5)}}{T_c^{(4)}} \right)^i \hat{\mu}_i^{(5)} - \hat{\mu}_i^{(4)} \quad , \qquad \text{II(55)}$$

$$q_0 = 1 \quad , \qquad q_1 = \frac{\rho_c^{(5)}}{\rho_c^{(4)}} \left(\frac{Z_c^{(4)}}{Z_c^{(5)}} \right)^{1/\delta} - 1 \quad , \qquad \text{II(56)}$$

$$\ell_0 = 1 \quad , \qquad \ell_1 = \frac{T_c^{(5)}}{T_c^{(4)}} \left(\frac{Z_c^{(5)}}{Z_c^{(4)}} \right)^{1/\beta\delta} - 1 \quad . \qquad \text{II(57)}$$

The first two terms in the expansion II(49) for $\hat{T}_c(\zeta)$, $\hat{\rho}_c(\zeta)$, $\hat{P}_1(\zeta)$, $H_1(\zeta)$, $q(\zeta)$, $\ell(\zeta)$ are thus completely specified by the properties of the pure components. In order to determine the coefficients of any higher-order terms in the expansions we need thermodynamic property data for the mixture. For this purpose we consider critical line-data and data for the dew-bubble curve discussed in Part I and listed in Tables I 5 and I 7.

The available experimental information is not sufficiently extensive to determine coefficients of the higher order terms in the expansion II(49) for all of the functions $\hat{T}_c(\zeta)$, $\hat{\rho}_c(\zeta)$, $\hat{P}_1(\zeta)$, $H_1(\zeta)$, $q(\zeta)$, $\ell(\zeta)$. In practice we only retain higher order terms in the expansions for $\hat{\rho}_c(\zeta)$, $\hat{P}_0(\zeta)$ and $\hat{P}_1(\zeta)$ and we restrict ourselves to the following truncated expansions:

$$\hat{T}_c(\zeta) = \hat{T}_{c0} + \hat{T}_{c1}\zeta \quad , \qquad\qquad \text{II(58)}$$

$$\hat{\rho}_c(\zeta) = \hat{\rho}_{c0} + \hat{\rho}_{c1}\zeta + \hat{\rho}_{c2}\zeta(1-\zeta) \quad , \qquad\qquad \text{II(59)}$$

$$\hat{P}_0(\zeta) = \hat{P}_{00} + \hat{P}_{01}\zeta + \hat{P}_{02}\zeta(1-\zeta) + \hat{P}_{03}\zeta^2(1-\zeta) \quad , \qquad\qquad \text{II(60)}$$

$$\hat{P}_1(\zeta) = \hat{P}_{10} + \hat{P}_{11}\zeta + \hat{P}_{12}\zeta(1-\zeta) \quad , \qquad\qquad \text{II(61)}$$

$$\hat{P}_2(\zeta) = \hat{P}_{20} + \hat{P}_{21}\zeta \quad , \qquad\qquad \text{II(62)}$$

$$\hat{P}_3(\zeta) = \hat{P}_{30} + \hat{P}_{31}\zeta \quad , \qquad\qquad \text{II(63)}$$

$$H_1(\zeta) = H_{10} + H_{11}\zeta \quad , \qquad\qquad\qquad \text{II(64)}$$

$$q(\zeta) = q_0 + q_1\zeta \quad , \qquad\qquad\qquad \text{II(65)}$$

$$\ell(\zeta) = \ell_0 + \ell_1\zeta \quad , \qquad\qquad\qquad \text{II(66)}$$

We repeat that the coefficients of the constant and linear terms in these expansions are determined by the constants in the equation for pure isobutane and isopentane. The coefficients of the higher order terms, i.e. $\hat{\rho}_{c2}$, $\hat{P}_{02}$, $\hat{P}_{03}$ and $\hat{P}_{12}$ are estimated, primarily on the basis of the critical-line data presented in Table I 5, as

$$\hat{\rho}_{c2} = 0.06 \quad , $$

$$\hat{P}_{02} = 0.16 \quad , \quad \hat{P}_{03} = -0.03 \qquad\qquad \text{II(67)}$$

$$\hat{P}_{12} = 7 \quad . $$

A complete set of coefficients for isobutane-isopentane mixtures is presented in Appendix D. Tables of thermodynamic properties calculated from the scaled fundamental equation are presented in Appendix E.

4. Discussion of results

4.1 · Comparison with experimental data

The scaled fundamental equation for the mixture was constructed in such a way as to reproduce the thermodynamic properties of the pure components. In addition we can make a comparison with the experimental data for the critical point and the coexistence curve data for the mixture as a function of concentration presented in Tables I 5 and I 7.

The critical parameters of the mixtures are given by the functions $\hat{T}_c(\zeta)$, $\hat{\rho}_c(\zeta)$ and $\hat{P}_c(\zeta)$, where ζ is related to the mole fraction x of isopentane by

$$x = \zeta + \frac{\zeta(1-\zeta)Q(\zeta)}{\hat{\rho}(\zeta)} \qquad \text{II(68)}$$

On the critical line $\hat{\rho}(\zeta) = \hat{\rho}_c(\zeta)$ and $Q(\zeta) = Q_c(\zeta)$ with

$$Q_c(\zeta) = \frac{d\hat{P}_0(\zeta)}{d\zeta} - \hat{P}_1(\zeta)\frac{d\hat{T}_c(\zeta)}{d\zeta} - \hat{\rho}_c(\zeta)\left[\frac{dH_0(\zeta)}{d\zeta} - H_1(\zeta)\frac{d\hat{T}_c(\zeta)}{d\zeta}\right] . \qquad \text{II(69)}$$

In Table II 2 we list the critical parameters of the mixture calculated from this equation for various values of the composition; these calculated values are to be compared with the experimental values given earlier in Table I 4. The comparison is made in Fig. II 1. We consider the agreement with the experimental data satisfactory.

42

The experimental coexistence curve data presented in Table I 7 are compared with coexistence curve data calculated from our fundamental equation at constant compositions x in Fig. II 2. Here the agreement is only approximate; there are systematic disagreements between the experimental and calculated slopes of the coexistence curve data.

We tried to improve the agreement between experiment and theory by allowing for nonzero values of the coefficients H_{02} and H_{12} in the expansion II(49) for $H_0(\zeta)$ and $H_1(\zeta)$. This procedure, however, did not lead to a significant change in the values obtained for the thermodynamic properties from our fundamental equation.

4.2 Comparison with global thermodynamic surface for isobutane-isopentane mixtures

The application of the scaled fundamental equation to the fluid mixture is at any given composition restricted to a region around the critical point approximately given by II(17). In Part I we have developed a global analytical fundamental equation using generalized corresponding states. This formulation is valid far away from the critical line but ceases to be valid near the critical line. One can investigate the consistency of the two procedures by comparing the two thermodynamic surfaces at temperatures and densities where both surfaces are expected to be applicable. In Part I, we discussed such a test for pure isobutane and found good consistency of the global and scaled surfaces at supercritical conditions. Here, we discuss such a comparison for an equimolar mixture of isobutane-isopentane (x = 0.5); at this composition the differences between the two prediction methods are likely to be largest.

43

An equimolar mixture of isobutane and isopentane has a critical temperature of 437.71 K and a critical density of 3.569 mol/dm^3. From II(17) it follows that our scaled fundamental equation should be valid at temperatures up to 452 K and at densities from 2.7 mol/dm^3 to 4.5 mol/dm^3. In Table II 3 we present a comparison between the pressure and its first derivatives as calculated from the global analytical fundamental equation at 452 K and those calculated from the scaled fundamental equation. It is seen that the differences are still substantial. The differences in the pressures are of the order of 5% and for the derivatives they increase up to 15% for the thermal pressure coefficient and up to 20% for the compressibility. In the absence of direct experimental PVT data for this mixture one cannot ascertain which of the two surfaces yields the more accurate values at this temperature. Moreover, the procedure for applying these fundamental equations to the mixture is not unique. If we compare the pressures calculated at 452 K from our fundamental equations with those calculated from the global surface but with a different set of coefficients, we find differences of the order of 3% but with the opposite sign! We conclude that the differences quoted in Table II 3 are a measure of the uncertainty with which the properties of these mixtures are predicted with currently available techniques, when the available data base for the mixture is modest to scant.

4.3 Concluding remarks

The procedure devised by Leung and Griffiths[39] leads to a scaled fundamental equation that correctly reproduces the scaled fundamental equation for the pure components near their respective critical points. In order to calculate the properties of the mixture one needs to specify the following

44

functions: $\hat{T}_c(\zeta)$, $\hat{\rho}_c(\zeta)$, $\hat{P}_1(\zeta)$, $H_1(\zeta)$, $q(\zeta)$ and $\ell(\zeta)$ as a function of ζ. For this purpose we considered an expansion of the form (of II(49))

$$f(\zeta) = f_0 + f_1\zeta + f_2\zeta(1-\zeta) + f_3\zeta^2(1-\zeta) + \ldots \quad . \qquad \text{II(70)}$$

The coefficients f_0 and f_1 for all the functions mentioned above are completely determined by the properties of the pure components as shown in Sec. 3.3 of Part II. Therefore, if we were to assume that all functions were linear functions of ζ, we could predict the properties of the mixtures from the properties of the pure components. Unfortunately, the assumption that $\hat{T}_c(\zeta)$, $\hat{\rho}_c(\zeta)$, $\hat{P}_1(\zeta)$, $H_1(\zeta)$, $q(\zeta)$ and $\ell(\zeta)$ are linear functions of ζ is not justified.

In our approach we took the energy and the entropy of the pure components to be zero at their respective critical points. This choice was made so as to bring the equations into their most simple form. A different choice of the reference points for zero energy and entropy would affect the variable ζ through its definition II(37). Hence if the functions $f(\zeta)$ were linear for one choice of reference points for zero energy and entropy, they would no longer be linear for another choice. We do not know a priori for which choice the linear approximation would be optimum. This problem has also been mentioned by Leung and Griffiths in their original paper. In our approach we took the reference points as the critical points of the pure fluids and retained nonlinear terms in the expansions for $\hat{\rho}_c(\zeta)$, $\hat{P}_0(\zeta)$ and $\hat{P}_1(\zeta)$ only. However, if we a take another set of reference points for zero energy and entropy and repeat the same procedure described in this report we do obtain different values for the pressures of the mixture.

45

The tables presented in this report are the best we can obtain with the information and methods presently available. However, in order to develop a method which can truly predict the thermodynamic properties of fluid mixtures near the critical points, it will be necessary to develop a procedure for applying the scaling laws to mixtures in a manner which is less sensitive to the choice of the reference points of zero energy and entropy.

Part III

Viscosities of Hydrocarbons and Their Mixtures

1. Experimental viscosity data obtained under this contract

1.1 Apparatus

Viscosity values are obtained from the damping of a piezoelectric quartz crystal, 5 cm long, 0.5 cm in diameter, mounted in a pressure cell filled with the fluid of interest. The apparatus is described in Refs. 12-14. The range is 100-300 K in temperature, at pressures up to 30 MPa. The apparatus is most suited for measurements in the saturated and compressed liquid. The viscosity is derived from the measured bandwidth of the resonance curve, Δf, by means of the relation

$$\eta = \frac{\pi f}{\rho} \left[\frac{M}{S} \right]^2 \left[\frac{\Delta f}{f} - \frac{\Delta f_{vac}}{f_{vac}} \right]^2 , \qquad \text{III(1)}$$

where ρ is the fluid density; M is the crystal mass; S is the crystal surface area adjusted for thermal expansion and hydrostatic compression; and f is the resonant frequency of the crystal.

Since the damping is related to the product of viscosity and density, while it is measured as function of pressure and temperature, it is necessary to have independent information on the equations of state of the fluids studied. In the cases we have studied, this information was always available, with an imprecision far smaller (about 0.2%) than that of the measured bandwidth (typically of the order of a percent). The inaccuracy of the reported viscosity data is estimated to be no larger than $\pm$ 2%, except for the butanes, where the imprecision occasionally was as much as $\pm$ 3%.

1.2 Data for methane, ethane and propane

The viscosity data for methane, ethane and propane have all been published in the archival literature.[14-17] We display the methane data in Fig. III 1, those for ethane in Fig. III 2 and those for propane in Fig. III 3. These figures make clear how the viscosity coefficient of a typical non-polar fluid depends on density and temperature. It is important to recall that the dependence on density is much 'simpler' than the dependence on pressure, especially at temperatures near the critical temperature of the fluid. Figure III 2 shows that, at reduced densities smaller than about 2.5 ρ_c (about 17 mol L^{-1} for ethane), the viscosity typically increases weakly with both temperature and density. However, at reduced densities larger than about 2.5, the viscosity increases strongly with density and decreases weakly with temperature at fixed density. We shall call these density ranges the 'gas-like' and 'liquid-like' density ranges, respectively.

For the listings of the original data we refer to the literature cited.

1.3 Data for nitrogen-ethane and methane-ethane mixtures.

The viscosities of pure nitrogen, pure methane and for approximately 30-70, 50-50 and 70-30 mol % mixtures are reported in Ref. 19. The data for the 50-50 mixture are displayed in Fig. III 4. The viscosities of approximately 30-70, 50-50 and 70-30 mol % mixtures of methane and ethane are reported in Ref. 20. The data for the 50-50 mixture are shown in Fig. III 5.

1.4 Viscosity data for normal and isobutane.

The viscosity of saturated and compressed liquid normal butane was measured at temperatures between 140 and 300 K, and at pressures to 30 MPa. Densities ranged from 9.8 to 12.8 mol/dm^3. The viscosities of the compressed liquid are listed in Table III 1, those of the saturated liquid normal butane in

Table III 2. The data are displayed in Fig. III 6.

The viscosity of saturated and compressed liquid isobutane was measured at temperatures between 120 and 300 K and at pressures to 30 MPa. Densities ranged from 9.4 to 12.9 mol/dm^3. The viscosities of compressed liquid isobutane are listed in Table III 3, those of saturated liquid isobutane in Table III 4. The data are displayed in Fig. III 7.

2. The representation of the viscosity of hydrocarbon mixtures.

2.1 Corresponding-states model

A program for predicting the viscosities of hydrocarbon mixtures was developed at NBS and is available in the literature under the acronym TRAPP.[10,11] This program is based on an extension of the generalized principle of corresponding states discussed in Part I, Sec. 2.2. The reference fluid is methane. The shape factors are not tailor-made for each substance; rather, they are generalized functions of volume and temperature that depend on the characteristics of the hydrocarbon of interest through only one parameter, the acentric factor, by a procedure developed by Leach and Leland.[28]

For the mixing rules used in the program TRAPP we refer to the literature.[10,11] The adjustable constants in the combining rules are set equal to unity.

The viscosity of the mixture at specified pressure, temperature and composition is obtained in the following steps. Starting points are the equation of state and viscosity formulations, in terms of density and temperature, for the reference fluid. The program begins by finding the density of the mixture and the equivalent density and temperature of the reference fluid, using the generalized principle of corresponding states for the mixture. Once the densities are known, a simple expression connects the viscosity of the mixture to that of the reference fluid at the corresponding

49

density and temperature. The program TRAPP claims an accuracy of about seven percent in the prediction of transport properties of hydrocarbon mixtures.[10,11]

2.2 Comparison of the corresponding-states model with experimental data for methane, ethane and propane

Figure III 8 compares our data for methane at 100 K with a correlating equation for methane only.[51] Figures III 9 and 10 compare our data for saturated and compresed liquid ethane and propane, respectively, with the corresponding-states model. The densities shown correspond to reduced densities between 1.6 and 3.2. The comparisons, along with others in the publications cited, support the observation that, in the 'gas-like' density range, most of the differences between our measurements and the model are smaller than 7 percent, and that the model is likely to be satisfactory for many engineering calculations. However, at reduced densities larger than about 2.5, we find that in most cases the differences are substantially larger than 7 percent, and that they typically increase strongly with density.

2.3 Comparison of the corresponding-states model with data for the mixtures of nitrogen and methane, and those of methane and ethane

The viscosity measurements on pure methane, ethane and propane have revealed some of the strengths and weaknesses of the corresponding-states model applied to pure fluids. The viscosity measurements that we have performed on nitrogen-methane and methane-ethane mixtures[19,20] serve to answer the question of whether the model degrades if applied to mixtures.

The case of the nitrogen-methane mixtures is not clear-cut. As is shown in Fig. III 11, the measured viscosities of the 30-70, 50-50 and 70-30

mol % mixtures depart systematically from the model, but the departures are generally within 5%. The concentration-dependence at fixed molar density and temperature is not particularly well-predicted (Fig. III 12) but the problem is caused by poor prediction of the pure-nitrogen viscosity, a result perhaps not surprising given that the model was developed for use in hydrocarbon mixtures.

The methane-ethane mixtures form a more interesting test case. In Fig. III 13, we show a comparison of pure-methane and pure-ethane viscosities with the corresponding-states model. Up to 15% departures, of opposite signs for the two fluids, are found at the highest densities. Note that the reference viscosity values of the model have been shifted with respect to the correlation for pure methane (Fig. III 8) in order to represent viscosities of the heavier hydrocarbons more closely. In Fig. III 14, we shown viscosities of the approximately 3565 mol % methane-ethane mixture over the entire range of densities. Since at the lowest densities the agreement is within 5%, and the largest departures are within 15%, there seems in this case to be no further degradation of the model if extended to mixtures.

2.4 Comparison of the corresponding-states model with data for normal and
     isobutane

Of most interest to the objectives of this project are, of course, our data on the viscosities of normal and isobutane.

Measured normal butane viscosities were compared with the generalized corresponding states model. Measured and calculated saturated liquid viscosities are shown in Fig. III 15. The differences between the measured and calculated values, for both compressed and saturated liquid, are shown in Fig. III 16. At lower densities ($\leq 2.5 \rho_c$) the differences are smaller than 5 percent, which is typical of other fluids we have examined in this reduced

51

density range. At densities larger than 2.5 ρ_c the differences increase with density to a maximum difference of about 25 percent, which is also typical of our comparisons for other fluids in this reduced density range.

Comparisons of measured saturated liquid isobutane viscosities with the same extended corresponding states model are shown in Figs. III 15, 16, Differences between measured and calculated viscosities, for both saturated and compressed liquid data, are shown. The differences increase with density from about 15 percent at the lowest densities to over 100 percent at the highest densities. At the highest densities the differences are much larger for isobutane than for normal butane, which is somewhat surprising considering that they are isomers.

Our measurements under this contract have therefore revealed an isomer effect on viscosity that is much larger than the generalized corresponding-states model is capable of giving. This suggests that the program TRAPP should be used with caution at densities higher than $2\rho_c$ for the isobutane-isopentane mixtures of interest in geothermal power cycles.

2.5 An improved formulation of hydrocarbon viscosities

Hildebrand[52] has shown that the equation,

$$\phi = B(V - V_o)/V_o , \qquad \qquad III(1)$$

where $\phi \equiv \eta^{-1}$ is called the fluidity, B is an empirical parameter, and V_o is the estimated molar volume at $\phi = 0$, can correlate a large amount of viscosity data for liquids at low reduced temperatures. It is known that equation III(1) is a satisfactory approximation only within limited ranges of temperatures and pressures.[53] Nevertheless, it provides a relatively simple way to characterize the viscosity behavior of liquids within these ranges.

Eq. III(1) suggests that a plot of the inverse viscosity versus the volume should be linear. The slope of such a plot should give the parameter B, the

52

extrapolated intercept with the $\eta^{-1} = 0$ axis the parameter V_o. We have made

such fluidity plots for the liquids ethane (Fig. III 17), propane (Fig. III 18),

and normal and isobutane (Fig. III 19). It is obvious that these representations

are simpler and more revealing than the viscosity vs. density plots. In the

cases of ethane and propane, the constant V_o seems to be virtually independent

of temperature, while the saturation boundary is closely approximated by a

straight line.

The dependence of the fluidities of the butanes on molar volume is

shown in Fig. III 19. The fluidities of the compressed liquid increase

linearly with volume at fixed temperature; the fluidities of the saturated

liquid also increase linearly with volume except at the lowest temperatures.

The parameter B is clearly dependent on temperature at low reduced

temperatures. Estimates of V_o, obtained by linear extrapolation of the

isotherms to $\phi = 0$, are also slightly dependent on temperature. The

literature[53] indicates that the compressed liquid isotherms would probably

be non-linear at volumes smaller than we have measured. The behavior shown

in Fig. III 19 suggests that equation III(1), if modified to include

dependences on temperature, can be used for correlating our data. We have

therefore examined our data making use of equation III(1), modified to

include dependences of B and V_o on temperature. For normal butane, the

temperature dependences are described by

$$B(T) = 0.287 \exp (-0.198 \times 10^5/T^2) \qquad \text{III(2)}$$

and

$$V_o(T) = 0.074 + 3.33 \times 10^{-6} T , \qquad \text{III(3)}$$

where T is in kelvins, V_o in L mol^{-1} and B in $\mu Pa^{-1} \cdot s^{-1}/(L \cdot mol^{-1})$. Figure III 20

shows a comparison of our data with equations III(1), (2) and (3). Most of the

differences between measured and calculated viscosities are smaller than 3 percent.

For isobutane the temperature dependences are described by

$$B(T) = 0.420 \exp(-0.354 \times 10^5/T^2) \qquad \text{III(4)}$$

and

$$V_o(T) = 0.0698 \times 10^{-5}T . \qquad \text{III(5)}$$

Figure III 21 shows a comparison of our data for isobutane with equations III(1), (4) and (5). As for normal butane, most of the differences between measured and calculated viscosities are smaller than 3 percent.

We conclude that a simple Hildebrand equation with few adjustable parameters seems to be effective in describing hydrocarbon viscosities in the range from 2 to 3 ρ_c. However, unlike TRAPP, the Hildebrand equation is not global and not predictive.

References

1. Sourcebook on the Production of Electricity from Geothermal Energy, J. Kestin, R. DiPippo, H. E. Khalifa and D. J. Ryley, Editors, U.S. Department of Energy, 1980.

2. M. Waxman and J. S. Gallagher, A Thermodynamic Surface for Isobutane, Proc. 8th Symposium on Thermophysical Properties, J. V. Sengers, Ed., ASME, New York, 1982, Vol. I, p. 88.

3. M. Waxman and J. S. Gallagher, Thermodynamics Properties of Isobutane for Temperature from 250 to 600 K and Pressures from 0.1 to 40 MPa, J. Chem. Eng. Data 28, 224 (1983).

4. W. M. Haynes, Measurements of Densities and Dielectric Constants of Liquid Isobutane from 120 to 300 K at Pressures to 35 MPa, J. Chem. Eng. Data 28, 367 (1983).

5. M. Waxman, H. A. Davis, J. M. H. Levelt Sengers and M. Klein, The Equation of State of Isobutane: An Interim Assessment, NBS Internal Report 79-1715, Sept. 1981.

6. M. Waxman, M. Klein, J. M. H. Levelt Sengers and J. S. Gallagher, Thermodynamic Properties of Isobutane, NBS Internal Report 81-2435, Feb. 1982.

7. J. M. H. Levelt Sengers, B. Kamgar-Parsi and J. V. Sengers, Thermodynamic Properties of Isobutane in the Critical Region, J. Chem. Eng. Data 28, 354, 1983.

8. J. S. Gallagher and J. M. H. Levelt Sengers, Thermodynamic Properties of Isobutane-Isopentane Mixtures, Geothermal Resources Council, Reno, Nevada, Aug. 1984.

9. J. S. Gallagher, J. M. H. Levelt Sengers, G. Morrison and J. V. Sengers, Thermodynamic Properties of Isobutane-Isopentane Mixtures from -40 to +600 °F and up to 1000 psia, NBS Internal Report, 1984, in preparation.

10. J. F. Ely and H. J. M. Hanley, A Computer Program for the Prediction of Viscosity and Thermal Conductivity in Hydrocarbon Mixtures, NBS Technical Note 1039, 1981.

11. J. F. Ely and H. J. M. Hanley, Prediction of Transport Properties I. Viscosity of Fluids and Mixtures, Ind. Eng. Chem. Fund. 20, 323 (1981).

12. W. M. Haynes, Viscosity of Gaseous and Liquid Argon, Physica 67, 440 (1973).

13. D. E. Diller, Measurements of the Viscosity of Compressed Gaseous and Liquid Nitrogen, Physica 119A, 92 (1983).

14. D. E. Diller, Measurements of the Viscosity of Compressed Gaseous and Liquid Methane, Physica 109A, 417 (1980).

15. D. E. Diller and J. M. Saber, Measurements of the Viscosity of Compressed Gaseous and Liquid Ethane, Physica 108A, 143 (1981).

16. D. E. Diller, Measurements of the Viscosity of Saturated and Compressed Liquid Propane, J. Chem. Eng. Data 27, 240 (1982).

17. D. E. Diller, Measurements of the Viscosity of Saturated and Compressed Liquid Methane, Ethane and Propane, Proc. 8th Symp. Thermophy. Prop., J. V. Sengers, Ed., ASME, New York, 1982, Vol. I, p. 219.

18. D. E. Diller and L. J. Van Poolen, Measurements of the Viscosities of Saturated and Compressed Liquid Normal Butane and Isobutane, Submitted, Int. J. Thermophysics.

19. D. E. Diller, Measurements of the Viscosity of Compressed Gaseous and Liquid Nitrogen and Methane Mixtures, Int. J. Thermophysics 3, 237 (1982).

20. D. E. Diller, Measurements of the Viscosity of Compressed Gaseous and Liquid Methane and Ethane Mixtures, J. Chem. Eng. Data. In press.

21. D. E. Diller, Shear Viscosity Coefficients of Nitrogen + Methane and Methane + Ethane Mixtures, ASME Winter Annual Meeting, Boston, MA, Nov. 1984, Paper 83-WA/HT-49.

22. American Institute of Physics Handbook, Dwight E. Gray, Ed. McGraw-Hill Book Company, 1972, Table 4f-3, p. 4-138.

23. J. J. M. Beenakker and C. A. Swenson, Total Thermal Contraction of Some Technical Metals to 4.2 °K, Rev. Sci. Instr. $\underline{26}$, 1204 (1955).

24. H. A. Davis, Low-Cost Tubular Sapphire Optical Cells for Study of Phase Separation in Fluid Mixtures, Rev. Sci. Instr. $\underline{54}$, 1412 (1983).

25. G. Morrison and J. M. Kincaid, Critical Point Measurements on Nearly Polydisperse Fluids, AIChE Journal $\underline{30}$, 257 (1984).

26. C. M. Knobler and R. L. Scott, Indirect Determination of Concentrations in Coexisting Phases, J. Chem. Phys. $\underline{73}$, 5390 (1980).

27. J. S. Rowlinson and I. D. Watson, The Prediction of the Thermodynamics Properties of Fluids and Fluid Mixtures-I. The Principle of Corresponding States and its Extensions, Chem. Eng. Sci. $\underline{24}$, 1565 (1969).

28. J. W. Leach, P. S. Chappelear and T. W. Leland, Use of Molecular Shape Factors in Vapor-Liquid Equilibrium Calculations with the Corresponding States Principle, AIChE Journal $\underline{14}$, 568 (1968).

29. T. W. Leland, Jr. and P. Chappelear, The Corresponding States Principle Ind. & Eng. Chemistry $\underline{60}$, 15 (1968).

30. S. Young, The Thermal Properties of Isopentane, Proc. Phys. Soc. London $\underline{13}$, 602 (1895).

31. P. W. Scott, The Chemical Thermodynamic Properties of Hydrocarbons and Related Substances-Properties of the Alkane Hydrocarbons, C_1 through C_{10} in the Ideal Gas State from 0 to 1500 K, Bulletin 666, U.S. Dept. of the Interior, Bur. Mines, 1974.

32. A Levelt Sengers, R. Hocken and J. V. Sengers, Critical-Point Universality and Fluids, Physics Today $\underline{30}$ (12), 42, 1977.

33. J. M. H. Levelt Sengers and J. V. Sengers, How Close is "Close to the Critical Point"? Ch. 14 in Perspectives in Statistical Physics, H. J. Raveché, Ed., North Holland Publ. Co., 1981.

34. L. P. Kadanoff, Scaling Laws for Ising Models Near T_c, Physics $\underline{2}$, 263 (1966).

35. K. G. Wilson and J. Kogut, The Renormalization Group and the ε-Expansion, Phys. Report $\underline{12C}$, 75 (1974).

36. F. J. Wegner, Corrections to Scaling Laws, Phys Rev. $\underline{B5}$, 4529 (1972).

37. J. V. Sengers and J. H. H. Levelt Sengers, A Universal Representation of the Thermodynamics Properties of Fluids in the Critical Region. The Fourth Japan Symposium on Thermophysical Properties 1983. Also Int. J. Thermophys. $\underline{5}$, 195 (1984).

38. R. B. Griffiths and J. C. Wheeler, Critical Points in Multicomponent Systems, Phys. Rev. $\underline{A2}$, 1047 (1970).

39. S. S. Leung and R. B. Griffiths, Thermodynamic Properties near the Liquid-Vapor Critical Line in Mixtures of He^3 and He^4, Phys. Rev. $\underline{A8}$, 2670 (1973).

40. M. R. Moldover and J. S. Gallagher, Phase Equilibria in the Critical Region: An Application of the Rectilinear Diameter and 1/3 Power Laws to Binary Mixtures, in A.C.S. Symposium Series No. 60, Phase Equilibria and Fluid Properties in the Chemical Industry, T. S. Storvick and S. I. Sandler, Editors. A.C.S. 1977. Chapter 30, p. 498.

41. J. C. Rainwater and M. R. Moldover, Thermodynamic Models for Fluid Mixtures Near Critical Conditions, in Chemical Engineering in Supercritical Fluid Conditions, M. E. Paulaitis et al., Editors, Ann Arbor Science Publishers, 1983, p. 199.

42. R. F. Chang and T. Doiron, Leung-Griffiths, Model for the Thermodynamic Properties of Mixtures of CO_2 and C_2H_6 Near the Gas-Liquid Critical Line, Int. J. Thermophysics, $\underline{4}$(4), 337 (1983).

43. J. M. H. Levelt Sengers, From van der Waals' Equation to the Scaling Laws, Physica $\underline{73}$, 73 (1974).

44. J. V. Sengers and J. M. H. Levelt Sengers, Critical Phenomena in Classical Fluids, in Progress in Liquid Physics, C. A. Croxton, Editors, Wiley, Chichester, U.K., 1978, p. 103.

45. J. C. Le Guillou and J. Zinn-Justin, Critical Exponents from Field Theory, Phys Rev. B21, 3976 (1980).

46. D. Z. Albert, Behavior of the Borel Resummations for the Critical Exponents of the n-Vector Model, Phys. Rev. B25, 4810 (1982).

47. M. Ley-Koo and J. V. Sengers, On Corrections to Scaling in the Thermodynamic Properties of Fluids Near the Critical Point, Proc. 8th Symp. Thermophys. Properties, J. V. Sengers, Editor, ASME, New York, 1982.

48. J. A. Beattie, D. G. Edwards and S. Marple, Jr., The Vapor Pressure, Orthobaric Liquid Density, and Critical Constants of Isobutane, J. Chem. Phys. 17, 576 (1949).

49. J. A. Beattie, S. Marple, Jr. and D. G. Edwards, The Compressibility of, and an Equation of State for Gaseous Isobutane, J. Chem. Phys. 18, 127 (1950).

50. B. Kamgar-Parsi, J. M. H. Levelt Sengers and J. V. Sengers, Thermodynamic Properties of D_2O in the Critical Region, J. Phys. Chem. Ref. Data 12, 513 (1983).

51. H. J. M. Hanley, W. M. Haynes and R. D. McCarty, The Viscosity and Thermal Conductivity Coefficients for Dense Gaseous and Liquid Methane, J. Phys. Chem. Ref. Data 6, 597 (1977).

52. J. H. Hildebrand, Viscosity and Diffusivity, J. Wiley and Sons (1977).

53. J. H. Dymond, K. J. Young and J. D. Isdale, Transport Properties of Nonelectrolyte Liquid Mixtures, Int. J. Thermophysics 1, 345 (1980).

Appendix A

List of publications resulting from this contract.

1. M. Waxman and J. S. Gallagher, A Thermodynamic Surface for Isobutane, Proc. 8th Symposium on Thermophysical Properties, J. V. Sengers, Ed., ASME, New York, 1982, Vol. I, p. 88.

2. M. Waxman and J. S. Gallagher, Thermodynamics Properties of Isobutane for Temperature from 250 to 600 K and Pressures from 0.1 to 40 MPa, J. Chem. Eng. Data 28, 224 (1983).

3. M. Waxman, H. A. Davis. J. M. H. Levelt Sengers and M. Klein, The Equation of State of Isobutane: An Interim Assessment, NBS Interal Report 79-1715, Sept. 1981.

4. M. Waxman, M. Klein, J. M. H. Levelt Sengers and J. S. Gallagher, Thermodynamic Properties of Isobutane, NBS Internal Report 81-2435, Feb. 1982.

5. J. M. H. Levelt Sengers, B. Kamgar-Parsi and J. V. Sengers, Thermodynamic Properties of Isobutane in the Critical Region, J. Chem. Eng. Data 28, 354, 1983.

6. D. E. Diller, Measurements of the Viscosity of Compressed Gaseous and Liquid Nitrogen, Physica 119A, 92 (1983).

7. D. E. Diller, Measurements of the Viscosity of Compressed Gaseous and Liquid Methane, Physica 109A, 417 (1980).

8. D. E. Diller and J. M. Saber, Measurements of the Viscosity of Compressed Gaseous and Liquid Ethane, Physica 108A, 143 (1981).

9. D. E. Diller, Measurements of the Viscosity of Saturated and Compressed Liquid Propane, J. Chem. Eng. Data 27, 240 (1982).

10. D. E. Diller, Measurements of the Viscosity of Saturated and Compressed Liquid Methane, Ethane and Propane, Proc. 8th Symp. Thermophy. Prop., J. V. Sengers, Ed., ASMF, New York, 1982, Vol. I, p. 219.

11. D. E. Diller and L. J. Van Poolen, Measurements of the Viscosities of Saturated and Compressed Liquid Normal Butane and Isobutane, Submitted, Int. J. Thermophysics.

12. D. E. Diller, Measurements of the Viscosity of Compressed Gaseous and Liquid Nitrogen and Methane Mixtures, Int. J. Thermophysics **3**, 237 (1982).

13. D. E. Diller, Measurements of the Viscosity of Compressed Gaseous and Liquid Methane and Ethane Mixtures, J. Chem. Eng. Data. In press.

14. D. E. Diller, Shear Viscosity Coefficients of Nitrogen + Methane and Methane + Ethane Mixtures, ASME Winter Annual Meeting, Boston, MA, Nov. 1984, Paper 83-WA/HT-49.

15. J. V. Sengers and J. M. H. Levelt Sengers, A Universal Representation of the Thermodynamic Properties of Fluids in the Critical Region. The Fourth Japan Symposium on Thermophysical Properties (1983).

Appendix B

Scaled equations for one-component fluids

B.1 Reduced thermodynamic quantities

$$\hat{T} = -\frac{T_c}{T} \quad , \quad \hat{\rho} = \frac{\rho}{\rho_c} \quad , \quad \hat{P} = \frac{P}{T} \cdot \frac{T_c}{P_c} \quad ,$$

$$\hat{\mu} = \frac{\mu}{T} \cdot \frac{\rho_c T_c}{P_c} \quad , \quad \hat{U} = \frac{U}{V} \cdot \frac{1}{P_c} \quad , \quad \hat{A} = \frac{A}{VT} \cdot \frac{T_c}{P_c} \quad ,$$

$$\hat{S} = \frac{S}{V} \cdot \frac{T_c}{P_c} \quad , \quad \hat{H} = \frac{H}{VT} \cdot \frac{T_c}{P_c} \quad , \quad \hat{\chi}_T = \left(\frac{\partial\hat{\rho}}{\partial\hat{\mu}}\right)_{\hat{T}} \quad ,$$

$$\hat{C}_v = \frac{C_v}{V} \cdot \frac{T_c}{P_c} \quad , \quad \hat{C}_p = \frac{C_p}{V} \cdot \frac{T_c}{P_c} \quad .$$

(B.1)

B.2 Thermodynamic relations

$$d\hat{P} = \hat{U}d\hat{T} + \hat{\rho}d\hat{\mu}$$

$$d\hat{A} = -\hat{U}d\hat{T} + \hat{\mu}d\hat{\rho}$$

$$d\hat{H} = -\hat{T}d\hat{U} + \hat{\rho}d\hat{\mu}$$

$$d\hat{S} = -\hat{T}d\hat{U} - \hat{\mu}d\hat{\rho}$$

(B.2)

with

$$\hat{A} = \widetilde{\rho\mu} - \hat{P}$$

$$\hat{H} = \hat{P} - \hat{T}\hat{U}$$

$$\hat{S} = \hat{H} - \widehat{\rho\mu} = -\hat{T}\hat{U} - \hat{A}$$

(B.3)

B.3 Fundamental equations

$$\Delta \hat{T} = \hat{T} + 1 \tag{B.4a}$$

$$\Delta \hat{\mu} = \hat{\mu} - \hat{\mu}_0(\Delta \hat{T}) \tag{B.4b}$$

$$\hat{P} = \hat{P}_0(\Delta \hat{T}) + \Delta \hat{\mu} + \Delta \hat{P} \tag{B.4c}$$

with

$$\hat{\mu}_0(\Delta \tilde{T}) = \hat{\mu}_c + \sum_{i=1}^{3} \hat{\mu}_i \Delta \hat{T}^i \tag{B.5a}$$

$$\hat{P}_0(\Delta \hat{T}) = 1 + \sum_{i=1}^{3} \hat{P}_i \Delta \hat{T}^i \tag{B.5b}$$

E2

B.4 Derived thermodynamic quantities

$$\hat{\rho} = 1 + \left(\frac{\partial \Delta \hat{P}}{\partial \Delta \hat{\mu}}\right)_{\Delta \hat{T}} \tag{B.6}$$

$$\hat{U} = \frac{d\hat{P}_0(\Delta \hat{T})}{d\hat{T}} - \hat{\rho}\,\frac{d\hat{\mu}_0(\Delta \hat{T})}{d\hat{T}} + \left(\frac{\partial \Delta \hat{P}}{\partial \Delta \hat{T}}\right)_{\Delta \hat{\mu}} \tag{B.7}$$

$$\hat{\chi}_T = \left(\frac{\partial^2 \Delta \hat{P}}{\partial \Delta \hat{\mu}^2}\right)_{\Delta \hat{T}} \tag{B.8}$$

$$\left(\frac{\partial \hat{P}}{\partial \hat{T}}\right)_{\hat{\rho}} = \frac{d\hat{P}_0(\Delta \hat{T})}{d\hat{T}} + \left(\frac{\partial \Delta \hat{P}}{\partial \Delta \hat{T}}\right)_{\Delta \hat{\mu}} - \frac{\hat{\rho}}{\hat{\chi}_T}\,\frac{\partial^2 \Delta \hat{P}}{\partial \Delta \hat{\mu} \partial \Delta \hat{T}} \tag{B.9}$$

$$\hat{C}_v = \hat{T}^2\left[\frac{d^2\hat{P}_0(\Delta \hat{T})}{d\hat{T}^2} - \hat{\rho}\,\frac{d^2\hat{\mu}_0(\Delta \hat{T})}{d\hat{T}^2} + \left(\frac{\partial^2 \Delta \hat{P}}{\partial \Delta \hat{T}^2}\right)_{\Delta \hat{\mu}} - \frac{1}{\hat{\chi}_T}\left(\frac{\partial^2 \Delta \hat{P}}{\partial \Delta \hat{\mu} \partial \Delta \hat{T}}\right)^2\right] \tag{B.10}$$

$$\hat{C}_p = \hat{C}_v + \frac{\hat{\chi}_T}{\hat{\rho}^2}\left[\hat{P} - \hat{T}\left(\frac{\partial \hat{P}}{\partial \hat{T}}\right)_{\hat{\rho}}\right]^2 \tag{B.11}$$

B.5 Parametric equations

$$\Delta\hat{T} = r(1-b^2\theta^2) \tag{B.12}$$

$$\Delta\hat{\mu} = r^{\beta\delta}a\theta(1-\theta^2) \tag{B.13}$$

$$\Delta\hat{P} = r^{\beta(\delta+1)}ak(p_0 + p_2\theta^2 + p_4\theta^4) \tag{B.14}$$

$$\left(\frac{\partial\Delta\hat{P}}{\partial\Delta\hat{\mu}}\right)_{\Delta\hat{T}} = r^\beta k\theta \tag{B.15}$$

$$\left(\frac{\partial\Delta\hat{P}}{\partial\Delta\hat{T}}\right)_{\Delta\hat{\mu}} = r^{1-\alpha}ak(s_0 + s_2\theta^2) \tag{B.16}$$

$$\left(\frac{\partial^2\Delta\hat{P}}{\partial\Delta\hat{\mu}^2}\right)_{\Delta\hat{T}} = r^{-\gamma}\frac{k}{a}\ \frac{1 - b^2(1-2\beta)\theta^2}{1 + q_2\theta^2 + q_4\theta^4} \tag{B.17}$$

$$\frac{\partial^2\Delta\hat{P}}{\partial\Delta\hat{\mu}\Delta\hat{T}} = r^{\beta-1}k\beta\theta\ \frac{1 - 3\theta^2 - \delta(1-\theta^2)}{1 + q_2\theta^2 + q_4\theta^4} \tag{B.18}$$

$$\left(\frac{\partial^2\Delta\hat{P}}{\partial\Delta\hat{T}^2}\right)_{\Delta\hat{\mu}} = r^{-\alpha}ak\ \frac{(1-\alpha)(1-3b^2)(s_0 + s_2b^2) - 2\beta\delta s_2\theta^2(1-b^2)}{1 + q_2\theta^2 + q_4\theta^4} \tag{B.19}$$

with

$$P_0 = \frac{\beta\delta - 3\beta - b^2\alpha\gamma}{2b^4(2-\alpha)(1-\alpha)\alpha} \qquad (B.20)$$

$$P_2 = -\frac{\beta\delta - 3\beta - b^2\alpha(2\beta\delta-1)}{2b^2(1-\alpha)\alpha} \qquad (B.21)$$

$$P_4 = \frac{2\beta\delta - 3}{2\alpha} \qquad (B.22)$$

$$s_0 = (2-\alpha)P_0 \qquad (B.23)$$

$$s_2 = -\frac{\beta(\delta-3)}{2b^2\alpha} \qquad (B.24)$$

$$q_2 = b^2(2\beta\delta-1) - 3 \qquad (B.25)$$

$$q_4 = -b^2(2\beta\delta-3) \qquad (B.26)$$

B.6 Thermodynamic properties in one-phase region

$$\hat{T} = -1 + r(1-b^2\theta^2) \tag{B.27}$$

$$\hat{\rho} = 1 + r^\beta k\theta \tag{B.28}$$

$$\hat{\mu} = \hat{\mu}_0(\Delta\hat{T}) + r^{\beta\delta}Q\theta(1-\theta^2) \tag{B.29}$$

$$\hat{P} = \hat{P}_0(\Delta\hat{T}) + r^{\beta\delta}a\theta(1-\theta^2) + r^{\beta(\delta+1)}ak(p_0 + p_2\theta^2 + P_4\theta^4) \tag{B.30}$$

$$\hat{U} = \frac{d\hat{P}_0(\Delta\hat{T})}{d\hat{T}} - \hat{P}\frac{d\hat{\mu}_0(\Delta\hat{T})}{d\hat{T}} + r^{1-\alpha}ak(s_0 + s_2\theta^2) \tag{B.31}$$

$$\hat{x}_T = r^{-\gamma}\frac{k}{a}\frac{1 - b^2(1-2\beta)\theta^2}{1 + q_2\theta^2 + q_4\theta^4} \tag{B.32}$$

$$\left(\frac{\partial\hat{P}}{\partial\hat{T}}\right)_{\hat{\rho}} = \frac{d\hat{P}_0(\Delta\hat{T})}{d\hat{T}} + r^{1-\alpha}ak(s_0 + s_2b^2) + \hat{\rho}r^{\beta\delta-1}a\beta\theta\frac{\delta(1-\theta^2) - (1-3\theta^2)}{1-b^2(1-2\beta)\theta^2} \tag{B.33}$$

$$\hat{C}_v = \hat{T}^2\left[\frac{d^2\hat{P}_0(\Delta\hat{T})}{d\hat{T}^2} - \hat{\rho}\frac{d^2\hat{\mu}_0(\Delta\hat{T})}{d\hat{T}^2} + r^{-\alpha}ak\frac{(1-\alpha)(s_0 + s_2\theta^2) - 3\beta s_2\theta^2}{1 - b^2(1-2\beta)\theta^2}\right] \tag{B.34}$$

$$\hat{C}_p = \hat{C}_v + \frac{\hat{x}_T}{\hat{\rho}^2}\left[P - T\left(\frac{\partial\hat{\rho}}{\partial\hat{T}}\right)_{\hat{\rho}}\right]^2 \tag{B.35}$$

B.7 Thermodynamic properties in two-phase region

$$\hat{T} = -1 + r(1-b^2) \tag{B.36}$$

$$\hat{\mu} = \hat{\mu}_0(\Delta\hat{T}) \tag{B.37}$$

$$\hat{P} = \hat{P}_0(\Delta\hat{T}) + r^{\beta(\delta+1)}ak(p_0 + p_2 + p_4) \tag{B.38}$$

$$\hat{U} = \frac{d\hat{P}_0(\Delta\hat{T})}{d\hat{T}} - \hat{\rho}\frac{d\hat{\mu}_0(\Delta\hat{T})}{d\hat{T}} + \frac{(2-\alpha)r^{1-\alpha}ak(p_0 + p_2 + p_4)}{1-b^2} \tag{B.39}$$

$$\hat{C}_v = \hat{T}^2\left[\frac{d^2\hat{P}_0(\Delta\hat{T})}{d\hat{T}^2} - \hat{\rho}\frac{d^2\hat{\mu}_0(\Delta\hat{T})}{d\hat{T}^2} + \frac{(2-\alpha)(1-\alpha)r^{-\alpha}ak(p_0 + p_2 + p_4)}{(1-b^2)^2}\right] \tag{B.40}$$

Appendix C

Scaled equations for fluid mixtures

C.1 Reduced thermodynamic quantities

$$T = -\frac{T_c^{(4)}}{T} \quad , \quad \hat{\rho} = \frac{\rho}{P_c^{(4)}} \quad , \quad \hat{P} = \frac{P}{T} \cdot \frac{T_c^{(4)}}{P_c^{(4)}}$$

$$\hat{\rho}_4 = \frac{\rho_4}{\rho_c^{(4)}} \quad , \quad \rho_5 = \frac{\rho_5}{\rho_c^{(4)}} \tag{C.1}$$

$$\hat{\mu}_4 = \frac{\mu_4}{T} \cdot \frac{\rho_c^{(4)} T_c^{(4)}}{P_c^{(4)}} \quad , \quad \hat{\mu}_5 = \frac{\mu_5}{T} \cdot \frac{\rho_c^{(4)} T_c^{(4)}}{P_c^{(5)}}$$

$$\hat{U} = \frac{U}{V P_c^{(4)}}$$

$$d\hat{P} = \hat{\rho}_4 d\hat{\mu}_4 + \hat{\rho}_5 d\hat{\mu}_5 + \hat{U} d\hat{T} \tag{C.2}$$

C1

C.2 Fundamental equations

$$\zeta = \frac{e^{\hat{\mu}_5}}{e^{\hat{\mu}_4} + e^{\hat{\mu}_5}} \tag{C.3}$$

$$\tau = \hat{T} - \hat{T}_c(\zeta) \tag{C.4}$$

$$h = \ln(e^{\hat{\mu}_4} + e^{\hat{\mu}_5}) - H(\zeta,\tau) \tag{C.5}$$

$$\hat{P} = \hat{P}_0(\zeta,\tau) + \tilde{\rho}_c(\zeta)h + q(\zeta)\Delta\hat{P}(\ell(\zeta)\tau,h) \tag{C.6}$$

with

$$H(\zeta,\tau) = \sum_{i=0}^{3} H_i(\zeta)\tau^i \tag{C.7}$$

$$\tilde{P}_0(\zeta,\tau) = \sum_{i=0}^{3} \hat{P}_i(\zeta)\tau^i \tag{C.8}$$

and

$$\hat{T}_c(\zeta) = \hat{T}_{c0} + \hat{T}_{c1}\zeta \tag{C.9}$$

$$\hat{\rho}_c(\zeta) = \hat{\rho}_{c0} + \hat{\rho}_{c1}\zeta + \hat{\rho}_{c2}\zeta(1-\zeta) \tag{C.10}$$

$$\hat{P}_0(\zeta) = \hat{P}_{00} + \hat{P}_{01}\zeta + \hat{P}_{02}\zeta(1-\zeta) + \hat{P}_{03}\zeta^2(1-\zeta) \tag{C.11}$$

$$\hat{P}_1(\zeta) = \hat{P}_{10} + \hat{P}_{11}\zeta + \hat{P}_{12}\zeta(1-\zeta) \tag{C.12}$$

$$\hat{P}_i(\zeta) = \hat{P}_{i0} + \hat{P}_{i1}\zeta \quad , \quad (i = 2, 3) \tag{C.13}$$

$$H_i(\zeta) = H_{i0} + H_{i1}\zeta \quad , \quad (i = 0, 1, 2, 3) \tag{C.14}$$

$$q(\zeta) = q_0 + q_1\zeta \tag{C.15}$$

$$\ell(\zeta) = \ell_0 + \ell_1\zeta \tag{C.16}$$

C.3 Parametric representation

$$\bar{\tau} = \ell(\zeta)\tau = r(1-b^2\theta^2) \qquad\qquad (C.17)$$

$$h = r^{\beta\delta}a\theta(1-\theta^2) \qquad\qquad (C.18)$$

$$\Delta\hat{P} = r^{\beta(\delta+1)}ak(p_0 + p_2\theta^2 + p_4\theta^4) \qquad\qquad (C.19)$$

C.4 Derived thermodynamic quantities[†]

Densities:
$$\hat{\rho} = \hat{\rho}_4 + \hat{\rho}_5 = \hat{P}_h \qquad (C.20)$$

$$\hat{\rho}_4 = (1-\zeta)\hat{\rho} - \zeta(1-\zeta)Q \qquad (C.21)$$

$$\hat{\rho}_5 = \zeta\hat{\rho} + \zeta(1-\zeta)Q \qquad (C.22)$$

Mole fraction of isopentane:

$$x = \frac{\hat{\rho}_5}{\hat{\rho}} = \zeta + \zeta(1-\zeta)\frac{Q}{\hat{\rho}} \qquad (C.23)$$

[†] Notation

$$g_\zeta = \left(\frac{\partial g}{\partial \zeta}\right)_{\tau,h} \quad , \quad g_\tau = \left(\frac{\partial g}{\partial \tau}\right)_{\zeta,h} \quad , \quad g_h = \left(\frac{\partial g}{\partial h}\right)_{\zeta,\tau}$$

$$g_{\zeta\zeta} = \left(\frac{\partial^2 g}{\partial \zeta^2}\right)_{\tau,h} \quad , \quad g_{\tau\tau} = \left(\frac{\partial^2 g}{\partial \tau^2}\right)_{\zeta,h} \quad , \quad g_{hh} = \left(\frac{\partial^2 g}{\partial h^2}\right)_{\zeta,\tau}$$

$$g_{\zeta\tau} = \frac{\partial^2 g}{\partial \zeta \partial \tau} \quad , \quad g_{\zeta h} = \frac{\partial^2 g}{\partial \zeta \partial h} \quad , \quad g_{\tau h} = \frac{\partial^2 g}{\partial \tau \partial h}$$

Specific energy:

$$U = \frac{P_c^{(4)}}{\rho_c^{(4)}} \cdot \frac{\hat{P}_\tau - \hat{\rho} H_\tau}{\hat{\rho}} \qquad (C.24)$$

Specific enthalpy:

$$H = U - \frac{P}{\rho} \qquad (C.25)$$

Isochoric thermal pressure coefficient:

$$\left(\frac{\partial P}{\partial T}\right)_{\rho x} = \frac{P_c^{(4)}}{T_c^{(4)}} \left(\hat{P} + \hat{T} \frac{D}{F}\right) \qquad (C.26)$$

Compressibility:

$$K_{Tx} = \frac{1}{\rho} \left(\frac{\partial P}{\partial P}\right)_{Tx} = -\frac{1}{P_c^{(4)}} \frac{\hat{T}}{\hat{\rho}} \frac{F}{0} \qquad (C.27)$$

Response function:

$$\left(\frac{\partial x}{\partial \Delta}\right)_{P,T} = \left(\frac{\partial x}{\partial(\mu_5 - \mu_4)}\right)_{P,T} = -\frac{1}{P_c^{(4)}} \frac{\hat{T}}{\hat{\rho}} \zeta(1-\zeta)G \qquad (C.28)$$

Specific heat at constant volume:

$$C_{vx} = \frac{-P_c^{(4)}}{\rho_c^{(4)}T_c^{(4)}} \frac{\hat{T}^2}{\hat{\rho}} \frac{E}{F} \qquad (C.29)$$

Specific heat at constant pressure:

$$C_{px} = C_{vx} + \frac{T}{\rho} K_{Tx} \left(\frac{\partial P}{\partial T}\right)_{\rho x}^2 \qquad (C.30)$$

C7

Auxiliary functions:

$$Q = \hat{P}_\zeta - \hat{P}_\tau \hat{T}_{c\zeta} - \hat{\rho}(H_\zeta - H_\tau \hat{T}_{c\zeta}) \tag{C.31}$$

$$D = \times_h(\hat{P}_\tau \hat{P}_{\zeta h} - \hat{P}_\zeta \hat{P}_{\tau h}) - \times_\tau(\hat{P}_h \hat{P}_{\zeta h} - \hat{P}_\zeta \hat{P}_{hh}) + \times_\zeta(\hat{P}_h \hat{P}_{\tau h} - \hat{P}_\tau \hat{P}_{hh}) \tag{C.32}$$

$$E = \times_h(\hat{P}_{\zeta h} \hat{P}_{\tau\tau} - \hat{P}_{\zeta\tau}\hat{P}_{\tau h}) - \times_\tau(\hat{P}_{\zeta h}\hat{P}_{\tau h} - \hat{P}_{\zeta\tau}\hat{P}_{hh}) + \times_\zeta(\hat{P}_{\tau h}^2 - \hat{P}_{\tau\tau}\hat{P}_{hh})$$

$$-\hat{\rho}\left[\times_h(H_{\tau\tau}P_{\zeta h} - H_{\zeta\tau}P_{\tau h}) + \times_\tau H_{\zeta\tau}P_{hh} - \times_\zeta H_{\tau\tau}P_{hh}\right] \tag{C.33}$$

$$F = \left[1 + (1-2\zeta)\frac{Q}{\hat{\rho}}\right]\hat{P}_{hh} + \frac{\zeta(1-\zeta)}{\hat{\rho}}\left\{\hat{\rho}\hat{P}_{hh}\left[-H_{\zeta\zeta} + 2H_{\zeta\tau}\hat{T}_{c\zeta} + H_\tau \hat{T}_{c\zeta\zeta} - H_{\tau\tau}\hat{T}_{c\zeta}^2\right]\right.$$

$$+ \hat{P}_{hh}\left[\hat{P}_{\zeta\zeta} - 2\hat{P}_{\tau\zeta}\hat{T}_{c\zeta} - \hat{P}_\tau \hat{T}_{c\zeta\zeta} + \hat{P}_{\tau\tau}\hat{T}_{c\zeta}^2\right]$$

$$\left. - \left[\hat{P}_{\zeta h} - \hat{P}_{\tau h}\hat{T}_{c\zeta}\right]^2 \right\} \tag{C.34}$$

$$g = \hat{\rho} + (1-2\zeta)Q +$$

$$\zeta(1-\zeta)\left\{-\hat{\rho}(H_{\zeta\zeta} - 2H_{\zeta\tau}\hat{T}_{c\zeta} + H_{\tau\tau}\hat{T}_{c\zeta}^2 - H_\tau \hat{T}_{c\zeta\zeta})\right.$$

$$+ (\hat{P}_{\zeta\zeta} - 2\hat{P}_{\zeta\tau}T_{c\zeta} + \hat{P}_{\tau\tau}\hat{T}_{c\zeta}^2 - \hat{P}_\tau \hat{T}_{c\zeta\zeta})$$

$$- \frac{2}{\hat{\rho}}(\hat{P}_\zeta - \hat{P}_\tau \hat{T}_{c\zeta})(\hat{P}_{\zeta h} - \hat{P}_{\tau h}\hat{T}_{c\zeta})$$

$$\left. + \frac{1}{\hat{\rho}^2}\hat{P}_{hh}(\hat{P}_\zeta - \hat{P}_\tau \hat{T}_{c\zeta})^2 \right\} \tag{C.35}$$

Appendix D

Parameters for isobutane - isopentane mixtures near the critical line

$\hat{T}_{c0}$ = -1 $\hat{T}_{c1}$ = 0.11437

$\hat{\rho}_{c0}$ = 1 $\hat{\rho}_{c1}$ = -0.15842 $\hat{\rho}_{c2}$ = 0.06

$\hat{P}_{00}$ = 1 $\hat{P}_{01}$ = -0.17735 $\hat{P}_{02}$ = 0.16 $\hat{P}_{03}$ = -0.03

$\hat{P}_{10}$ = 5.8840 $\hat{P}_{11}$ = -0.15089 $\hat{P}_{12}$ = 7

$\tilde{P}_{20}$ = -15.789 $\hat{P}_{21}$ = -3.1202

$\hat{P}_{30}$ = 0 $\hat{P}_{31}$ = 23.089

H_{00} = 1 H_{01} = -0.022491

H_{10} = 5.8840 H_{11} = 0.92834

H_{20} = -28.659 H_{21} = -23.22

H_{30} = -25.543 H_{31} = 3.7432

q_0 = 1 q_1 = -0.15401

ℓ_0 = 1 ℓ_1 = 0.11264

Tables of thermodynamic properties

In this Appendix we present tables of thermodynamic properties for isobutane – isopentane mixtures calculated from the scaled fundamental equation. Specifically we list the pressure in MPa, the thermal pressure coefficient $(\partial P/\partial T)_{\rho,x}$ in Mpa/K, the isothermal compressibility $K_T = \rho^{-1}(\partial \rho/\partial P)_{T,x}$ in 1/MPa, the specific heat C_v in kJ/kg K, the specific heat C_p in kJ/kg K and the specific enthalpy H in kJ/kg as a function of the density ρ in kg/m^3 and temperature in K for two compositions, namely x = 0.1 and x = 0.5, where x represents the mole fraction of isobutane.

Table E1.   Pressure in MPa as a function of ρ in kg/m^3 and T in K for x = 0.1

Table E2.   Thermal pressure coefficient $(\partial p/\partial T)_{\rho,x}$ in MPa/K as a function of ρ in kg/m^3 and T in K for x = 0.1

Table E3.   Isothermal compressibility $K_T = \rho^{-1}(\partial\rho/\partial P)_{T,x}$ in 1/Mpa as a function of ρ in kg/m^3 and T in K for x = 0.1

Table E4.   Specific heat $C_{v,x}$ in kJ/kg K as a function of ρ in kg/m^3 and T in K for x = 0.1

Table E5.   Specific heat $C^{p,x}$ in kJ/kg K as a function of ρ in kg/m^3 and T in K for x = 0.1

Table E6.   Specific enthalpy H in kJ/kg as a function of ρ in kg/m^3 and T in K for x = 0.1

Table E1

Pressure

CENSITY:	140.0	170.0	180.0	190.0	200.0	210.0	220.0	230.0	240.0	250.0	260.0	270.0	280.0	290.0	300.0
TEPI															
427.00	4.177	4.251	4.317	4.375	4.428	4.479	4.528	4.577	4.628	4.683	4.745	4.815	4.899	4.995	5.123
426.00	4.129	4.201	4.264	4.319	4.370	4.418	4.464	4.510	4.558	4.609	4.667	4.733	4.812	4.907	5.025
425.00	4.082	4.151	4.211	4.264	4.312	4.357	4.400	4.443	4.488	4.536	4.590	4.652	4.726	4.816	4.928
424.00	4.035	4.101	4.158	4.208	4.254	4.296	4.336	4.376	4.418	4.462	4.512	4.570	4.640	4.725	4.831
423.00	3.987	4.051	4.105	4.153	4.195	4.235	4.272	4.309	4.348	4.389	4.435	4.489	4.554	4.634	4.734
422.00	3.940	4.001	4.052	4.097	4.137	4.174	4.209	4.243	4.278	4.316	4.359	4.409	4.469	4.544	4.638
421.00	3.892	3.950	4.000	4.042	4.079	4.113	4.145	4.177	4.209	4.244	4.283	4.328	4.384	4.454	4.543
420.00	3.844	3.900	3.947	3.986	4.021	4.053	4.082	4.111	4.140	4.171	4.207	4.249	4.300	4.364	4.448
419.00	3.796	3.850	3.894	3.931	3.963	3.992	4.019	4.045	4.071	4.107	4.131	4.169	4.216	4.275	4.353
418.00	3.749	3.799	3.841	3.875	3.905	3.932	3.956	3.979	4.003	4.029	4.056	4.090	4.132	4.187	4.259
417.00	3.701	3.749	3.788	3.820	3.847	3.871	3.893	3.914	3.935	3.957	3.982	4.012	4.050	4.095	4.165
416.00	3.654	3.698	3.734	3.764	3.789	3.811	3.831	3.849	3.867	3.886	3.908	3.934	3.967	4.012	4.072
415.00	3.604	3.647	3.681	3.708	3.731	3.751	3.768	3.784	3.800	3.816	3.835	3.857	3.886	3.925	3.980
414.00	3.555	3.596	3.627	3.653	3.673	3.691	3.706	3.720	3.734	3.747	3.762	3.781	3.805	3.835	3.888
413.00									3.668	3.679	3.691	3.705	3.725	3.755	3.798
412.00												3.632	3.647	3.671	3.708
411.00														3.588	3.619
410.00														3.995	3.531

Table E2

DP/DT

DENSITY:	150.0	170.0	180.0	190.0	200.0	210.0	220.0	230.0	240.0	250.0	260.0	270.0	280.0	290.0	300.0
TEMP															
427.10	.047	.050	.053	.056	.058	.061	.064	.067	.071	.074	.078	.082	.087	.092	.098
426.00	.047	.050	.053	.056	.058	.061	.064	.067	.070	.074	.078	.082	.087	.092	.097
425.00	.047	.050	.053	.056	.058	.061	.064	.067	.070	.074	.077	.082	.086	.091	.097
424.00	.047	.050	.053	.055	.058	.061	.064	.067	.070	.073	.077	.081	.086	.091	.097
423.00	.048	.050	.053	.055	.058	.061	.064	.067	.070	.073	.077	.081	.085	.091	.096
422.00	.048	.050	.053	.055	.058	.061	.063	.066	.069	.073	.076	.080	.085	.090	.096
421.00	.048	.050	.053	.055	.058	.061	.063	.066	.069	.073	.076	.080	.085	.090	.095
420.00	.048	.050	.053	.055	.058	.061	.063	.066	.069	.072	.076	.080	.084	.089	.095
419.00	.048	.050	.053	.056	.058	.060	.063	.066	.069	.072	.075	.079	.084	.089	.094
418.00	.048	.051	.053	.056	.058	.060	.063	.065	.068	.071	.075	.079	.083	.088	.094
417.00	.048	.051	.053	.056	.058	.060	.063	.065	.068	.071	.074	.078	.083	.088	.093
416.00	.048	.051	.053	.056	.058	.060	.062	.065	.067	.070	.074	.077	.082	.087	.093
415.00	.048	.051	.053	.056	.058	.060	.062	.064	.067	.070	.073	.077	.081	.086	.092
414.00	.049	.051	.054	.056	.058	.060	.062	.064	.066	.069	.072	.076	.080	.085	.091
413.00									.064	.067	.071	.075	.079	.084	.090
412.00												.073	.078	.083	.089
411.00														.082	.088
410.00															.087

Table E3

Comp KT

DENSITY:	160.0	170.0	180.0	190.0	200.0	210.0	220.0	230.0	240.0	250.0	260.0	270.0	280.0	29C.C	300.0
TEMP															
427.00	.777	.847	.905	.947	.967	.963	.930	.871	.789	.691	.587	.486	.392	.311	.243
426.00	.805	.882	.947	.996	1.023	1.022	.991	.930	.843	.738	.626	.516	.414	.327	.255
425.00	.834	.919	.993	1.050	1.086	1.089	1.059	.996	.904	.791	.669	.549	.439	.343	.267
424.00	.866	.959	1.043	1.110	1.152	1.163	1.137	1.072	.974	.852	.719	.587	.467	.363	.281
423.00	.900	1.003	1.097	1.176	1.229	1.247	1.224	1.159	1.054	.921	.775	.631	.499	.387	.296
422.00	.936	1.050	1.158	1.249	1.314	1.343	1.325	1.259	1.147	1.002	.841	.681	.535	.413	.312
421.00	.975	1.102	1.224	1.331	1.411	1.452	1.441	1.375	1.256	1.097	.918	.739	.577	.440	.331
420.00	1.017	1.159	1.297	1.423	1.521	1.577	1.576	1.512	1.385	1.210	1.009	.807	.625	.473	.352
419.00	1.063	1.221	1.379	1.527	1.647	1.722	1.735	1.675	1.540	1.346	1.119	.889	.682	.510	.376
418.00	1.113	1.290	1.471	1.646	1.791	1.891	1.923	1.871	1.729	1.513	1.253	.988	.750	.554	.404
417.00	1.168	1.366	1.574	1.778	1.956	2.090	2.148	2.109	1.964	1.722	1.422	1.111	.832	.606	.436
416.00	1.227	1.451	1.691	1.932	2.152	2.324	2.418	2.404	2.260	1.997	1.639	1.268	.935	.670	.474
415.00	1.294	1.547	1.825	2.109	2.376	2.598	2.743	2.771	2.644	2.349	1.930	1.475	1.067	.748	.518
414.00	1.369	1.658	1.980	2.312	2.650	2.912	3.128	3.230	3.153	2.849	2.343	1.763	1.244	.848	.573
413.00									3.886	3.617	2.988	2.200	1.495	.981	.642
412.00												3.009	1.895	1.169	.731
411.00														1.467	.853
410.00														.999	1.035

E5

Table E4

Spec Heat CV

DENSITY:	160.0	170.0	180.0	190.0	200.0	210.0	220.0	230.0	240.0	250.0	260.0	270.0	280.0	290.0	300.0
TEMP															
427.00	2.475	2.478	2.480	2.479	2.475	2.469	2.460	2.448	2.435	2.419	2.403	2.386	2.368	2.350	2.333
426.00	2.476	2.482	2.485	2.485	2.481	2.475	2.465	2.453	2.439	2.423	2.406	2.388	2.370	2.352	2.334
425.00	2.481	2.488	2.491	2.491	2.486	2.481	2.472	2.459	2.445	2.429	2.410	2.391	2.372	2.353	2.334
424.00	2.486	2.494	2.498	2.498	2.495	2.489	2.479	2.466	2.451	2.433	2.414	2.395	2.374	2.354	2.335
423.00	2.472	2.501	2.506	2.507	2.504	2.498	2.487	2.474	2.458	2.440	2.420	2.399	2.377	2.356	2.336
422.00	2.499	2.509	2.515	2.517	2.514	2.508	2.497	2.483	2.466	2.447	2.425	2.403	2.381	2.359	2.337
421.00	2.507	2.518	2.525	2.528	2.526	2.520	2.509	2.494	2.476	2.455	2.432	2.409	2.385	2.361	2.339
420.00	2.517	2.529	2.538	2.542	2.541	2.535	2.523	2.508	2.488	2.465	2.441	2.415	2.389	2.364	2.341
419.00	2.528	2.543	2.553	2.559	2.559	2.553	2.541	2.524	2.502	2.477	2.450	2.423	2.395	2.368	2.343
418.00	2.542	2.559	2.572	2.580	2.581	2.575	2.563	2.544	2.520	2.492	2.462	2.432	2.402	2.373	2.345
417.00	2.556	2.580	2.596	2.607	2.610	2.605	2.591	2.570	2.543	2.511	2.477	2.443	2.410	2.378	2.349
416.00	2.574	2.606	2.629	2.644	2.651	2.646	2.631	2.606	2.574	2.536	2.497	2.457	2.420	2.385	2.353
415.00	2.607	2.643	2.675	2.701	2.714	2.711	2.693	2.661	2.619	2.572	2.523	2.476	2.432	2.393	2.358
414.00	2.646	2.700	2.758	2.813	2.846	2.849	2.818	2.764	2.698	2.629	2.563	2.502	2.449	2.403	2.364
413.00									2.967	2.761	2.634	2.543	2.473	2.417	2.372
412.00												2.628	2.510	2.436	2.382
411.00														2.466	2.396
410.00															2.416

E6

Table E5

Spec Heat CP

TEMP / DENSITY:	160.0	170.0	180.0	190.0	200.0	210.0	220.0	230.0	240.0	250.0	260.0	270.0	280.0	290.0	300.0
427.00	7.115	7.808	8.463	9.041	9.500	9.794	9.884	9.753	9.412	8.896	8.241	7.569	6.878	6.229	5.647
426.00	7.250	8.024	8.732	9.368	9.879	10.213	10.327	10.198	9.836	9.279	8.589	7.838	7.090	6.391	5.768
425.00	7.460	9.257	9.027	9.727	10.298	10.681	10.824	10.699	10.313	9.709	8.958	8.139	7.325	6.568	5.899
424.00	7.653	8.510	9.350	10.123	10.765	11.205	11.383	11.265	10.854	10.197	9.374	8.476	7.586	6.765	6.043
423.00	7.862	9.787	9.706	10.564	11.287	11.796	12.018	11.910	11.473	10.755	9.848	8.858	7.880	6.982	6.200
422.00	8.099	9.090	10.099	11.055	11.874	12.465	12.743	12.651	12.185	11.398	10.393	9.294	8.212	7.226	6.374
421.00	8.335	9.422	10.535	11.605	12.538	13.228	13.576	13.509	13.014	12.147	11.025	9.796	8.590	7.500	6.568
420.00	8.604	9.791	11.023	12.225	13.293	14.105	14.541	14.511	13.988	13.029	11.768	10.380	9.026	7.811	6.784
419.00	8.900	10.200	11.571	12.930	14.159	15.119	15.669	15.694	15.147	14.081	12.652	11.071	9.533	8.167	7.027
418.00	9.228	10.659	12.192	13.735	15.157	16.300	16.997	17.104	16.543	15.357	13.722	11.898	10.131	8.580	7.303
417.00	9.594	11.179	12.903	14.665	16.317	17.665	18.574	18.804	18.251	16.931	15.043	12.910	10.850	9.064	7.621
416.00	10.007	11.775	13.728	15.750	17.676	19.316	20.456	20.871	20.373	18.919	16.717	14.179	11.732	9.643	7.989
415.00	10.433	12.475	14.707	17.038	19.281	21.237	22.696	23.395	23.050	21.497	18.907	15.821	12.844	10.345	8.424
414.00	11.049	13.335	15.935	18.643	21.210	23.470	25.292	26.429	26.460	24.951	21.912	18.047	14.300	11.231	8.947
413.00									30.700	29.818	26.367	21.299	16.316	12.385	9.590
412.00												26.918	19.398	13.572	10.410
411.00														16.392	11.504
410.00															13.088

E7

Table E6

Enthalpy

DENSITY:	160.0	170.0	180.0	190.0	200.0	210.0	220.0	230.0	240.0	250.0	260.0	270.0	280.0	290.0	300.0
TEMP															
427.00	55.914	50.921	46.177	41.644	37.293	33.096	29.030	25.071	21.196	17.381	13.602	9.832	6.045	2.211	-1.700
426.00	53.735	49.736	43.988	39.455	35.106	30.915	26.859	22.912	19.053	15.256	11.497	7.749	3.985	.176	-3.708
425.00	51.552	46.546	41.793	37.259	32.913	28.729	24.681	20.747	16.903	13.125	9.387	5.662	1.923	-1.806	-5.718
424.00	49.365	44.350	39.592	35.057	30.713	26.534	22.496	18.575	14.747	10.988	7.271	3.570	-.143	-3.900	-7.729
423.00	47.173	42.148	37.384	32.846	28.504	24.331	20.302	16.395	12.584	8.844	5.150	1.474	-2.213	-5.942	-9.743
422.00	44.975	39.939	35.168	30.627	26.295	22.118	18.099	14.205	10.411	6.697	3.022	-.628	-4.288	-7.988	-11.760
421.00	42.769	37.721	32.942	28.397	24.056	19.893	15.884	12.004	8.229	4.537	.887	-2.737	-6.368	-10.038	-13.779
420.00	40.556	35.493	30.704	26.154	21.812	17.654	13.655	9.791	6.035	2.361	-1.258	-4.853	-8.453	-12.092	-15.801
419.00	38.332	33.254	28.453	23.896	19.553	15.399	11.411	7.562	3.827	.179	-3.413	-6.977	-10.546	-14.151	-17.828
418.00	36.097	31.000	26.185	21.619	17.274	13.124	9.145	5.313	1.601	-2.020	-5.581	-9.112	-12.646	-16.217	-19.858
417.00	33.848	28.729	23.897	19.319	14.966	10.822	6.855	3.041	-.646	-4.237	-7.764	-11.259	-14.756	-18.285	-21.893
416.00	31.590	26.435	21.581	16.987	12.629	8.485	4.529	.737	-2.922	-6.478	-9.966	-13.421	-16.877	-20.365	-23.934
415.00	29.290	24.111	19.227	14.610	10.240	6.095	2.153	-1.613	-5.237	-8.751	-12.194	-15.602	-19.011	-22.454	-25.981
414.00	26.968	21.743	16.813	12.156	7.760	3.612	-.311	-4.040	-7.614	-11.072	-14.457	-17.807	-21.163	-24.561	-28.037
413.00									-10.132	-13.482	-16.776	-20.050	-23.339	-26.678	-30.102
412.00												-22.355	-25.548	-28.815	-32.179
411.00														-30.980	-34.271
410.00															-36.384

E2.   Thermodynamic properties of isobutane - isopentane at x = 0.5

Table E7.   Pressure in MPa as a function of ρ in kg/m^3 and T in K
for x = 0.5

Table E8.   Thermal pressure coefficient $(\partial p / \partial T)_{\rho, x}$ in Mpa/K as a function
of ρ in kg/m^3 and T in K for x = 0.5

Table E9.   Isothermal compressibility $K_T = \rho^{-1} (\partial \rho / \partial P)_{T, x}$ in 1/MPa as a
function of ρ in kg/m^3 and T in K for x = 0.5

Table E10.   Specific heat $C_{v, x}$ in kJ/kg K as a function of ρ in kg/m^3 and
T in K for x = 0.5

Table E11.   Specific heat $C_{p, x}$ in kJ/kg K as a function of ρ in kg/m^3 and
T in K for x = 0.5

Table E12.   Specific enthalpy H in kJ/kg as a function of ρ in kg/m^3 and
T in K for x = 0.5

Table E7

Pressure

DENSITY:	150.0	170.0	190.0	190.0	200.0	210.0	220.0	230.0	240.0	250.0	260.0	270.0	280.0	290.0	300.0
TEMP															
454.00	3.981	4.053	4.120	4.185	4.249	4.312	4.375	4.441	4.509	4.563	4.663	4.753	4.856	4.975	5.115
453.00	3.943	4.013	4.079	4.142	4.203	4.264	4.325	4.389	4.455	4.524	4.603	4.690	4.789	4.904	5.040
452.00	3.906	3.973	4.037	4.098	4.157	4.216	4.276	4.337	4.400	4.469	4.544	4.627	4.722	4.833	4.965
451.00	3.868	3.934	3.995	4.054	4.112	4.169	4.226	4.285	4.346	4.412	4.484	4.564	4.656	4.762	4.890
450.00	3.83_	3.894	3.954	4.011	4.056	4.121	4.176	4.233	4.292	4.355	4.424	4.502	4.590	4.693	4.815
449.00	3.792	3.854	3.912	3.967	4.021	4.073	4.127	4.181	4.238	4.299	4.365	4.439	4.524	4.623	4.741
448.00	3.754	3.814	3.870	3.923	3.975	4.026	4.077	4.130	4.184	4.243	4.306	4.377	4.458	4.554	4.667
447.00	3.716	3.774	3.828	3.879	3.929	3.978	4.028	4.078	4.131	4.186	4.247	4.315	4.393	4.464	4.593
446.00	3.678	3.734	3.786	3.835	3.884	3.931	3.978	4.027	4.077	4.131	4.189	4.254	4.328	4.415	4.520
445.00	3.643	3.693	3.744	3.791	3.838	3.883	3.929	3.975	4.024	4.075	4.130	4.192	4.263	4.347	4.447
444.00	3.601	3.653	3.701	3.747	3.792	3.836	3.880	3.924	3.970	4.019	4.072	4.131	4.199	4.278	4.374
443.00	3.562	3.612	3.659	3.703	3.746	3.789	3.831	3.873	3.917	3.964	4.014	4.070	4.134	4.210	4.301
442.00	3.523	3.571	3.616	3.659	3.700	3.741	3.782	3.822	3.864	3.909	3.956	4.009	4.070	4.143	4.229
441.00	3.484	3.530	3.574	3.615	3.655	3.694	3.733	3.772	3.812	3.854	3.899	3.949	4.007	4.075	4.157
440.00	3.445			3.570	3.609	3.646	3.684	3.721	3.759	3.799	3.842	3.889	3.943	4.008	4.086
439.00							3.635	3.671	3.707	3.745	3.785	3.829	3.880	3.941	4.015
438.00								3.622	3.656	3.691	3.729	3.770	3.818	3.874	3.944
437.00										3.639	3.673	3.712	3.756	3.808	3.873
436.00											3.619	3.654	3.694	3.742	3.804
435.00													3.633	3.678	3.734

Table E8

DP/DT

DENSITY:	160.0	170.0	180.0	190.0	200.0	210.0	220.0	230.0	240.0	250.0	260.0	270.0	280.0	290.0	300.0
TEMP															
454.0	.037	.040	.042	.044	.046	.048	.050	.052	.055	.057	.060	.063	.067	.071	.076
453.0	.036	.040	.042	.044	.046	.048	.050	.052	.054	.057	.060	.063	.067	.071	.075
452.0	.036	.040	.042	.044	.046	.048	.050	.052	.054	.057	.060	.063	.066	.070	.075
451.0	.036	.040	.042	.044	.046	.048	.050	.052	.054	.057	.060	.063	.066	.070	.075
450.0	.038	.040	.042	.044	.046	.048	.050	.052	.054	.057	.059	.062	.066	.070	.074
449.0	.038	.040	.042	.044	.046	.048	.050	.052	.054	.056	.059	.062	.066	.070	.074
448.0	.038	.040	.042	.044	.046	.048	.049	.052	.054	.054	.059	.062	.065	.065	.074
447.0	.038	.040	.042	.044	.046	.048	.049	.051	.054	.054	.059	.062	.065	.065	.074
446.0	.038	.040	.042	.044	.046	.047	.049	.051	.053	.056	.059	.062	.065	.065	.073
445.0	.038	.040	.042	.044	.046	.047	.049	.051	.053	.056	.058	.061	.065	.065	.073
444.0	.039	.041	.042	.044	.046	.047	.049	.051	.053	.055	.058	.061	.064	.068	.073
443.0	.039	.041	.042	.044	.046	.047	.049	.051	.053	.055	.058	.061	.064	.068	.072
442.0	.039	.041	.043	.044	.046	.047	.049	.051	.053	.055	.058	.060	.064	.068	.072
441.0	.039	.041	.043	.044	.046	.047	.049	.051	.053	.055	.057	.060	.064	.067	.072
440.0	.039			.045	.046	.047	.049	.050	.052	.054	.057	.060	.063	.067	.071
439.0							.048	.050	.052	.054	.057	.059	.063	.067	.071
438.0								.048	.051	.053	.056	.059	.062	.066	.071
437.0										.052	.055	.058	.062	.066	.070
436.0											.053	.057	.061	.065	.070
435.0													.060	.065	.069

Table E9

Comp KT

DENSITY:	160.0	170.0	180.0	190.0	200.0	210.0	220.0	230.0	240.0	250.0	260.0	270.0	280.0	290.0	300.0
TEMP															
454..0	.844	.846	.840	.822	.794	.755	.707	.651	.588	.522	.454	.387	.325	.265	.218
453.'0	.865	.872	.866	.849	.820	.761	.732	.674	.610	.541	.471	.402	.336	.277	.225
452..0	.894	.899	.894	.877	.848	.808	.758	.699	.633	.562	.489	.417	.349	.287	.233
451.C0	.921	.928	.923	.907	.876	.837	.786	.725	.657	.584	.508	.433	.362	.297	.241
450.C9	.950	.958	.954	.938	.909	.867	.815	.753	.683	.608	.529	.451	.376	.308	.249
449.10	.913	.990	.987	.971	.941	.899	.846	.783	.711	.631	.551	.469	.391	.320	.258
448.:0	1.012	1.023	1.021	1.005	.976	.933	.879	.815	.741	.660	.575	.490	.408	.332	.268
447.C0	1.040	1.059	1.057	1.042	1.012	.969	.914	.849	.773	.689	.601	.512	.426	.347	.279
446.C0	1.091	1.096	1.096	1.080	1.050	1.007	.951	.884	.807	.721	.629	.535	.445	.363	.290
445.C0	1.119	1.136	1.136	1.121	1.090	1.046	.990	.923	.844	.755	.659	.561	.466	.375	.303
444.10	1.160	1.178	1.179	1.163	1.132	1.088	1.032	.963	.883	.792	.692	.590	.489	.397	.316
443.C0	1.203	1.223	1.225	1.208	1.176	1.132	1.075	1.007	.925	.832	.729	.621	.515	.417	.331
442.C0	1.250	1.272	1.273	1.255	1.222	1.177	1.121	1.053	.971	.874	.769	.655	.543	.438	.346
441.C0	1.300	1.323	1.323	1.303	1.269	1.224	1.169	1.102	1.020	.924	.813	.694	.574	.462	.364
440.C0	1.354			1.352	1.315	1.271	1.218	1.154	1.074	.975	.862	.737	.609	.485	.383
439.C0							1.270	1.210	1.133	1.036	.918	.786	.649	.515	.405
438.C0								1.284	1.201	1.107	.982	.842	.694	.553	.429
437.C0										1.193	1.060	.908	.747	.593	.457
436.'0											1.179	.992	.811	.635	.489
435.C0													.892	.694	.526

Spec Heat CV

DENSITY:	160.0	170.0	180.0	190.0	200.0	210.0	220.0	230.0	240.0	250.0	260.0	270.0	280.0	290.0	300.0
TEMP															
454.00	1.933	1.946	1.954	1.958	1.959	1.956	1.951	1.943	1.934	1.922	1.910	1.897	1.883	1.865	1.854
453.00	1.925	1.939	1.948	1.953	1.954	1.951	1.946	1.939	1.929	1.918	1.906	1.893	1.879	1.865	1.850
452.00	1.916	1.932	1.942	1.947	1.949	1.947	1.942	1.935	1.925	1.914	1.902	1.889	1.875	1.861	1.846
451.00	1.910	1.926	1.937	1.943	1.945	1.943	1.939	1.931	1.922	1.911	1.898	1.885	1.871	1.857	1.843
450.00	1.904	1.920	1.932	1.939	1.941	1.940	1.936	1.928	1.919	1.908	1.895	1.882	1.868	1.854	1.840
449.00	1.896	1.915	1.928	1.936	1.939	1.938	1.934	1.926	1.917	1.905	1.893	1.879	1.865	1.851	1.837
448.00	1.893	1.911	1.925	1.934	1.937	1.937	1.933	1.925	1.916	1.904	1.891	1.877	1.863	1.849	1.834
447.00	1.888	1.908	1.923	1.933	1.937	1.937	1.933	1.925	1.915	1.903	1.890	1.876	1.861	1.847	1.832
446.00	1.884	1.906	1.922	1.933	1.938	1.938	1.934	1.926	1.916	1.903	1.890	1.875	1.860	1.845	1.831
445.00	1.882	1.906	1.924	1.935	1.941	1.942	1.937	1.929	1.918	1.905	1.890	1.875	1.860	1.844	1.829
444.00	1.881	1.907	1.927	1.940	1.947	1.948	1.943	1.934	1.921	1.907	1.892	1.876	1.860	1.844	1.829
443.00	1.881	1.910	1.933	1.948	1.956	1.957	1.951	1.941	1.927	1.911	1.895	1.878	1.861	1.844	1.829
442.00	1.884	1.917	1.943	1.962	1.971	1.971	1.964	1.951	1.936	1.918	1.899	1.881	1.863	1.845	1.829
441.00	1.890	1.928	1.961	1.985	1.996	1.995	1.984	1.968	1.948	1.927	1.906	1.885	1.866	1.847	1.830
440.00	1.900			2.032	2.046	2.038	2.019	1.994	1.967	1.940	1.915	1.891	1.870	1.850	1.832
439.00							2.099	2.042	1.998	1.961	1.928	1.900	1.875	1.854	1.834
438.00								2.233	2.064	1.995	1.948	1.912	1.883	1.858	1.837
437.00									2.080	1.983	1.931	1.894	1.865	1.841
436.00										2.083	1.961	1.909	1.874	1.847
435.00											1.932	1.865	1.854

E13

Table E11

Spec Heat CP

DENSITY:	160.0	170.0	180.0	190.0	200.0	210.0	220.0	230.0	240.0	250.0	260.0	270.0	280.0	290.0	300.0
TEMP															
454.00	5.291	5.479	5.617	5.696	5.715	5.675	5.580	5.436	5.248	5.024	4.775	4.511	4.243	3.963	3.739
453.00	5.390	5.585	5.726	5.806	5.825	5.783	5.685	5.535	5.341	5.110	4.852	4.578	4.300	4.030	3.777
452.00	5.495	5.697	5.842	5.925	5.942	5.898	5.796	5.641	5.441	5.202	4.935	4.650	4.362	4.081	3.818
451.00	5.608	5.817	5.967	6.051	6.067	6.020	5.914	5.754	5.548	5.301	5.024	4.729	4.428	4.136	3.863
450.00	5.729	5.946	6.101	6.185	6.201	6.150	6.040	5.875	5.662	5.407	5.120	4.813	4.500	4.196	3.911
449.00	5.859	6.085	6.244	6.329	6.343	6.289	6.174	6.004	5.784	5.521	5.223	4.904	4.578	4.260	3.963
448.00	5.999	6.234	6.398	6.483	6.494	6.437	6.317	6.141	5.915	5.643	5.335	5.003	4.663	4.331	4.019
447.00	6.151	6.395	6.563	6.649	6.656	6.594	6.469	6.288	6.055	5.775	5.456	5.110	4.755	4.407	4.080
446.00	6.315	6.569	6.741	6.826	6.829	6.761	6.631	6.445	6.205	5.917	5.587	5.227	4.855	4.489	4.147
445.00	6.493	6.758	6.934	7.016	7.013	6.939	6.803	6.611	6.366	6.070	5.728	5.353	4.964	4.579	4.219
444.00	6.687	6.964	7.143	7.220	7.210	7.127	6.985	6.788	6.538	6.235	5.882	5.492	5.083	4.678	4.298
443.00	6.900	7.191	7.371	7.441	7.419	7.326	7.176	6.975	6.721	6.412	6.049	5.642	5.213	4.786	4.384
442.00	7.136	7.441	7.622	7.681	7.643	7.536	7.377	7.172	6.916	6.603	6.230	5.808	5.356	4.904	4.478
441.00	7.401	7.724	7.904	7.945	7.892	7.755	7.585	7.377	7.122	6.808	6.428	5.989	5.514	5.034	4.581
440.00	7.705			8.251	8.144	7.962	7.797	7.588	7.337	7.027	6.643	6.189	5.689	5.175	4.695
439.00							9.006	7.796	7.558	7.259	6.877	6.410	5.884	5.346	4.821
438.00								7.982	7.773	7.501	7.131	6.656	6.102	5.520	4.962
437.00									7.744	7.408	6.932	6.349	5.723	5.119	
436.00										7.712	7.245	6.633	5.956	5.297	
435.00												6.967	6.226	5.501	

E14

Table E12

Enthalpy

DENSITY:	160.0	170.0	180.0	190.0	200.0	210.0	220.0	230.0	240.0	250.0	260.0	270.0	280.0	290.0	300.0
TIME															
454.00	62.011	59.106	54.374	50.798	47.361	44.047	40.838	37.715	34.659	31.647	28.659	25.671	22.660	19.595	16.461
453.00	60.316	56.397	52.654	49.072	45.633	42.321	39.116	36.001	32.954	29.955	26.982	24.011	21.017	17.976	14.860
452.00	58.629	54.694	50.941	47.352	43.910	40.599	37.398	34.290	31.254	28.267	25.308	22.353	19.378	16.357	13.262
451.00	56.951	52.999	49.233	45.637	42.192	38.880	35.634	32.583	29.556	26.587	23.637	20.699	17.742	14.741	11.667
450.00	55.280	51.310	47.531	43.926	40.477	37.168	33.973	30.878	27.861	24.899	21.969	19.048	16.109	13.127	10.075
449.00	53.616	49.627	45.834	42.219	38.765	35.453	32.264	29.176	26.168	23.219	20.303	17.398	14.477	11.515	8.484
448.00	51.958	47.949	44.140	40.515	37.055	33.742	30.556	27.474	24.477	21.539	18.638	15.750	12.848	9.905	6.896
447.00	50.306	46.275	42.450	38.813	35.347	32.032	28.848	25.773	22.785	19.860	16.974	14.103	11.219	8.297	5.308
446.00	48.659	44.604	40.761	37.111	33.638	30.321	27.139	24.071	21.093	18.181	15.310	12.456	9.591	6.488	3.721
445.00	47.016	42.936	39.072	35.409	31.927	28.607	25.428	22.366	19.399	16.500	13.645	10.808	7.962	5.081	2.135
444.00	45.376	41.268	37.382	33.703	30.211	26.888	23.712	20.658	17.701	14.817	11.978	9.159	6.333	3.474	.549
443.00	43.737	39.598	35.689	31.991	28.489	25.163	21.989	18.943	15.998	13.129	10.308	7.508	4.702	1.862	-1.038
442.00	42.098	37.925	33.987	30.269	26.755	23.425	20.255	17.218	14.287	11.435	8.633	5.854	3.069	.252	-2.626
441.00	40.455	36.244	32.273	28.531	25.002	21.669	18.504	15.480	12.565	9.732	6.951	4.194	1.433	-1.362	-4.216
440.00	38.807			26.760	23.214	19.880	16.726	13.719	10.827	8.017	5.261	2.528	-.209	-2.978	-5.809
439.00							14.895	11.923	9.063	6.284	3.558	.854	-1.856	-4.600	-7.404
438.00								10.034	7.252	4.523	1.836	-.833	-3.512	-6.221	-9.004
437.00										2.706	.086	-2.537	-5.178	-7.861	-10.609
436.00											-1.724	-4.267	-6.860	-9.504	-12.219
435.00													-8.562	-11.155	-13.838

Table I 1

Supercritical PVT data for isobutane

T = 423.15 K		T = 448.15K	
P, MPa	ρ, kg/m^3	P, MPa	ρ, kg/m^3
20.750	457.9	10.024	349.6
4.754	257.2	5.770	196.3
10.840	406.9	4.377	110.3
4.600	228.5	3.018	61.97
3.977	128.3	10.024	349.6
6.426	349.3	5.770	196.4
4.452	196.2	4.377	110.3
3.747	110.2	6.757	261.2
5.403	314.1	5.060	146.7
4.352	176.4	3.675	82.39
3.571	99.91	7.480	292.5
15.982	438.4	5.328	164.2
4.690	246.3	3.946	92.24
4.078	138.3		
uncertainty		0.01%	0.1%

Table I 2

Virial coefficients of isobutane

T,K	10^5B. m^3/kg	10^6C. $(m^3/kg)^2$	10^9D. $(m^3/kg)^3$	10^{11}E. $(m^3/kg)^4$	ρ_{max}. kg/m^3
377.594	-647.4 ± 0.7	9.86 ± 0.16			41
394.261	-592.2 ± 0.2	10.66 ± 0.08			81
423.15	-501.5 ± 0.3	8.91 ± 0.07	7.9 ± 0.8	-3.0 ± 0.3	150
448.15	-440.3 ± 0.1	8.62 ± 0.01			100

B, second virial; C, third virial; D, fourth virial, E, fifth virial.
Virial coefficients correspond to the coefficients of a finite density
series representation of the compressibility factor.

Table I 3

Vapor pressure of isobutane

T,K	P,MPa	T,K	P,MPa
298.15	0.3500	333.15	0.8676
303.15	0.4043	343.15	1.0867
308.15	0.4641	353.15	1.3432
313.15	0.5304	363.15	1.6408
318.15	0.6032	373.15	1.9855
323.15	0.6836	383.15	2.3819
328.15	0.7725	393.15	2.8361
333.15	0.8683	398.15	3.0879
Uncertainty		0.002	0.01%

.

Table I 4

Isochoric PρT data near the critical line
65.07/34.93 mol % isobutane/isopentane mixture

T,K	P,MPa	T,K	P,MPa
ρ = 251.9 kg/m^3		ρ = 241.2 kg/m^3	
157.535	3.801	156.582	3.729
157.424	3.795	156.520	3.726
157.362	3.791	156.444	3.721
156.558	3.804	156.468	3.722
157.415	3.796	156.328	3.714
157.918	3.766	156.113	3.701
156.635	3.747	155.708	3.676
156.563	3.742	155.536	3.666
156.474	3.735	ρ = 230.8 kg/m^3	
156.389	3.730		
156.333	3.726	156.503	3.703
156.330	3.726	156.369	3.696
		156.286	3.691
155.811	3.693	155.974	3.675
155.761	3.693	155.865	3.668
155.697	3.690		
155.719	3.692	ρ = 216.7 kg/m^3	
155.628	3.686	156.606	3.700
155.497	3.678	156.533	3.696
155.425	3.673	155.972	3.665
155.245	3.661	156.233	3.681
uncertainty		156.364	3.689
0.02	0.004	156.413	3.691
		156.458	3.693
		156.529	3.698

Table I 5

Critical-line data in isobutane/isopentane mixtures

x, mol % iC_5	T_c	ρ_c	P_c
	K	mol/dm^3	MPa
0	407.84	3.880	3.629
0.2001	419.92	3.781	3.677
0.3493	428.71	3.662	3.650
0.5073	437.35	3.649	3.615
1	460.51	3.265	3.371
uncertainty	0.02	1%	0.004

Table I 6

Vapor pressure of isopentane

T,K	P_{exp}, MPa	P_{calc}, MPa	$P_{exp}-P_{calc}$	$(P_{exp}-P_{calc})/P_{exp}$, %
400.529	1.2477	1.2467	.0010	.08
411.407	1.5208	1.5230	−.0022	−.15
411.390	1.5222	1.5226	−.0004	−.03
425.513	1.9387	1.9373	.0014	.07
437.593	2.3593	2.3570	.0023	.10
447.995	2.7761	2.7770	−.0009	−.03
454.576	3.0728	3.0755	−.0027	−.09
458.582	3.2698	3.2718	−.0020	−.06
459.562	3.3192	3.3218	−.0026	−.08
460.504	3.3698	3.3707	−.0009	−.03
0.02	0.004	uncertainty		

Fitting equation II(25).

Table I 7

Dew-bubble curve data

x mol % iC_5	T, K	ρ, mol/dm^3	P, MPa
0.2001	419.75	3.993	-
0.2001	419.88	3.832	-
0.2001	420.01	3.673	3.676
0.3493	427.99	4.336^4	-
0.3493	428.14	4.161^0	-
0.3493	428.41	3.996^8	3.661
0.3493	428.56	3.826^8	3.658
0.3493	428.71	3.661^9	3.650
0.3493	428.89	3.438^3	3.650
0.5073	436.88	4.005^7	-
0.5073	437.11	3.825^1	3.62^8
0.5073	437.28	3.662^5	3.637^5
0.5073	437.42	3.629^1	3.62
uncertainty			
0.001	0.02	1%	0.004 (x = 0.20 and 0.35) 0.01 (x = 0.50)

Table I 8

VLE data

T	x, mol % iC_s	P, MPa	ρ, mol/dm^3
288.890	0.4968	0.1685	9.3110
	0.5010	0.1653	9.3041
	0.5097	0.1632	9.2790
298.337	0.4968	0.2270	9.1483
	0.5010	0.2238	9.1449
308.327	0.4968	0.3045	8.9542
	0.5010	0.2994	8.9469
318.496	0.4968	0.4029	8.8137
	0.5010	0.3965	8.7712
	0.5097	0.3894	8.8082
328.480	0.4968	0.5145	8.6170
	0.5010	0.5139	8.5955

Table I 9

Parameters of the dimensionless Helmholtz function of isobutane

Primary reference constants

$T* = 407.84K$

$\rho* = 3.8796 \text{ mol/dm}^3$

$P* = 3.6290 \text{ MPa}$

Secondary reference constants

$A** = \dfrac{P*}{\rho*} = 0.93541 \text{ kJ/mol}$

$S** = \dfrac{P*}{\rho*T*} = 2.29356 \text{ J/(mol.K)}$

$a** = \left(\dfrac{P*}{\rho*}\right)^{1/2} = 126.86 \text{ m/s}$

Physical constants

$M = 0.0581243 \text{ kg/mol}$

$R = 8.31441 \text{ J/(mol.K)}$

Table I 9 (Continued)

Coefficients of dimensionless Helmholtz function

XO = 7.9688113

A00 =	27.849029	A05 =	2.5515510
A0L =	58.138236	A06 =	−53.012165
A02 =	−.050937	A07 =	3.343460
A03 =	2.525250	A08 =	−.119451
A04 =	346.65236	A09 =	−38.124442

YO = .15388314	A20 =	.30020353+001
Y1 = −.39169870−001	A21 =	−.61529971+001
Y2 = −.25198404−003	A22 =	−.14570002−001
Y3 = .98801205−006	A23 =	.13342155
	A24 =	−.90043710−004

ZO = .38796166   A10 = 3.6250

B11 = −.96153074+001	B23 = −.50009149+002
B21 = .27935713+002	B43 = .23153999+003
B41 = −.12569635+003	B63 = −.38080769+003
B51 = .54406550+003	B83 = .26120687+003
B61 = −.47948565+003	B14 = −.22934154+002
B81 = .14134133+003	B64 = −.14503027+002
B12 = −.12372626+002	B15 = −.10167777+002
B32 = −.34731447+002	B25 = .30142576+002
B52 = −.57569010+003	B55 = −.33549797+002
B62 = .53210066+003	B85 = .25502886+002
B72 = .41502454+003	B26 = −.53441617
B82 = −.42359614+003	B86 = .37213690−001
B13 = .58118955+002	

Table I 10

Coefficients determining shape factors θ and ϕ

	θ		ϕ
a_1	1	b_1	1
a_2	+0.0065	b_2	−0.021
a_3	−0.015	b_3	−0.065

Table I 11

Critical parameters of isobutane and isopentane

$T_4^c = 407.84$ K $\qquad\qquad$ $T_5^c = 460.51$ K

$V_4^c = 0.2578$ dm^3/mol $\qquad$ $V_5^c = 0.3079$ dm^3/mol

$P_4^c = 3.629$ MPa $\qquad\qquad$ $P_5^c = 3.3707$ MPa

$Z_4^c = 0.2759$ $\qquad\qquad\qquad$ $Z_5^c = 0.2711$

Table I 12

Combining-rule parameters k and ℓ

$$k = 0.995$$

$$\ell = 1.002$$

Table I 13

Parameters of the revised and extended
scaled thermodynamic potential of near-critical isobutane

Critical Parameters

T_c = 407.84 K P_c = 3.6290 MPa

ρ_c = 225.5 kg/m^3

Critical Exponents

β = 0.325 Δ_1 = 0.50

δ = 4.82

Parameters in Scaling Functions

α = 22.0163 c = -0.0096833

k_o = 1.19385 b^2 = 1.3757

k_1 = 0.50552

Pressure Background Parameters

$\tilde{P}_1$ = 5.8858 $\tilde{P}_{11}$ = -0.068209[e]

$\tilde{P}_2$ = -22.0805

Thermal Background Parameters

$\tilde{\mu}_c$ = -4.9535 $\tilde{\mu}_2$ = -32.2295

$\tilde{\mu}_1$ = -21.6912 $\tilde{\mu}_3$ = -33.5271

Table II 1

Parameters for the simple scaled equations of isobutane and isopentane

	isobutane	isopentane
Molar mass	$M = 0.0581243$ kg/mol	$M = 0.0721512$ kg/mol
Critical parameters	$T_c^{(4)} = 407.84$ K	$T_c^{(5)} = 460.51$ K
	$\rho_c^{(4)} = 3.8796$ mol/dm^3	$\rho_c^{(5)} = 3.265$ mol/dm^3
	$P_c^{(4)} = 3.62906 \times 10^6$ Pa	$P_c^{(5)} = 3.371 \times 10^6$ Pa
Parameters in scaling functions	$\beta = 0.355$	$\beta = 0.355$
	$\delta = 4.352$	$\delta = 4.352$
	$a = 20.7234$	$a = 20.7234$
	$k = 1.44675$	$k = 1.44675$
	$b^2 = 1.3909$	$b^2 = 1.3909$
Pressure background parameters	$\hat{P}_1^{(4)} = 5.8840$	$\hat{P}_1^{(5)} = 6.1720$
	$\hat{P}_2^{(4)} = -15.7886$	$\hat{P}_2^{(5)} = -18.0281$
	$\hat{P}_3^{(4)} = 0$	$\hat{P}_3^{(5)} = 19.4960$
Caloric background parameters	$\hat{\mu}_c = 1$	$\hat{\mu}_c = 1$
	$\hat{\mu}_1^{(4)} = \hat{P}_1^{(4)}$	$\hat{\mu}_1^{(5)} = \hat{P}_1^{(5)}$
	$\hat{\mu}_2^{(4)} = -28.6595$	$\hat{\mu}_2^{(5)} = -41.6268$
	$\hat{\mu}_3^{(4)} = -25.5431$	$\hat{\mu}_3^{(5)} = -15.4912$
Range of validity	407.6 K < T < 420.1 K	460.3 K < T < 474.3 K
	2.908 mol/dm^3 < ρ < 4.852 mol/dm^3	2.449 mol/dm^3 $\leq \rho \leq 4.081$ mol/dm^3

Table II 2

Calculated critical-point parameters of isobutane-isopentane mixtures as a function of the mole fraction x of isopentane.

x	T_c K	ρ_c mol/dm^3	P_c MPa
0	407.84	3.880	3.629
0.2001	419.40	3.774	3.677
0.3493	429.14	3.670	3.662
0.5	437.71	3.569	3.616
0.5073	438.09	3.564	3.613
1	460.51	3.265	3.371

Table II 3

Differences between thermodynamic property values F_{global} calculated from the global equation (Sec. 2.2 of Part I) and thermodynamic property values F_{scaled} calculated from the scaled fundamental equation for an equimolar mixture of isobutane and isopentane (x = 0.5) at T = 452 K.

Quantity listed: $(F_{global} - F_{scaled})/F_{scaled}$ in %

ρ mol/dm^3	$F = P$ %	$F = \left(\dfrac{\partial P}{\partial T}\right)_{\rho,x}$ %	$F = \left(\dfrac{\partial P}{\partial \rho}\right)_{T,x}$ %
2.702	6.1	0.8	− 5.6
2.886	5.8	3.4	−10.9
3.070	5.5	5.8	−15.1
3.255	5.1	8.0	−17.9
3.439	4.6	10.0	−19.5
3.623	4.2	11.8	−19.8
3.807	3.7	13.2	−19.3
3.992	3.2	14.3	−18.1
4.176	2.7	15.1	−16.5
4.360	2.2	15.5	−14.8

Note: T_c = 437.71 K, ρ_c = 3.569 mol/dm^3, M = 0.065137 kg/mol.

Table III 1

Viscosities of compressed liquid normal butane

P, MPa	ρ, mol·L^{-1}	η, μPa·s
	T = 300.00 K	
33.9166	10.548	221.4
30.6994	10.495	217.9
28.1542	10.450	212.9
24.7677	10.389	205.9
21.5095	10.327	201.3
17.7614	10.252	192.3
14.4315	10.181	188.2
10.2694	10.086	175.8
7.6515	10.021	170.8
4.8175	9.947	164.3
1.7289	9.859	157.8
	T = 250.00 K	
30.0269	11.201	337.3
27.0472	11.162	327.3
24.6018	11.130	322.7
21.4561	11.087	316.2
17.9370	11.037	305.9
14.6209	10.988	299.3
11.7832	10.945	292.5
7.9407	10.884	283.6
5.1172	10.837	275.9
1.8463	10.781	267.1

Table III 1 (Continued).

P, MPa	ρ, mol·L^{-1}	η, μPa·s
	T = 200.00 K	
31.0293	11.928	646.1
30.2055	11.920	632.7
27.9013	11.898	618.5
24.6365	11.865	606.0
21.3166	11.831	587.0
17.9753	11.797	573.8
14.4286	11.759	560.9
11.1406	11.723	550.1
7.9864	11.687	533.8
5.1249	11.654	519.1
2.0330	11.618	507.6
	T = 180.00 K	
31.2351	12.219	880.7
28.0523	12.191	851.9
24.7734	12.162	835.6
21.1814	12.129	813.8
17.7851	12.098	797.9
14.3967	12.065	782.3
11.3084	12.035	760.8
8.1990	12.004	745.4
5.4201	11.976	729.9
2.1837	11.942	703.7

Table III 1 (Continued)

P, MPa	ρ, mol·L^{-1}	η, μPa·s
	T = 160.00 K	
32.2269	12.519	1381.8
30.0563	12.503	1368.3
27.0460	12.479	1317.8
24.4627	12.458	1282.6
21.1290	12.430	1248.5
16.9623	12.395	1230.0
14.4448	12.374	1196.0
11.4659	12.348	1169.8
8.0570	12.317	1130.3
4.6655	12.286	1098.3
1.4602	12.257	1073.4
	T = 150.00 K	
29.1128	12.644	1809.5
26.6361	12.625	1785.9
24.0565	12.605	1736.8
21.4113	12.585	1663.2
17.8222	12.556	1641.7
14.6675	12.530	1562.4
7.9562	12.474	1512.4
5.0882	12.450	1443.8
1.7692	12.420	1400.2

Table III 1 (Continued)

P, MPa	ρ, mol·L^{-1}	η, uPa.s
	T = 140.00 K	
30.2935	12.802	2565.4
27.7097	12.784	2486.9
24.6230	12.761	2440.3
21.2652	12.736	2384.6
17.4590	12.707	2320.1
15.4894	12.692	2264.0
12.8373	12.672	2199.7
10.2410	12.651	2117.4
7.4174	12.628	2055.3
4.6766	12.606	2012.5
1.5161	12.579	1952.4

Table III 2

Viscosities of saturated liquid normal butane

T, K	ρ, mol·L^{-1}	η, μPa·s
136.00	12.634	2234.9
138.00	12.601	2013.1
140.00	12.566	1899.7
145.00	12.486	1592.1
150.00	12.405	1332.7
155.00	12.324	1200.4
160.00	12.243	1047.2
170.00	12.081	816.9
180.00	11.920	690.3
190.00	11.757	571.5
200.00	11.593	485.2
220.00	11.262	368.2
240.00	10.922	288.7
250.00	10.749	259.8
260.00	10.572	233.4
280.00	10.204	189.0

Table III 3

Viscosities of compressed liquid isobutane

P, MPa	ρ, mol·L^{-1}	η, µPa·s
	T = 300.00 K	
32.0838	10.250	223.8
28.5975	10.182	215.6
25.1765	10.112	206.3
24.3531	10.094	203.4
21.5145	10.032	197.7
18.2143	9.957	188.2
16.6258	9.919	188.2
14.8533	9.875	181.8
14.6597	9.870	184.7
13.4571	9.839	181.5
11.4848	9.787	175.0
7.6669	9.679	166.0
4.1001	9.568	155.9
.8064	9.453	148.2
.4145	9.439	147.1
	T = 250.00 K	
31.6827	10.970	377.8
27.9692	10.917	364.3
24.5552	10.866	349.7
21.0180	10.811	338.7
19.2675	10.784	327.8
17.5178	10.755	327.7

Table III 3   (Continued)

P, MPa	ρ, mol·L^{-1}	η, μPa·s
15.5723	10.723	314.7
14.0358	10.697	316.8
11.6838	10.656	302.7
10.7614	10.640	304.7
7.3892	10.578	295.0
3.1925	10.496	279.9

T = 200.00 K

31.2686	11.687	748.8
28.1272	11.654	731.7
24.8552	11.619	711.1
21.3494	11.580	682.6
17.6364	11.538	658.1
16.8536	11.528	643.6
14.0934	11.496	638.0
12.6896	11.479	609.6
10.7472	11.455	620.2
7.3582	11.412	601.4
3.0687	11.356	583.8

Table III 3   (Continued)

P, MPa	ρ, mol·L^{-1}	η, μPa·s
	T = 180.00 K	
31.4359	11.978	1093.6
28.0430	11.947	1064.2
24.4960	11.913	1017.0
21.0666	11.880	979.9
17.6586	11.846	945.5
13.9976	11.808	909.3
10.5922	11.772	884.3
7.4037	11.737	858.0
3.3993	11.691	836.7
	T = 160.00 K	
34.1087	12.291	1842.7
30.6682	12.263	1802.2
27.1278	12.235	1688.6
25.6699	12.223	1694.5
21.9056	12.191	1656.0
18.3818	12.160	1584.2
14.8377	12.128	1505.8
11.1760	12.095	1469.4
7.9163	12.064	1441.0
4.4249	12.029	1381.8
1.6752	12.002	1346.0

Table III 3   (Continued)

P, MPa	ρ, mol·L^{-1}	η, μPa·s
	T = 150.00 K	
32.3674	12.423	2459.5
29.3326	12.400	2412.6
25.9258	12.374	2341.6
22.6434	12.348	2246.8
18.5270	12.315	2145.4
14.9878	12.286	2077.1
14.8903	12.285	2116.8
11.5634	12.256	1972.2
10.8120	12.250	1981.1
7.7792	12.223	1906.1
7.3933	12.219	1944.2
3.3096	12.182	1890.5
	T = 140.00 K	
34.4848	12.584	3540.8
31.4535	12.564	3482.9
27.5545	12.536	3226.3
24.0140	12.510	3156.6
20.3420	12.483	3014.1
16.9883	12.457	2957.9
15.1308	12.443	2966.6
12.4894	12.422	2826.7
9.7485	12.400	2722.5

Table III 3   (Continued)

P, MPa	ρ, mol·L^{-1}	η, uPa·s
7.5270	12.381	2640.4
4.9825	12.359	2597.0
2.2351	12.335	2512.6

T = 135.00 K

32.8042	12.647	4404.4
29.3833	12.624	4310.2
26.0042	12.600	4143.9
22.4957	12.576	3994.0
18.9878	12.550	3878.8
15.4475	12.524	3671.2
11.9075	12.496	3523.9
7.2201	12.459	3352.1
2.9658	12.424	3137.1

T = 130.00 K

32.3245	12.717	5358.4
29.1835	12.697	5239.7
25.8556	12.675	5049.6
22.4324	12.651	4849.0
19.0082	12.628	4708.6
15.4097	12.602	4515.2
11.8763	12.576	4359.5
7.7479	12.544	4214.7
2.7303	12.504	4028.7

Table III 3   (Continued)

P, MPa	ρ, mol·L^{-1}	η, μPa·s
	T = 125.00 K	
33.4321	12.798	7088.0
30.2429	12.778	6803.0
27.1840	12.759	6562.1
23.9961	12.738	6244.6
20.3856	12.714	6078.9
16.9765	12.691	5742.6
13.1952	12.665	5553.6
9.8415	12.640	5366.3
6.4430	12.615	5138.3
2.8559	12.587	4800.9
	T = 120.00 K	
33.1409	12.870	9302.9
30.2300	12.853	8772.1
27.0404	12.834	8604.2
23.9612	12.815	8269.6
20.2683	12.791	7925.3
16.8658	12.769	7516.3
13.1879	12.744	7371.2
10.4375	12.725	7198.2
7.5484	12.704	6908.2
3.2824	12.673	6471.3

Table III 4

Viscosities of saturated liquid isobutane

T, K	ρ, mol·L^{-1}	η, uPa·s
115.00	12.733	8188.7
115.00	12.733	8224.1
116.00	12.716	7652.4
118.00	12.683	6919.0
120.00	12.647	6334.7
125.00	12.567	4694.8
130.00	12.481	3751.5
135.00	12.401	2999.1
140.00	12.315	2447.3
140.00	12.315	2412.9
145.00	12.235	2091.6
150.00	12.150	1747.5
155.00	12.070	1480.5
160.00	11.984	1272.1
160.00	11.984	1287.2
160.00	11.984	1301.5
170.00	11.817	975.3
180.00	11.651	829.3
180.00	11.651	803.5
180.00	11.651	797.5
190.00	11.483	651.9
200.00	11.313	539.0
200.00	11.313	531.5

Table III 4   (Continued)

T, K	ρ, mol·L^{-1}	η, uPa·s
220.00	10.969	396.2
220.00	10.969	393.1
240.00	10.614	301.8
240.00	10.614	298.7
250.00	10.431	262.2
260.00	10.243	231.9
260.00	10.243	234.2
280.00	9.853	183.9
280.00	9.853	184.9

long-stem Pt Thermometer

thermostated bath

pressure
transducer

to
gasometer
or to
dead-weight gage

optical cell
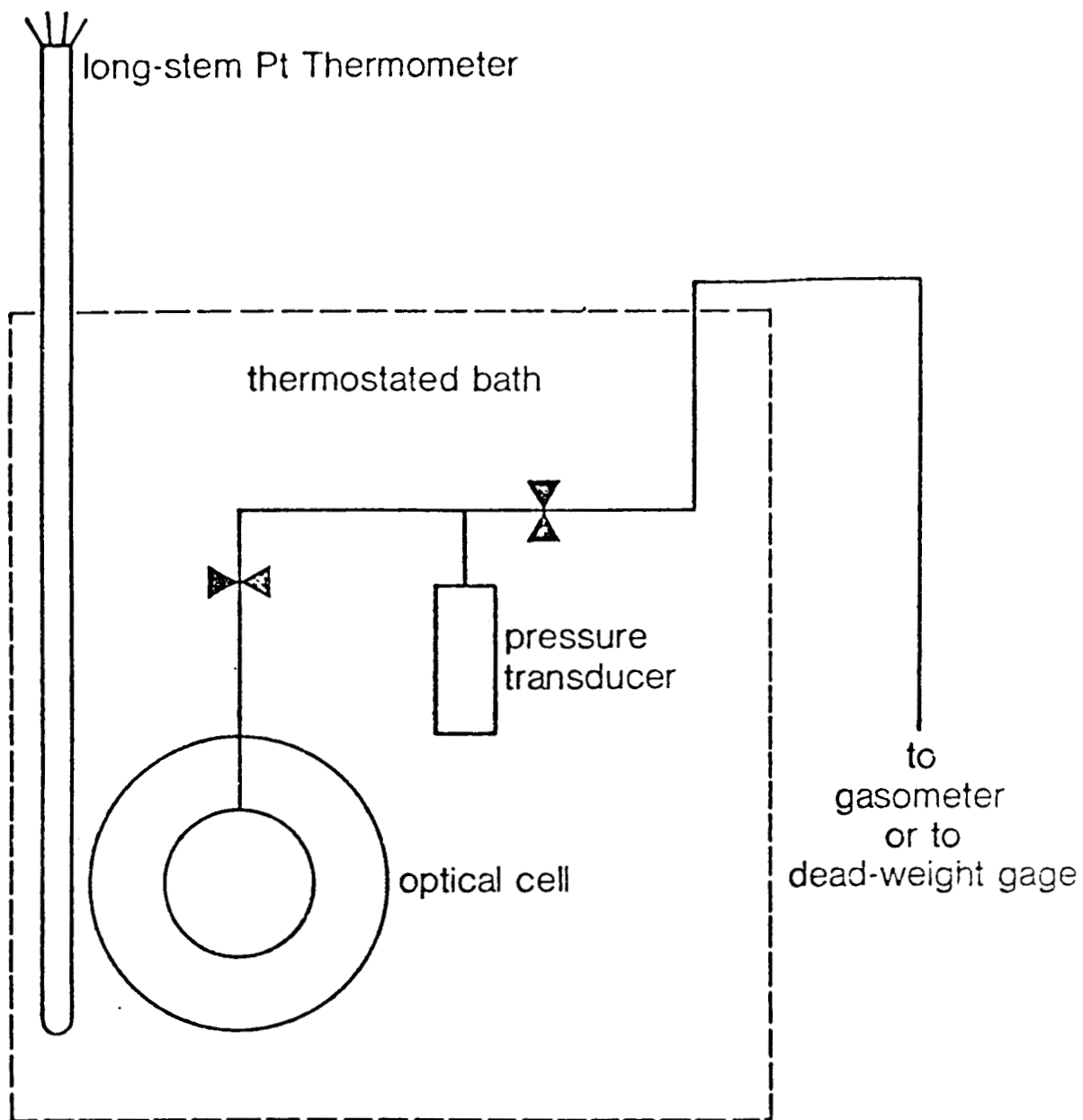
Fig. I 1   Arrangement of visual cell, pressure transducer,
thermostated bath and thermometer for the oberserva-
tion of meniscus disappearance in pure fluids and
mixtures.
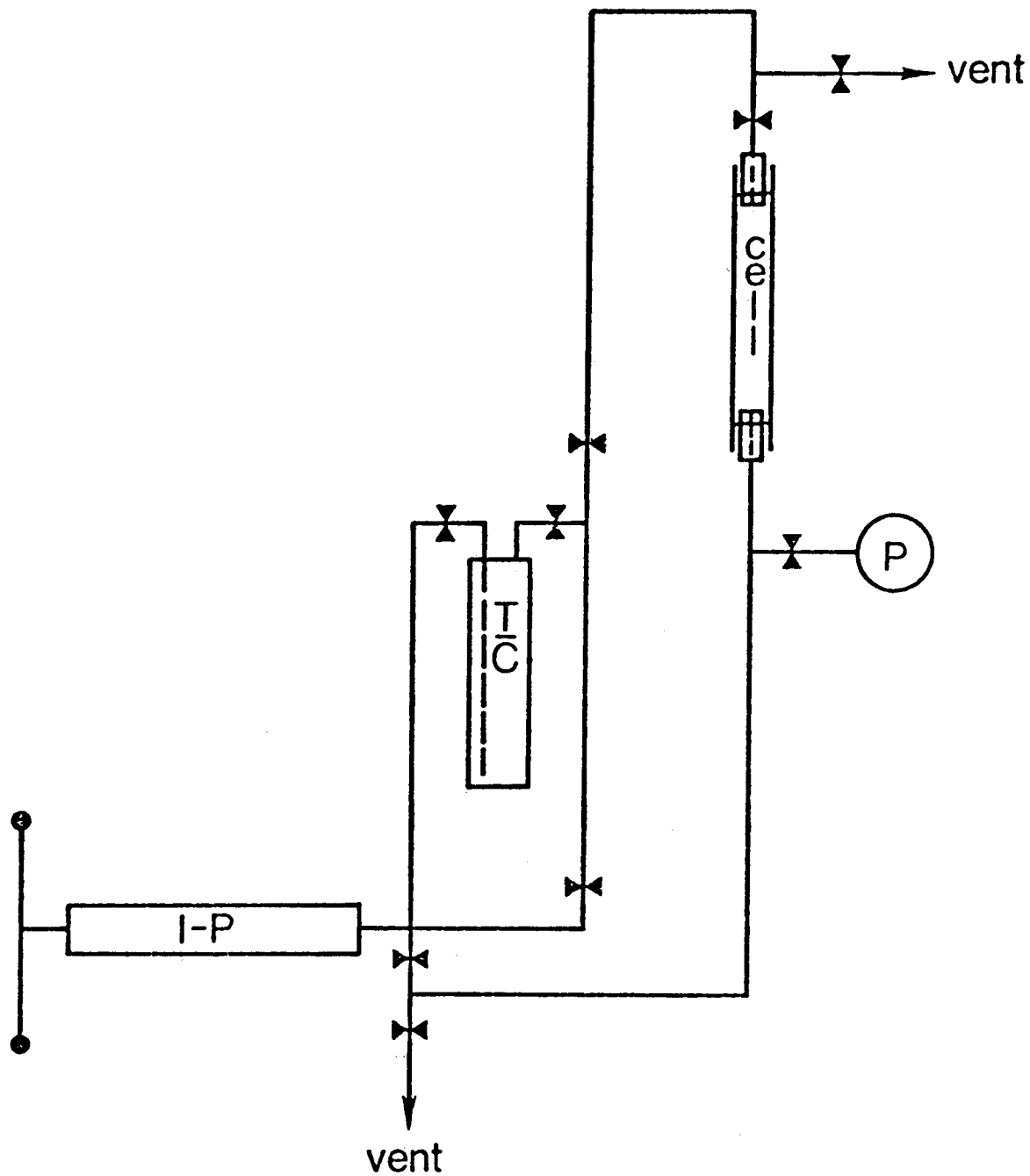
Fig. I 2   Arrangement of visual cell, thermal compressor (T-C),
injector pump (I-P) and pressure transducer (P) used for
density and composition determinations in binary fluid
mixtures. During oberservations, the entire manifold
is filled with mercury, and the cell in part.

F2
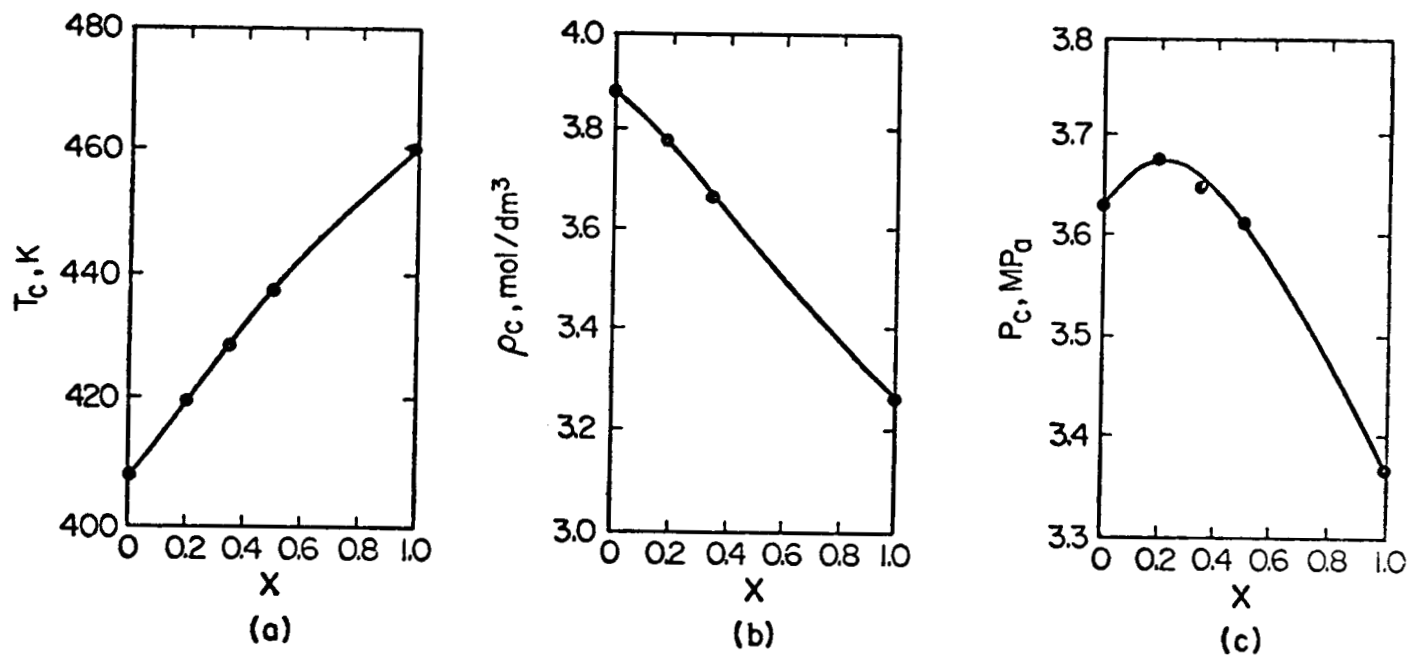
Fig. II 1   The critical line of isobutane-isopentane
            mixtures plotted against the mole fraction x of
            isopentane: (a) critical temperature, (b) critical
            density and (c) critical pressures. The points
            represent the experimental data of Table I 5 and the
            curves are calculated from the Leung-Griffiths equations.
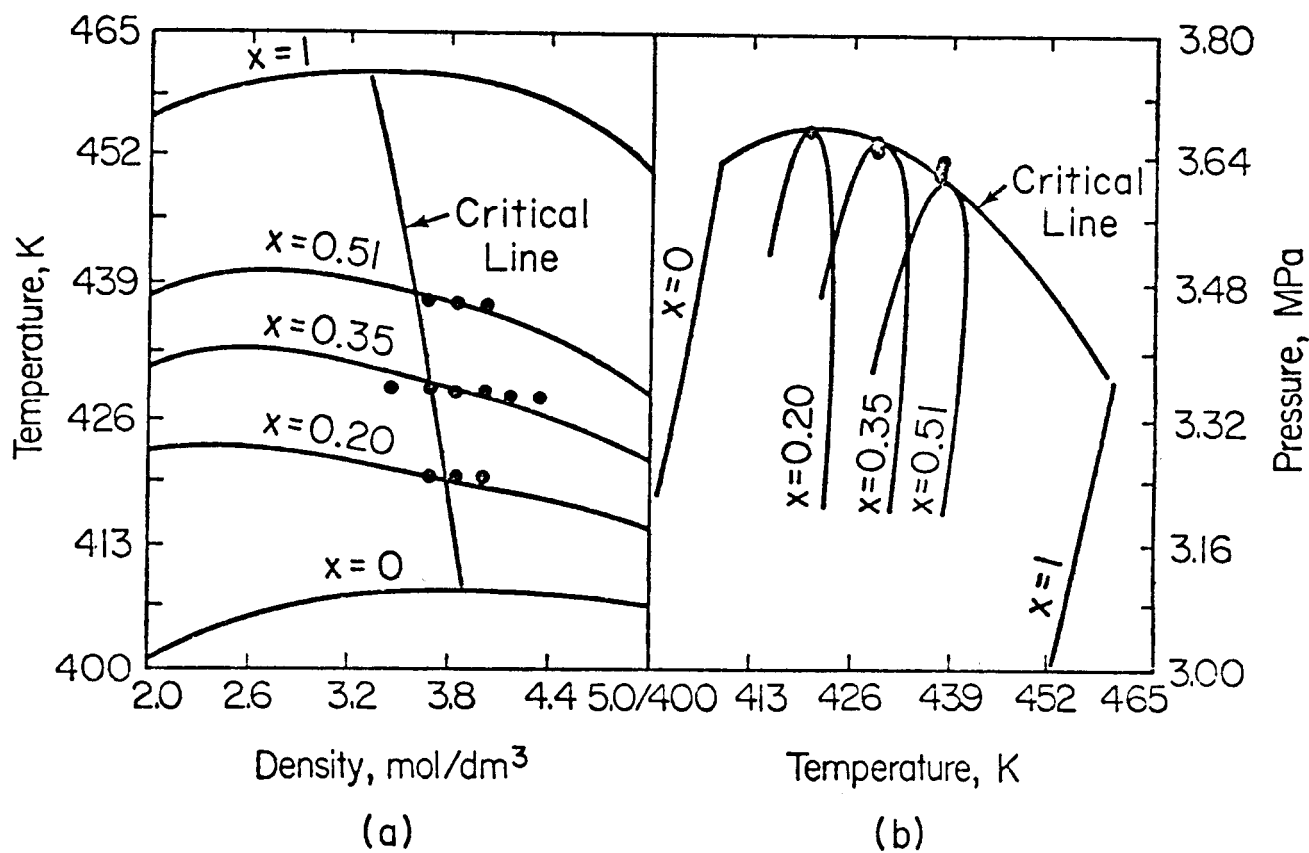
Fig. II 2   Comparison between experimental and calculated dew-
bubble curve data at various mole fractions x of isopentane
(a) coexistence curves near the top of the dome in the
temperature density plane, and (b) vapor-pressure
curves in the pressure – temperature plane. The points
represent the experimental data of Table I 7 and the curves
the values calculated from the Leung-Griffiths
equation.
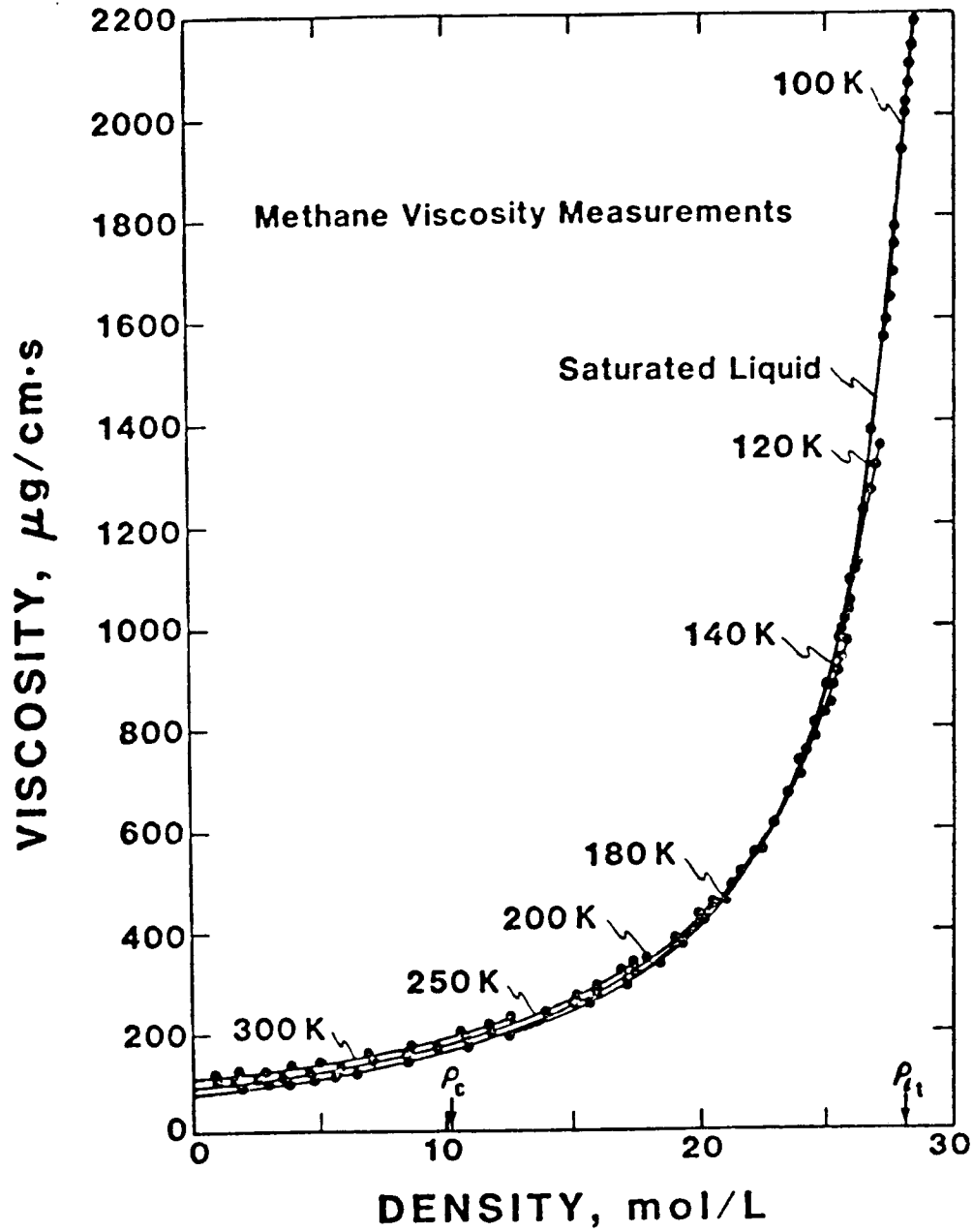
Fig. III 1   Viscosity of compressed gaseous and liquid methane as
a function of density along various isotherms.
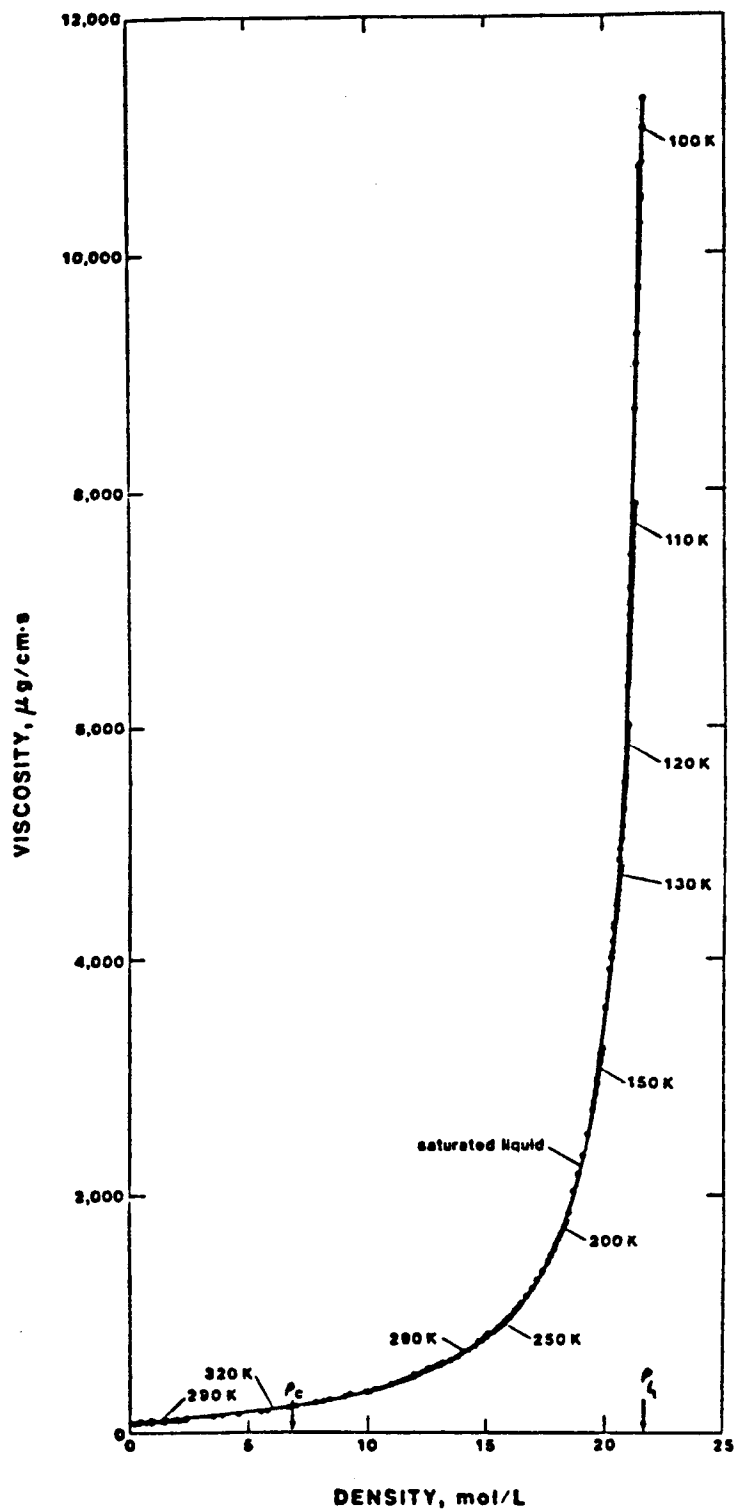
Fig. III 2 Viscosity of compressed gaseous and liquid ethane as
a function of density. (ρ_c is the critical density;
ρ_{lt} is the density of the liquid at the triple point
temperature.)
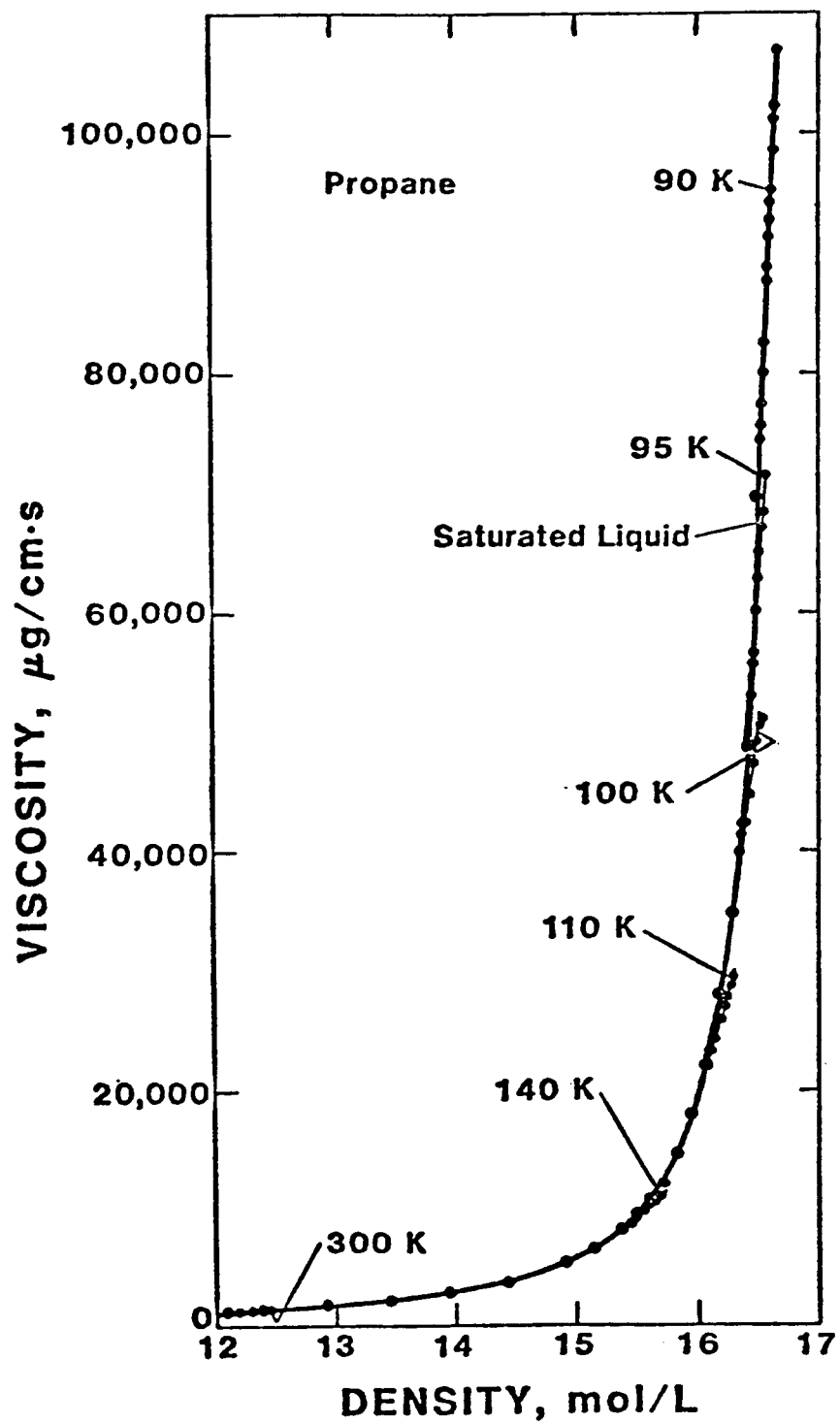
Fig. III 3 Viscosity of compressed gaseous and liquid propane as
a function of density along various isotherms.
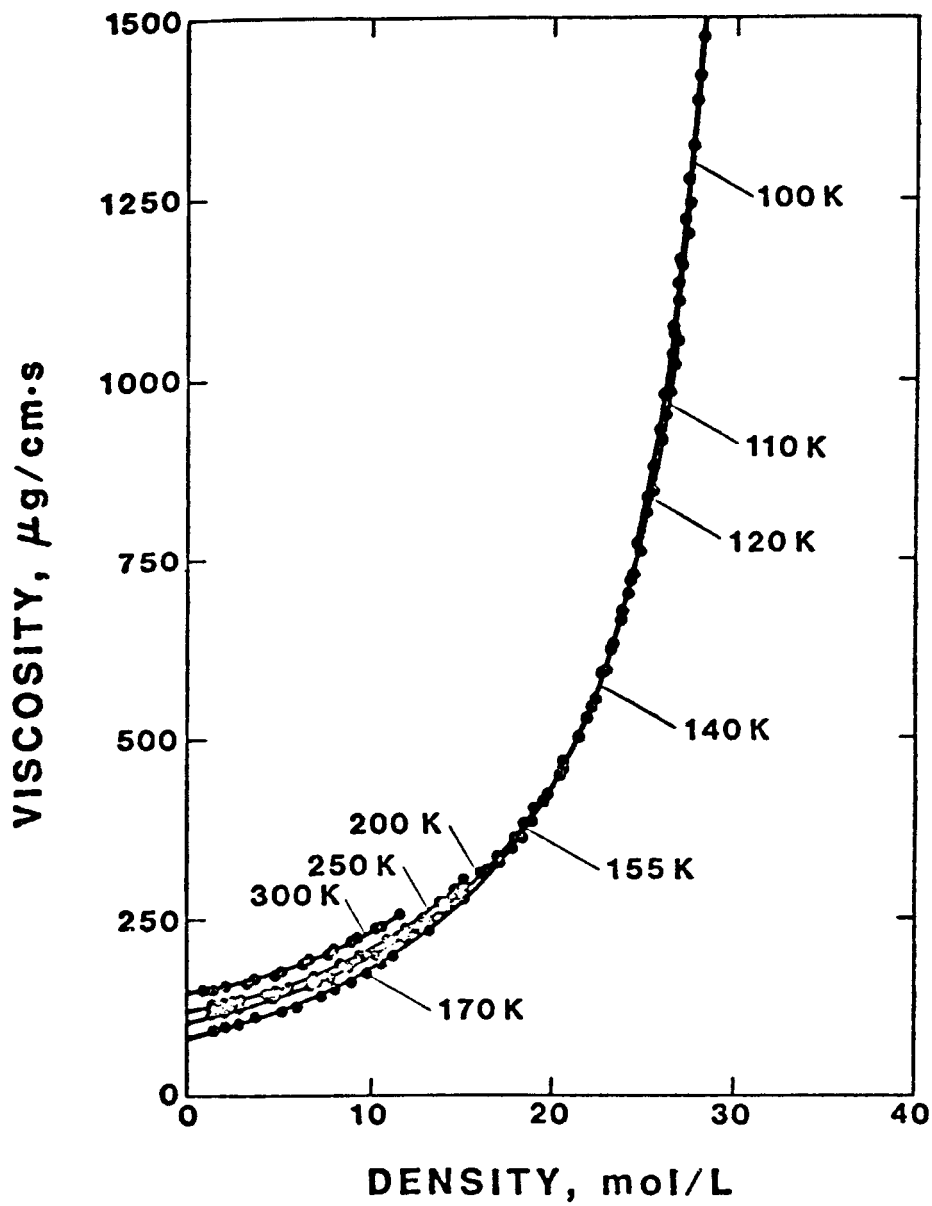
Fig. III 4 Viscosity of compressed gaseous and liquid 50.115 mol % nitrogen + 49.885 mol % methane as a function of density along various isotherms.
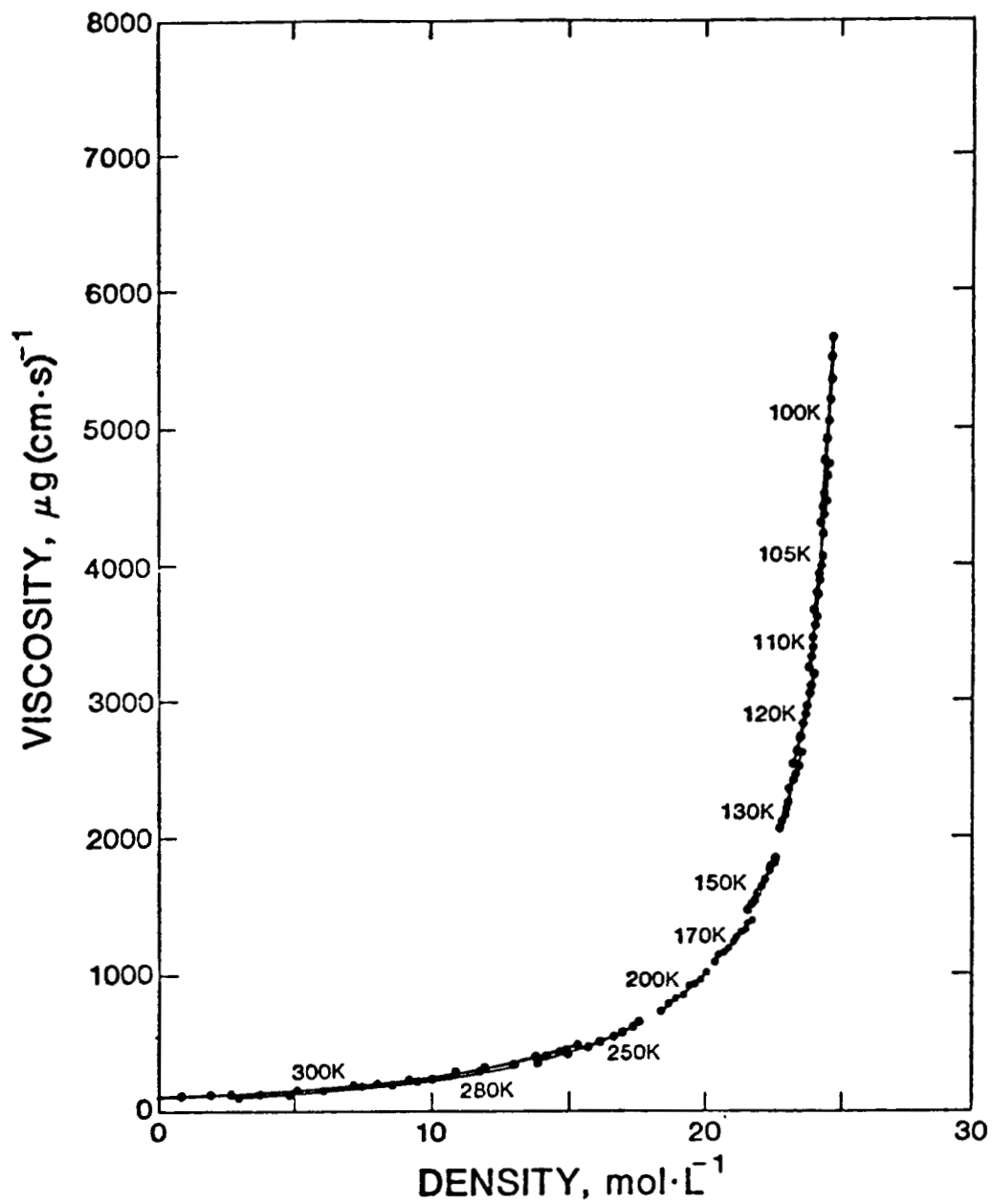
Fig. III 5 Viscosity of compressed gaseous and liquid 0.50217 mol %
methane + 49.783 mol % ethane as a function of density.
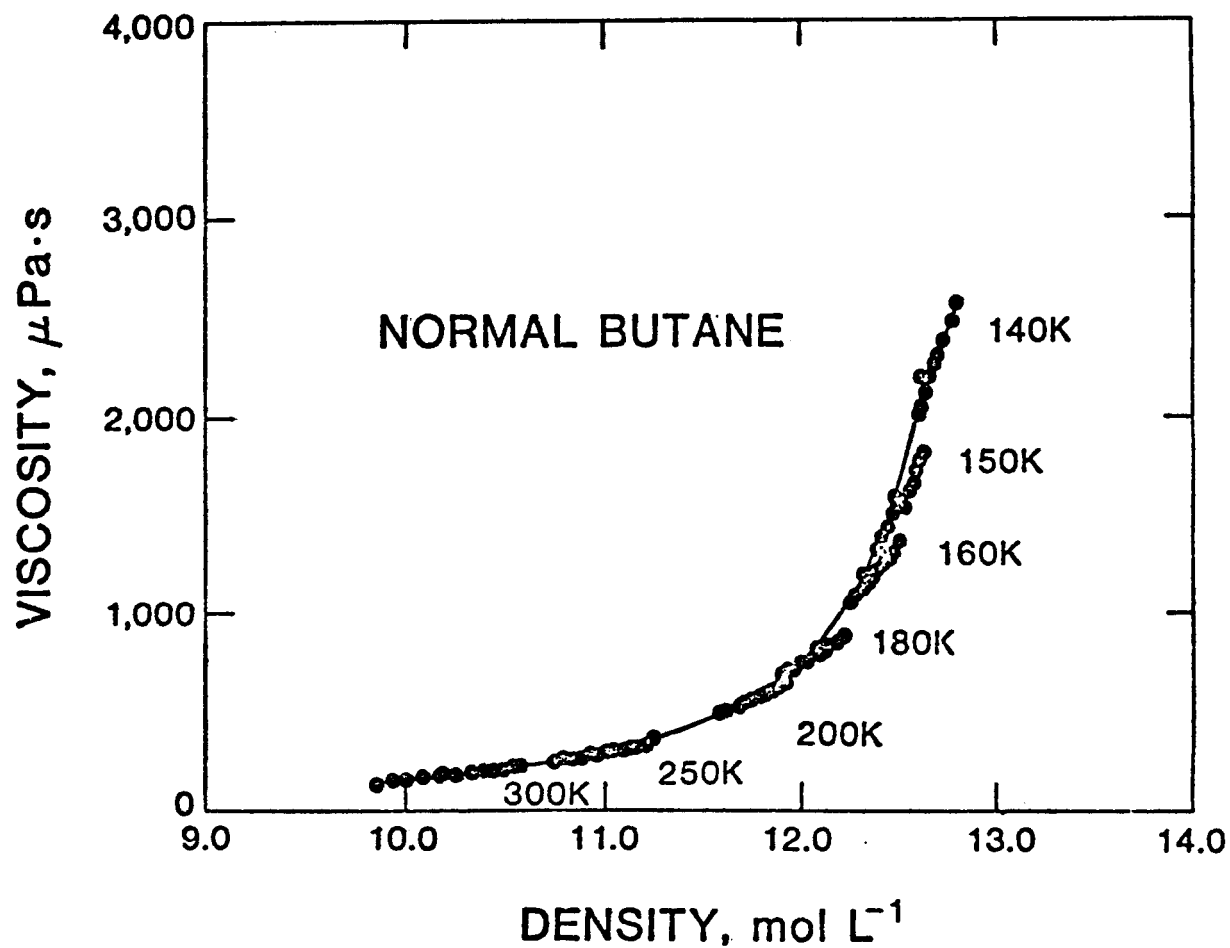
Fig. III 6 Viscosity of compressed gaseous and liquid normal butane at saturation and along various isotherms.
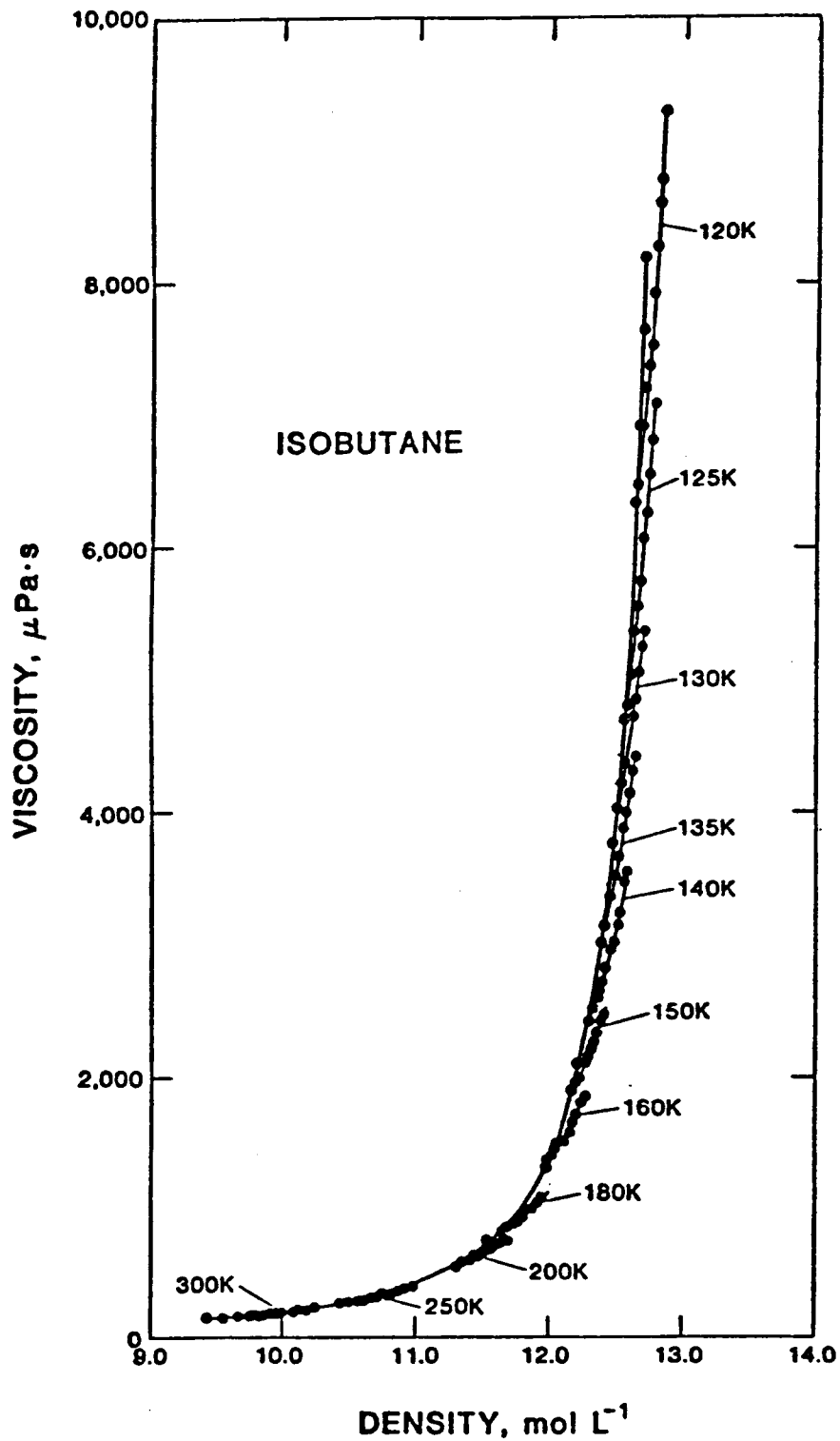
Fig. III 7 Viscosity of compressed gaseous and liquid isobutane
at saturation and along various isotherms.
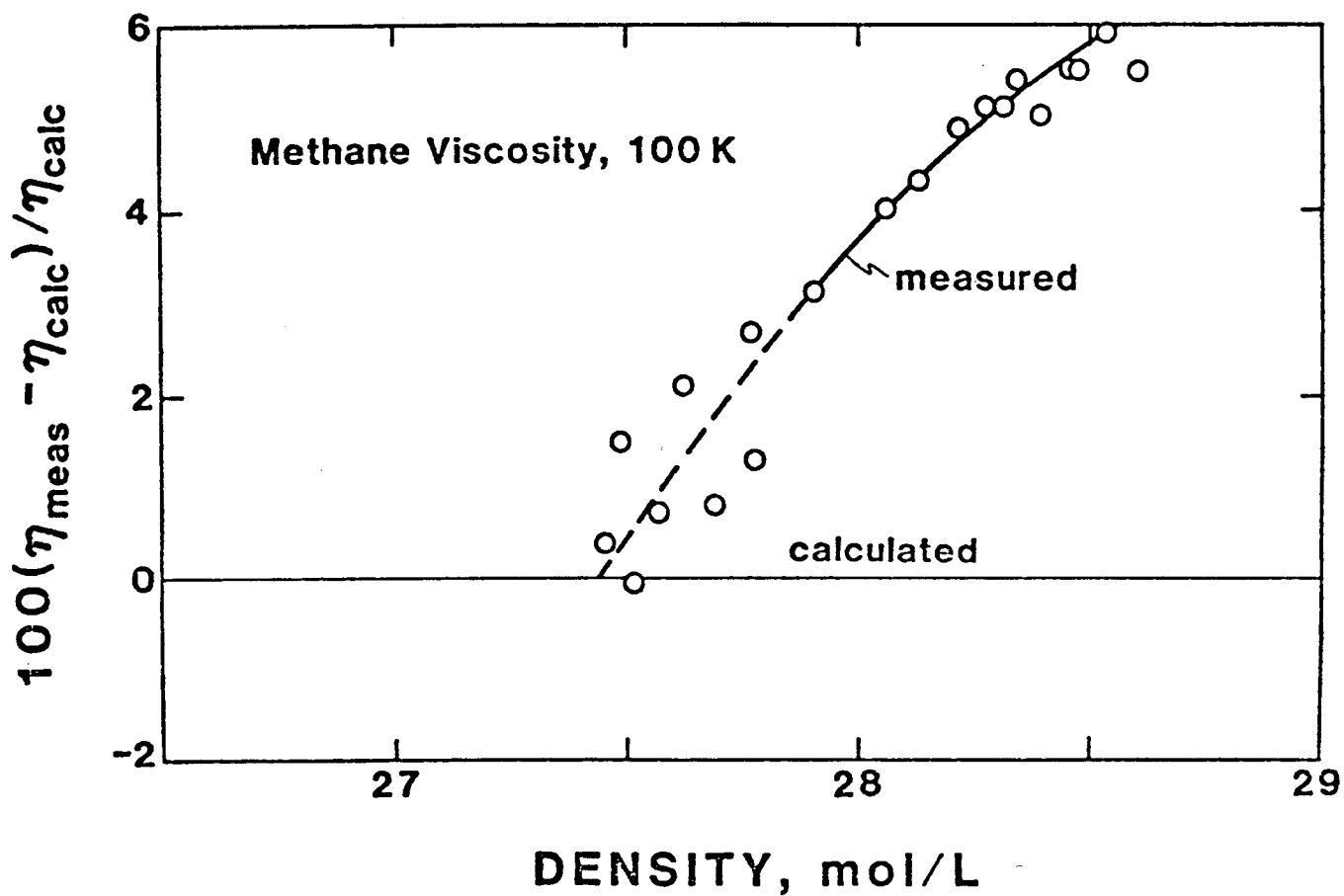
Fig. III 8   Comparison of the viscosity of methane at 100 K with
the correlation of Ref. 51.
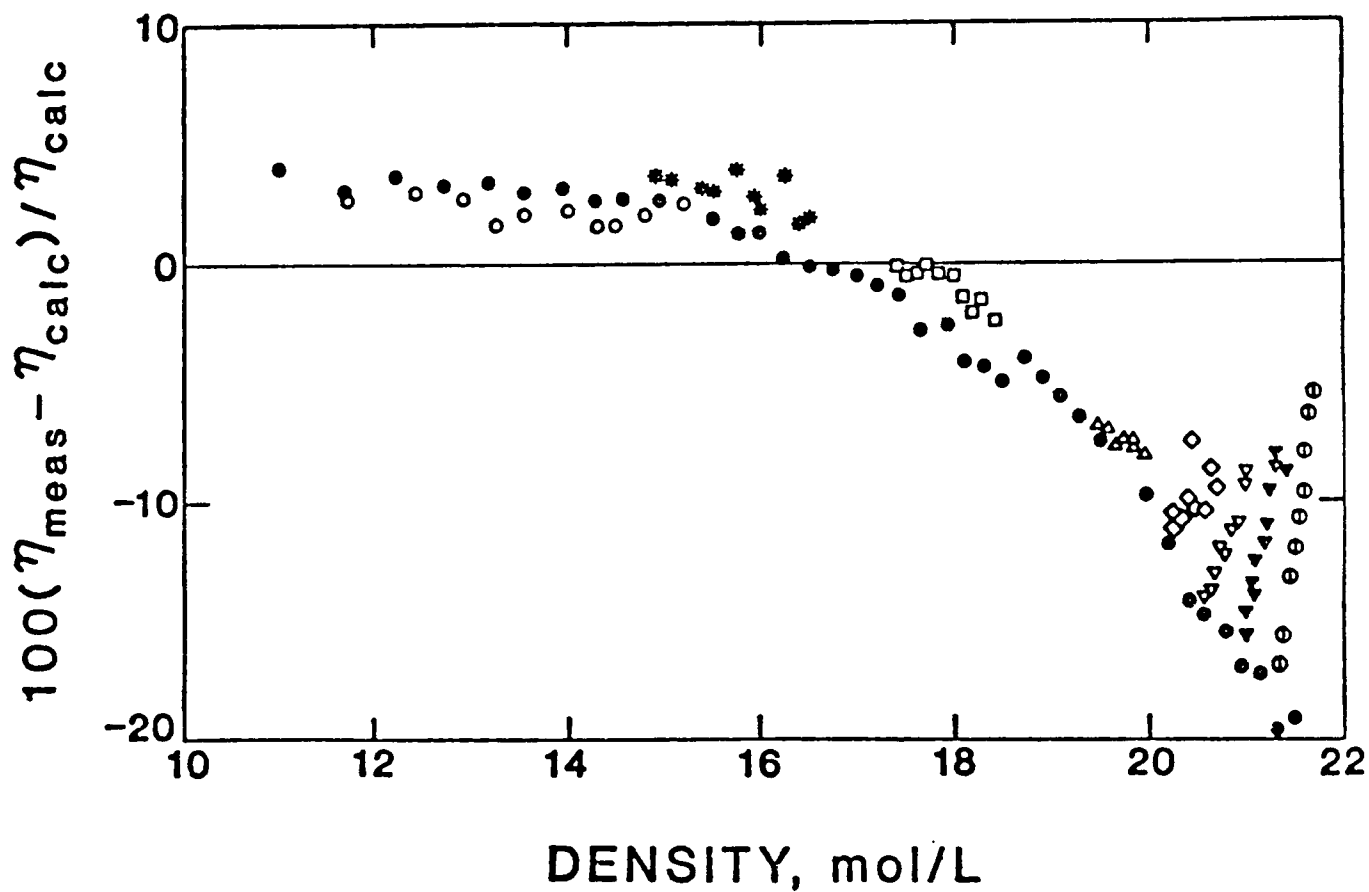
Fig. III 9 Comparison of the viscosity of ethane with that pre-
dicted by the generalized corresponding-states model.
⊙, 290 K; *, 250 K; □, 200 K; Δ, 150 K; ◊,130 K; ▽ ,
120 K; ▼ , 110 K; ⊕, 100 K; ◉ , saturated liquid.
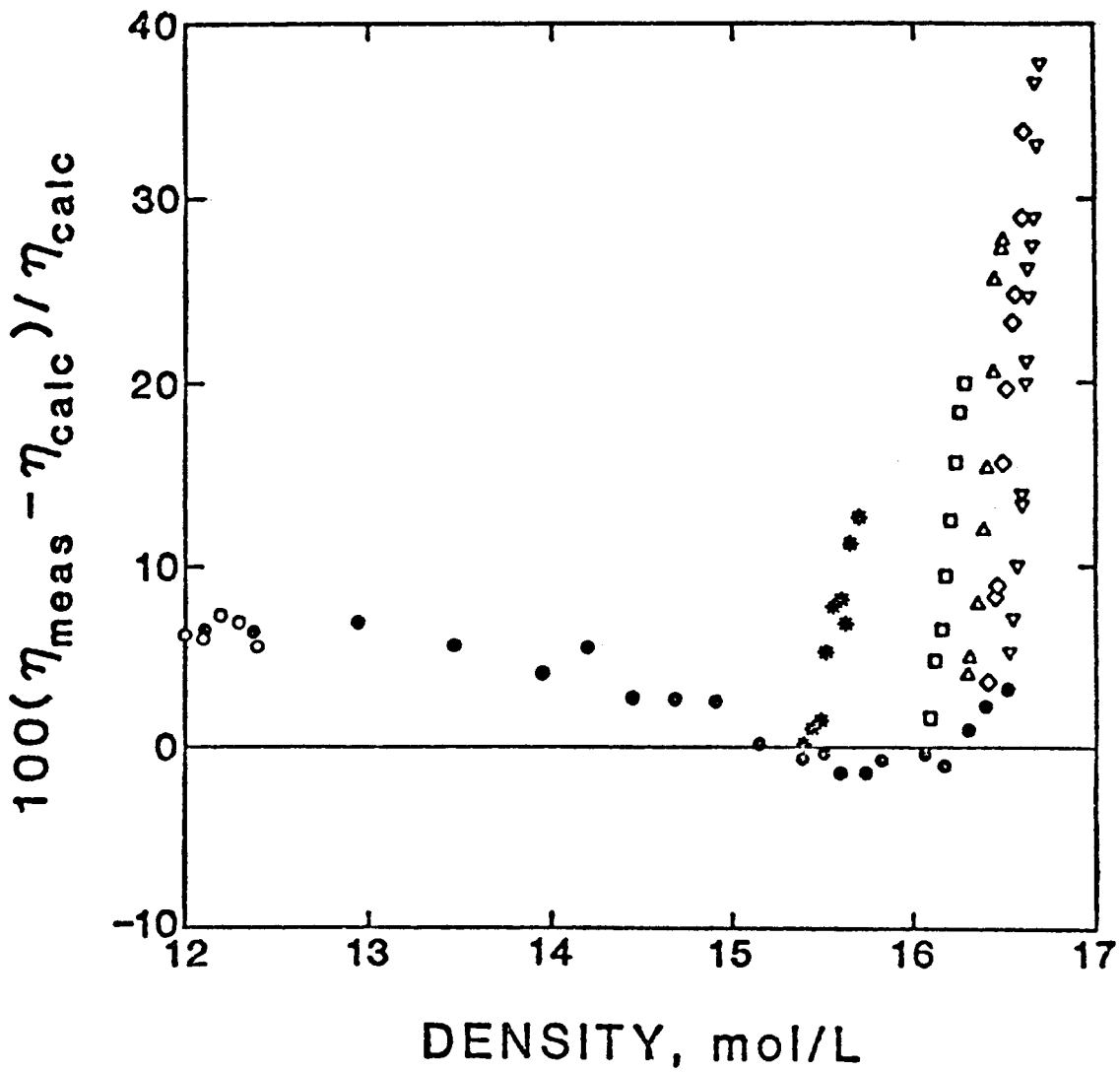
Fig. III 10 Comparison of the viscosity of propane with that
predicted by the generalized corresponding-states
model. ⊙, 300 K; *, 140 K; □, 110 K; Δ, 100 K; ◊,
95 K; ▽ , 90 K. ●, saturated liquid.
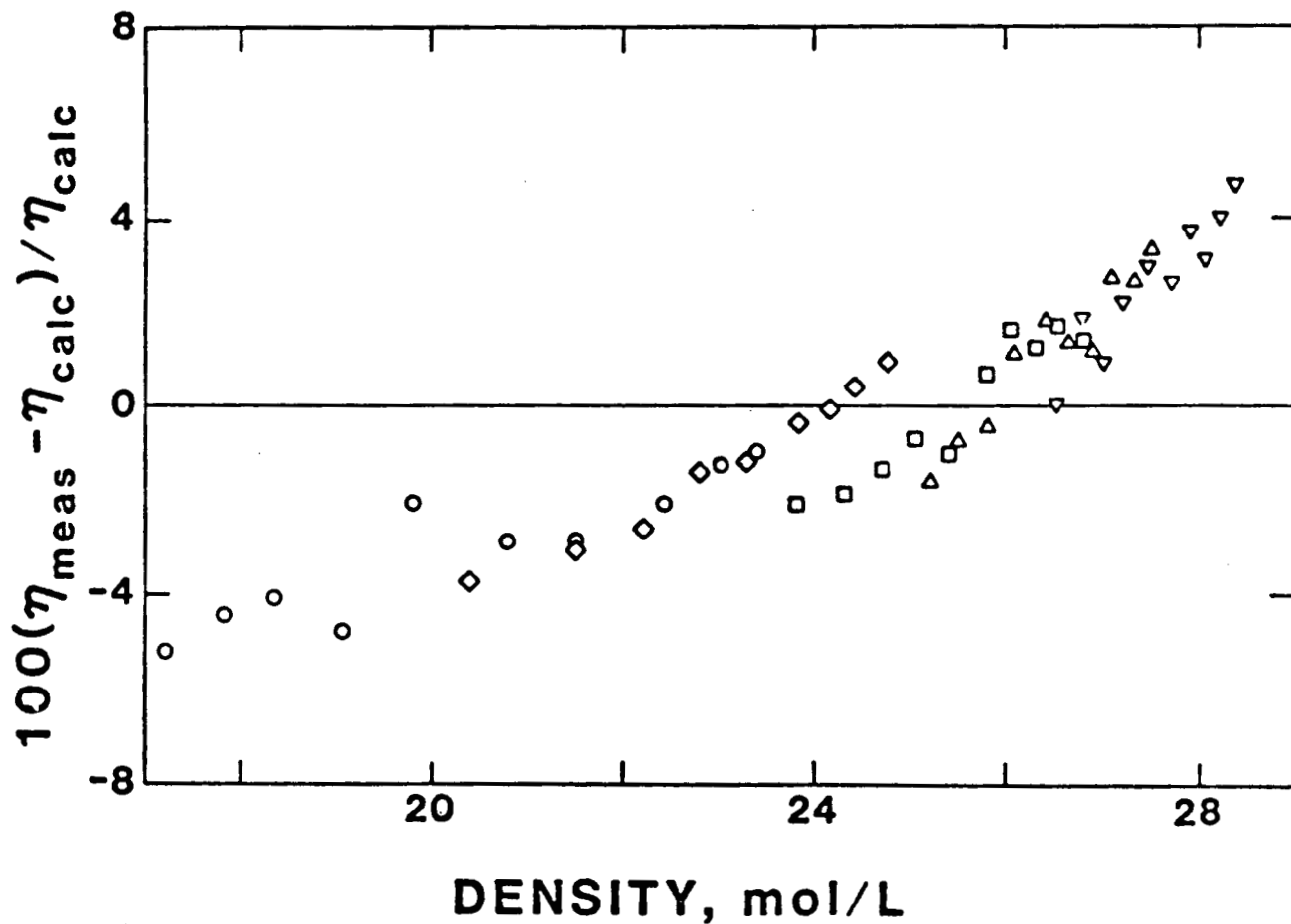
Fig. III 11   Comparison of the viscosity of a 50.115 mol %
              nitrogen--49.885 mol % methane mixture with that
              predicted by the generalized corresponding-states
              model. ⊙, 155 K; ◊, 140 K; □, 120 K; Δ, 110 K;
              ▽ , 100 K.
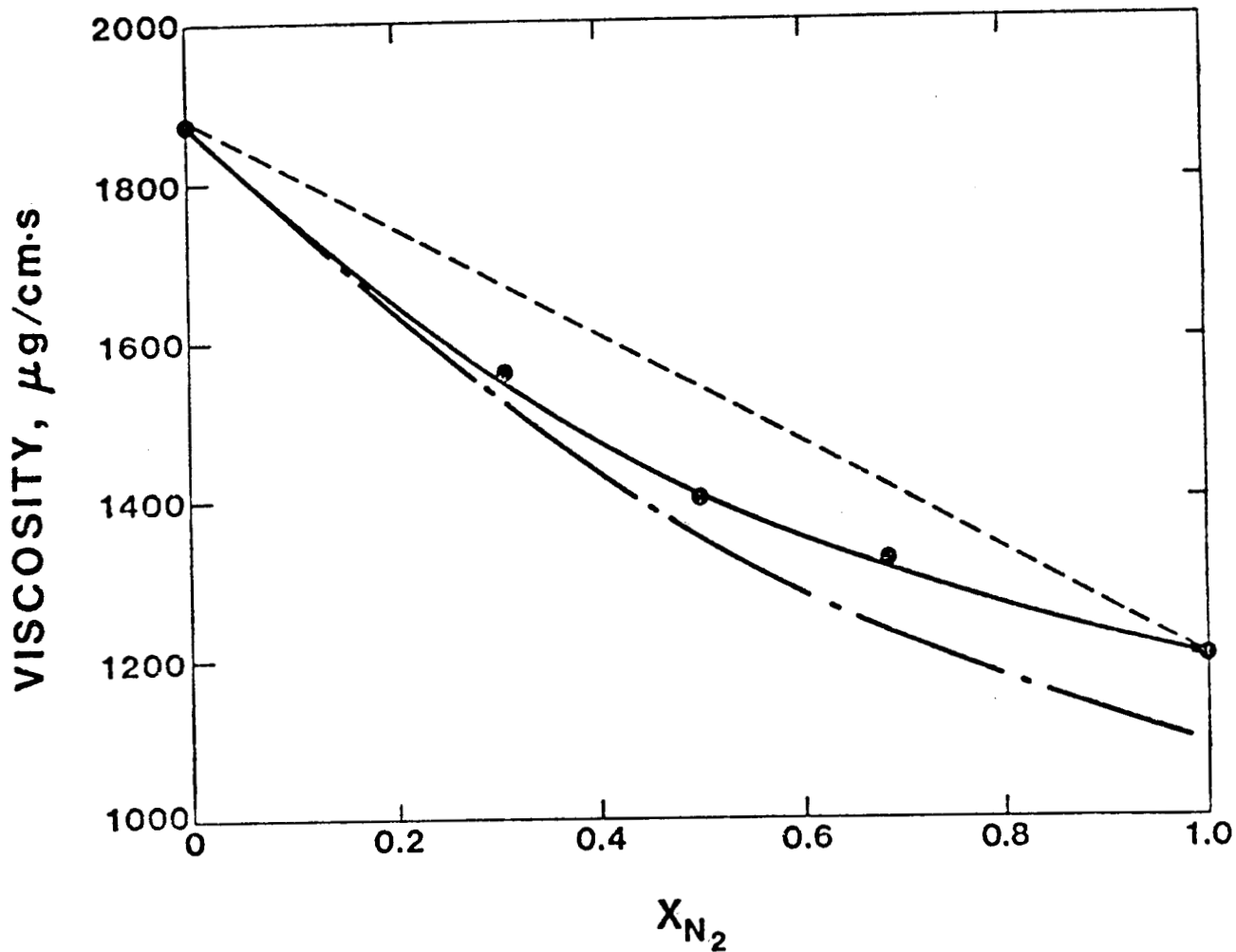
Fig. III 12 Viscosity of compressed liquid nitrogen + methane
mixtures and their pure components as a function of
composition at fixed molar density (28.0 $mol \cdot liter^{-1}$)
and at fixed temperature (100 K). The present mea-
surements, ; mole fraction average of the pure
component viscosities, — — — ; generalized corre-
sponding states model, —·—·— .
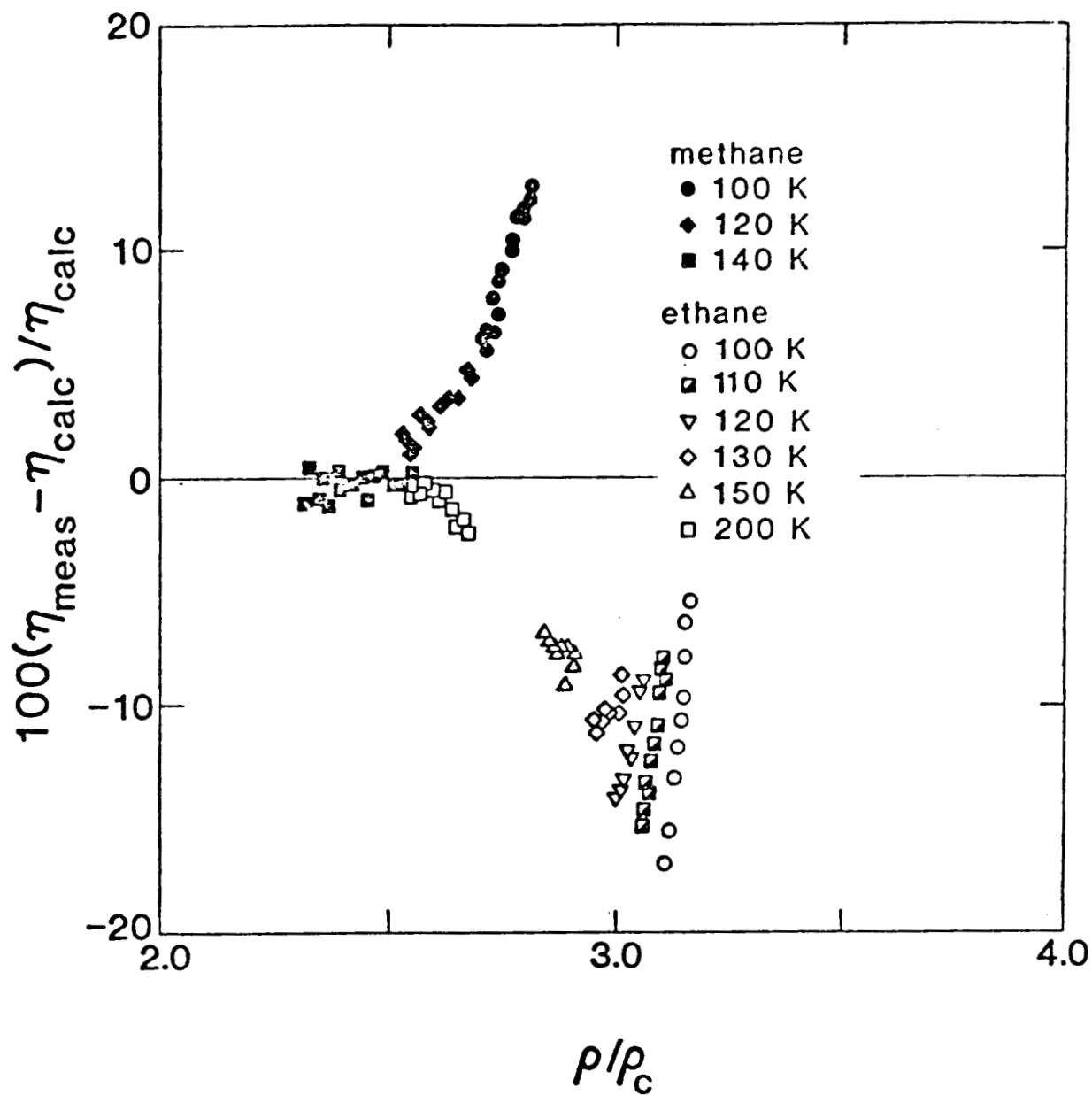
Fig. III 13 Comparison of the viscosity of compressed liquid
methane and ethane with the generalized corre-
sponding-states model.
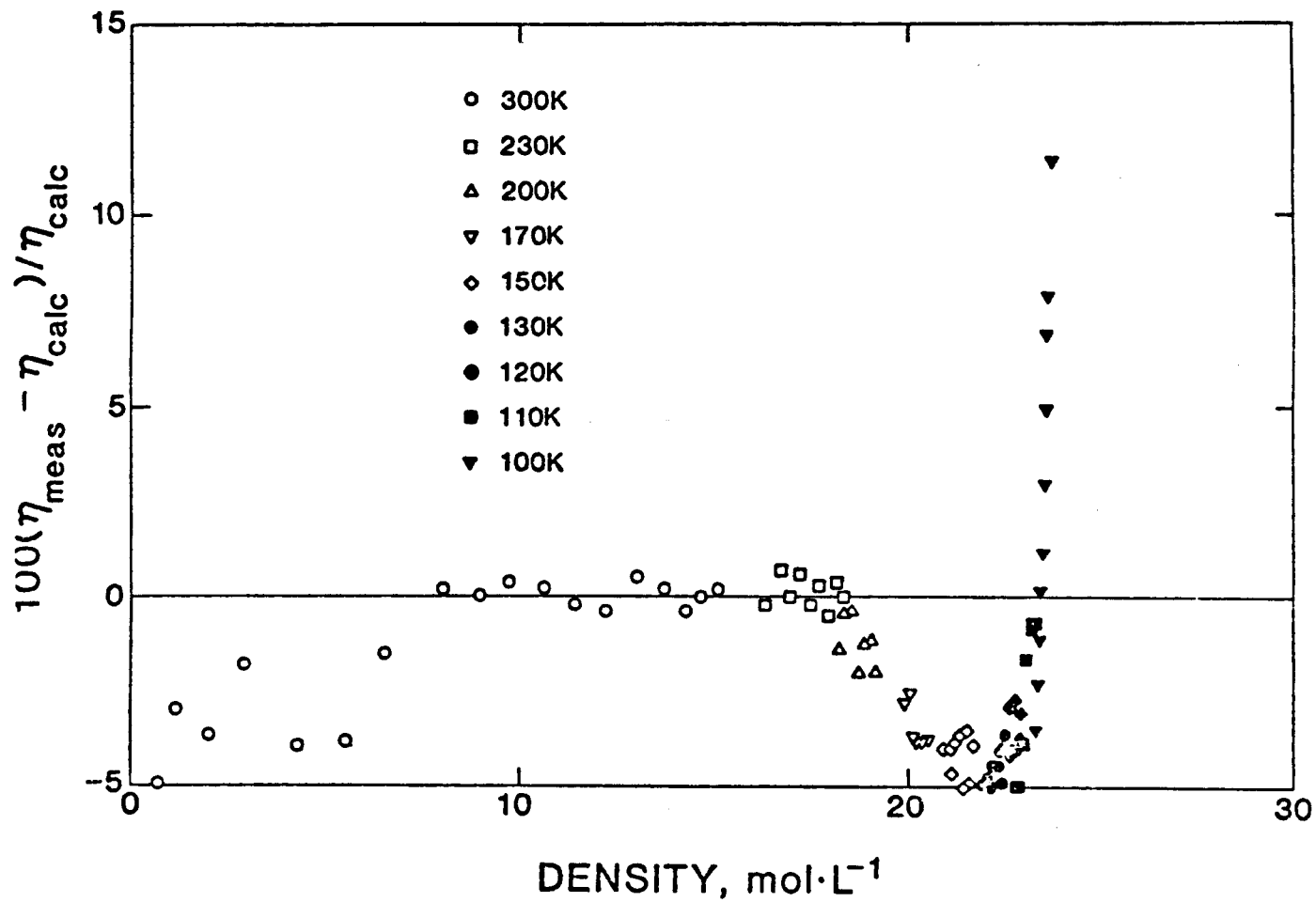
Fig. III 14 Comparison of the viscosity of a 35.528 mol %
methane-65.472 mol % ethane mixture with the gener-
alized corresponding-states model.
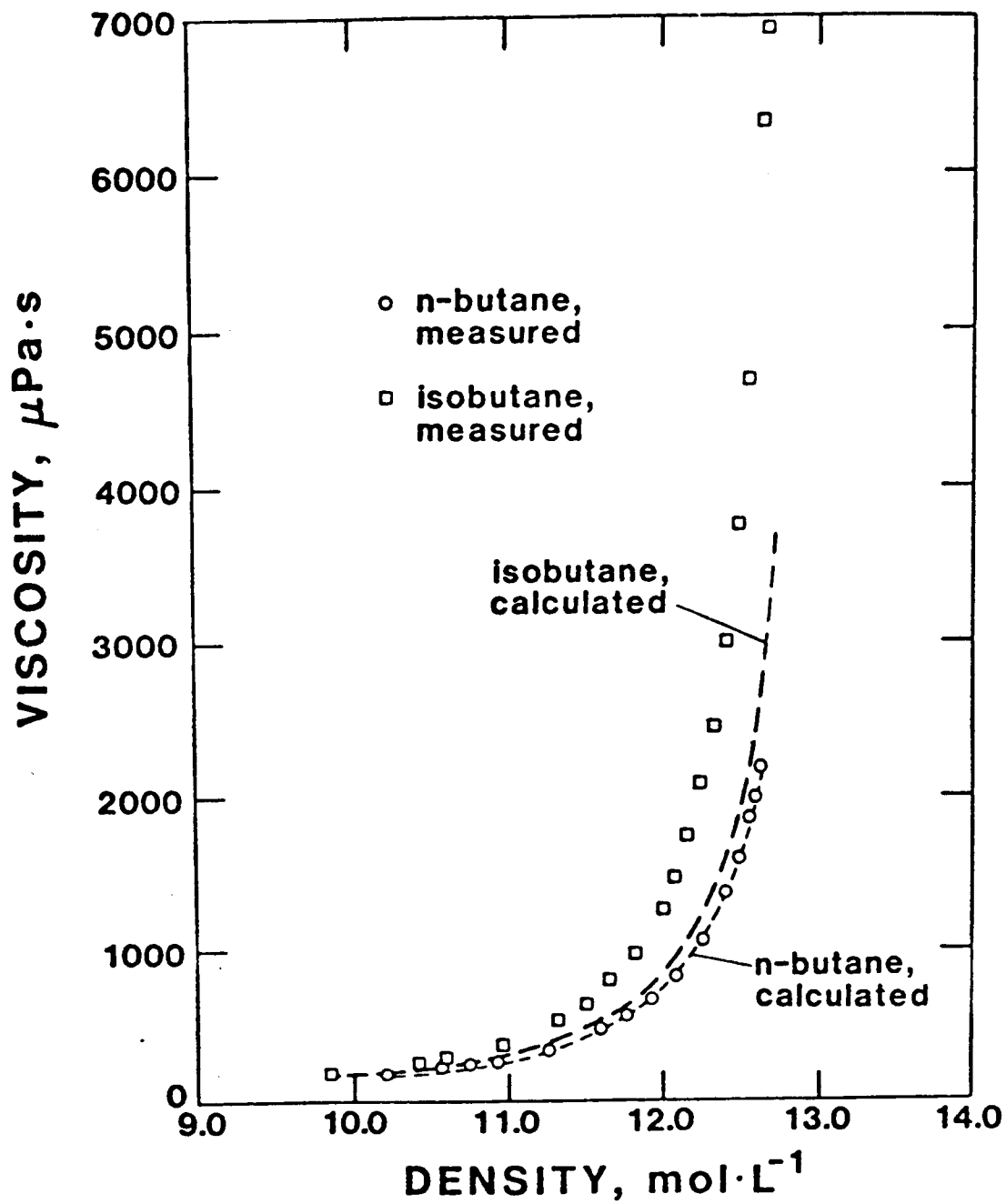
Fig. III 15 Dependences of the viscosities of saturated liquid normal butane and saturated liquid isobutane on density. Normal butane: ⊙, measured viscosities; generalized corresponding states model. Isobutane □, measured viscosities;— — —,generalized corresponding states model.
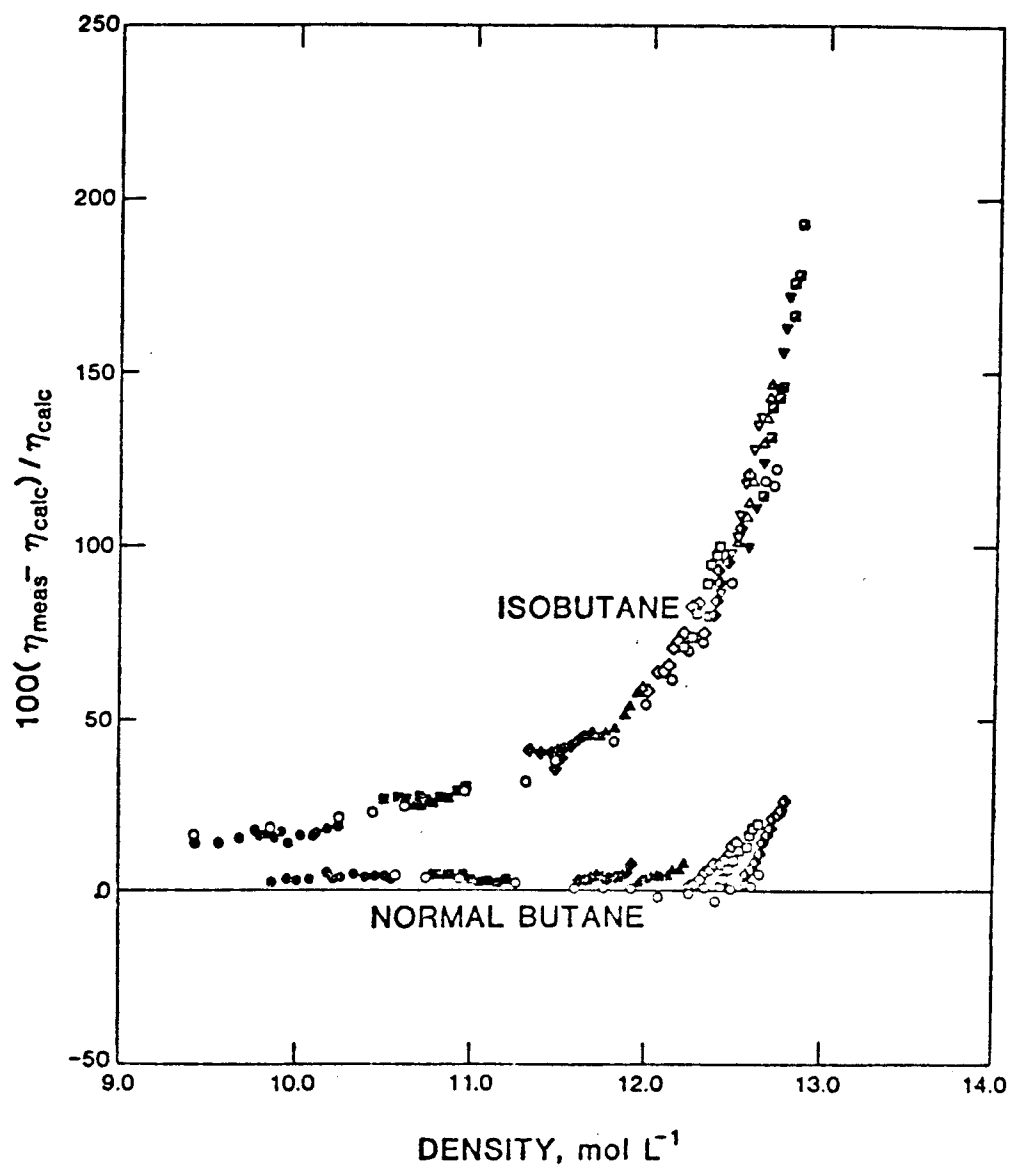
Fig. III 16 Differences between measured normal butane visco-
sities, measured isobutane viscosities and a gener-
alized corresponding states model.
●,300 K; ■, 250 K; ◆, 200 K;▲, 180 K; ◊,160 K; ▫,
150 K; ◈ , 140 K; ▽ , 135 K; △, 130 K; ▼ ,125 K;◪
,120 K; ○, saturated liquid.
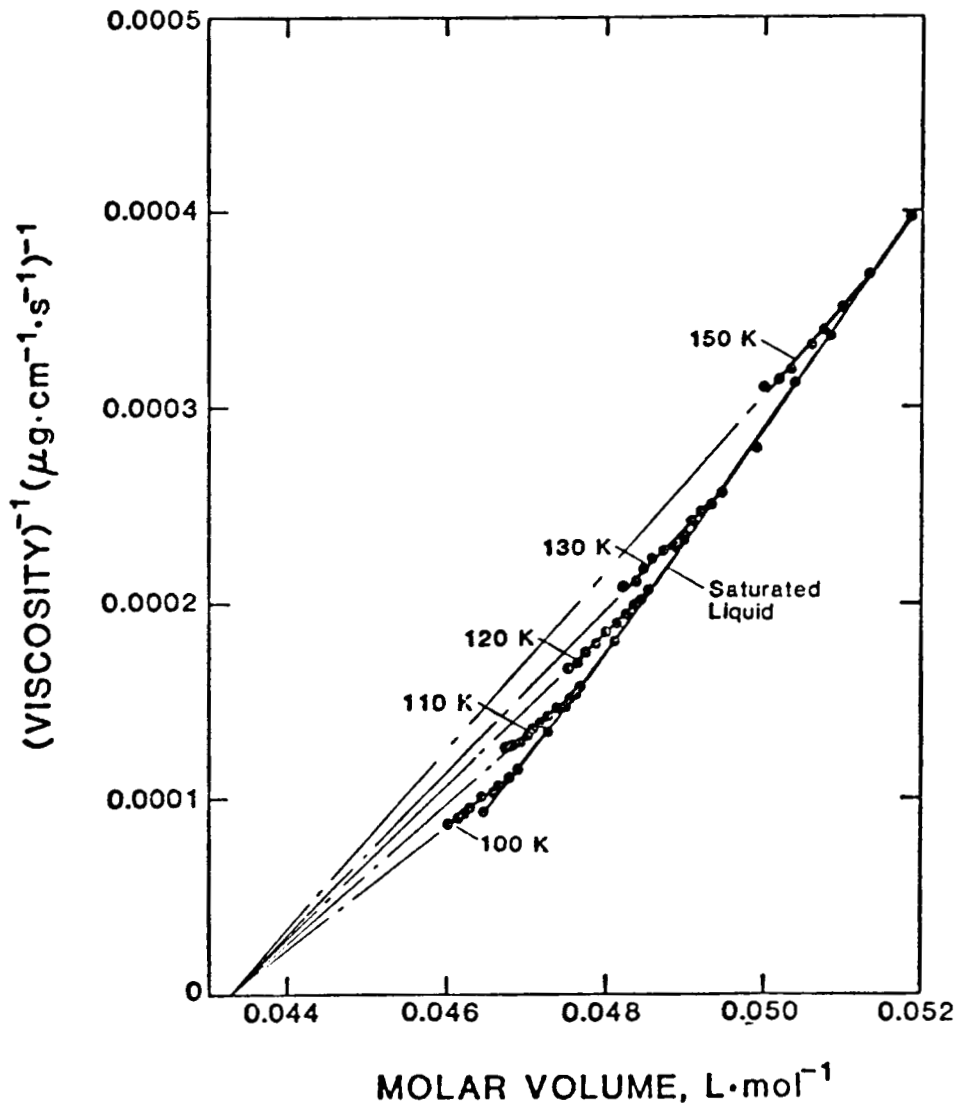
Fig. III 17 Dependence of the fluidity of ethane on molar volume and temperature.
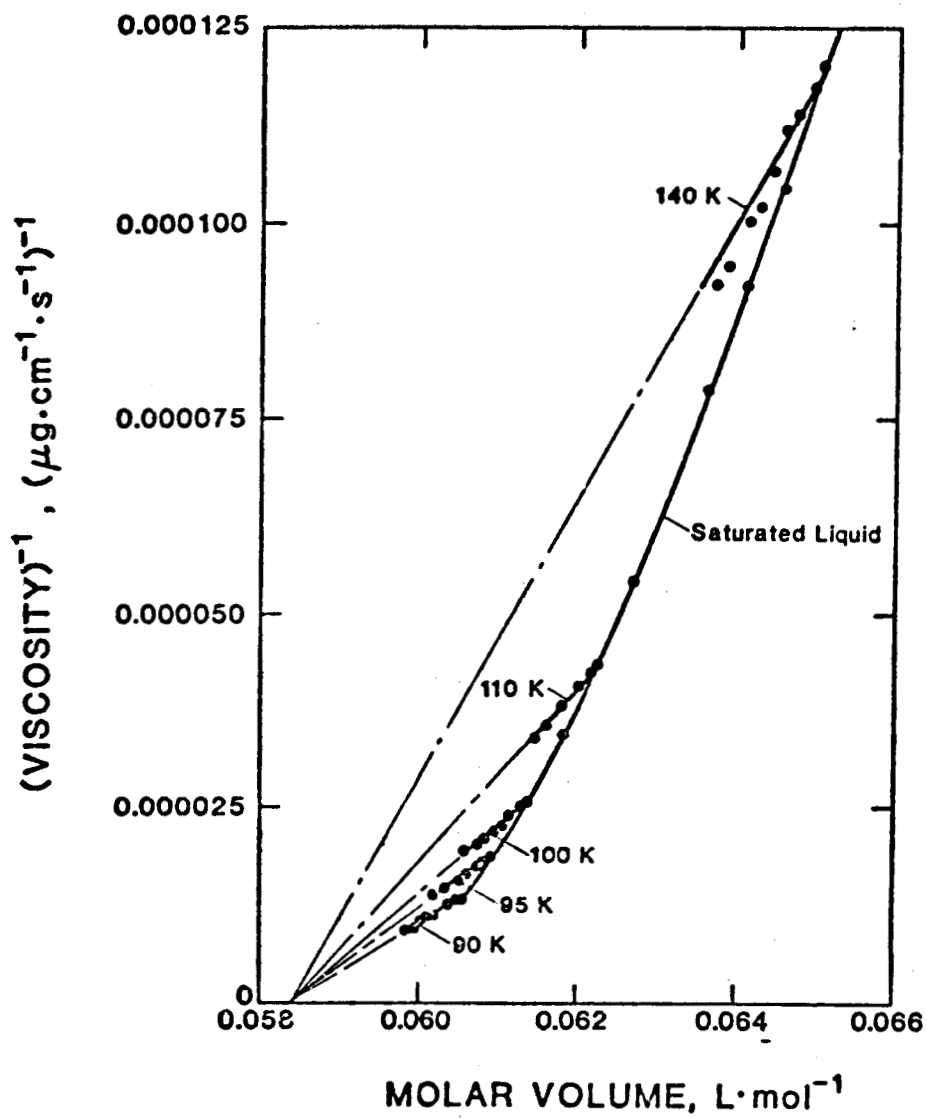
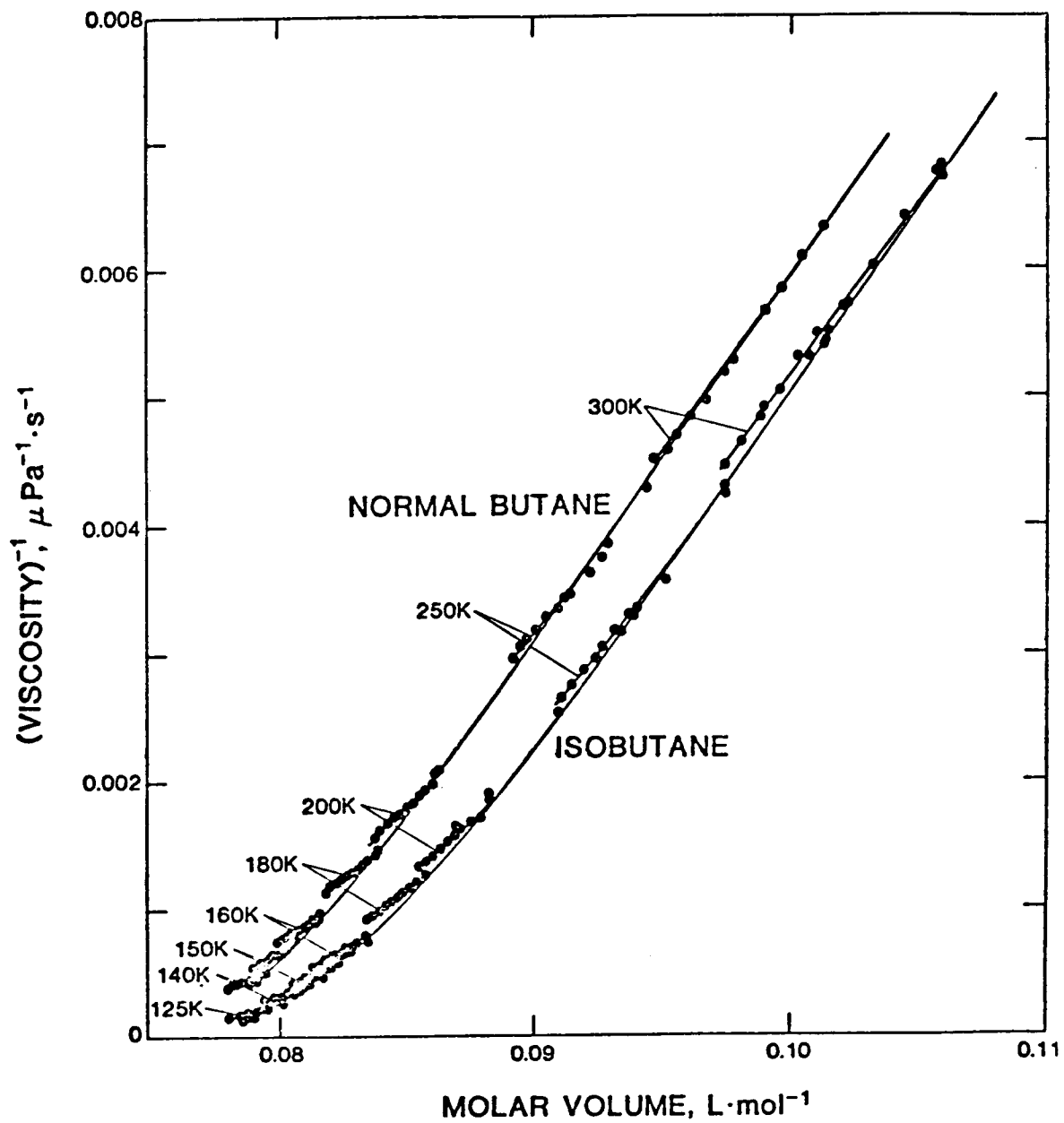Fig. III 18 Dependence of the fluidity of propane on molar volume and temperature.

Fig. III 19 Dependence of the fluidities of saturated and compressed liquid normal butane and isobutane on molar volume and temperature.
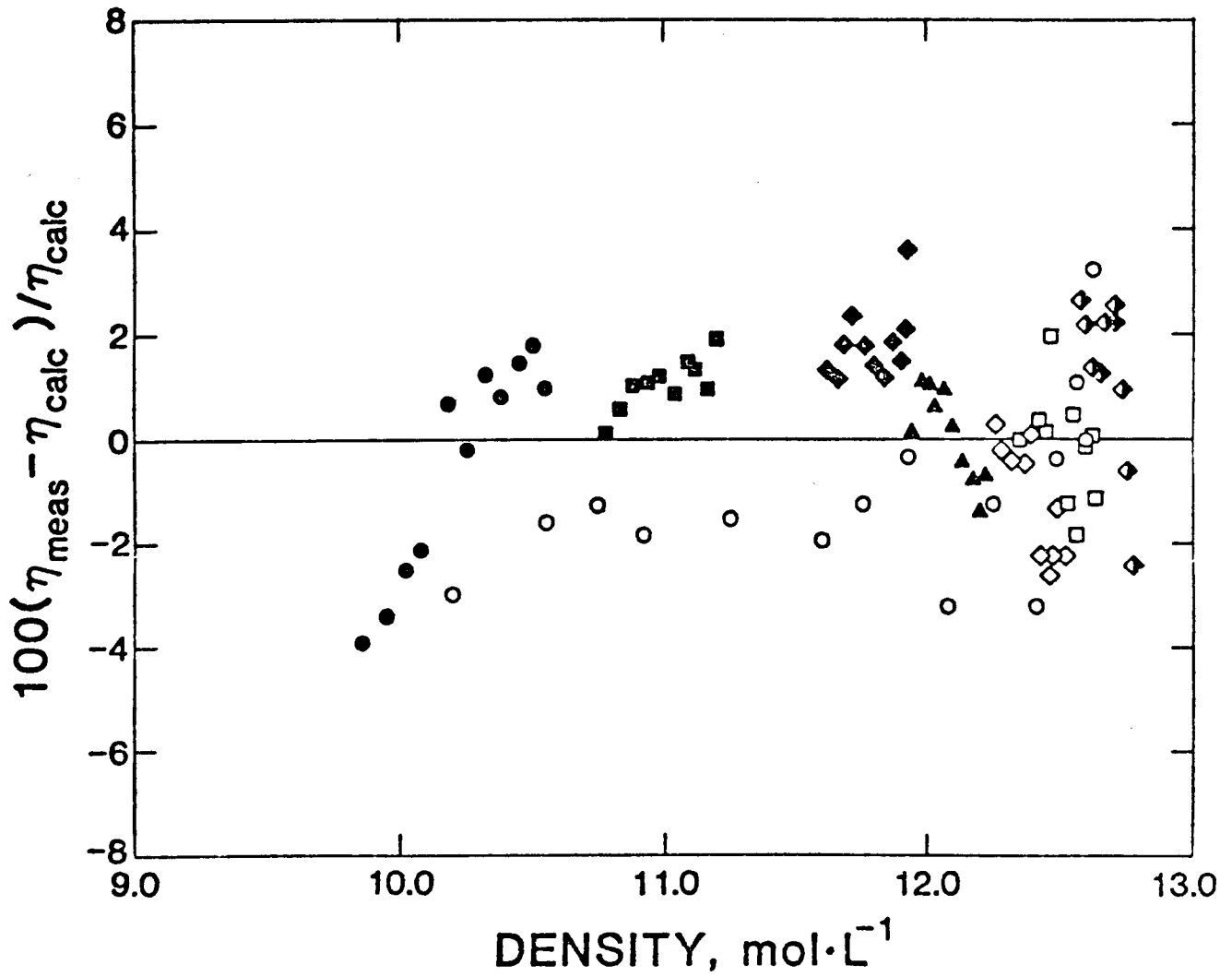
F23

Fig. III 20 Percentage departures of the viscosity of normal
butane from a Hildebrand-type correlating equation.
●, 300 K; ◼, 250 K; ◆, 200 K; ▲, 180 K; ◊, 160 K; □,
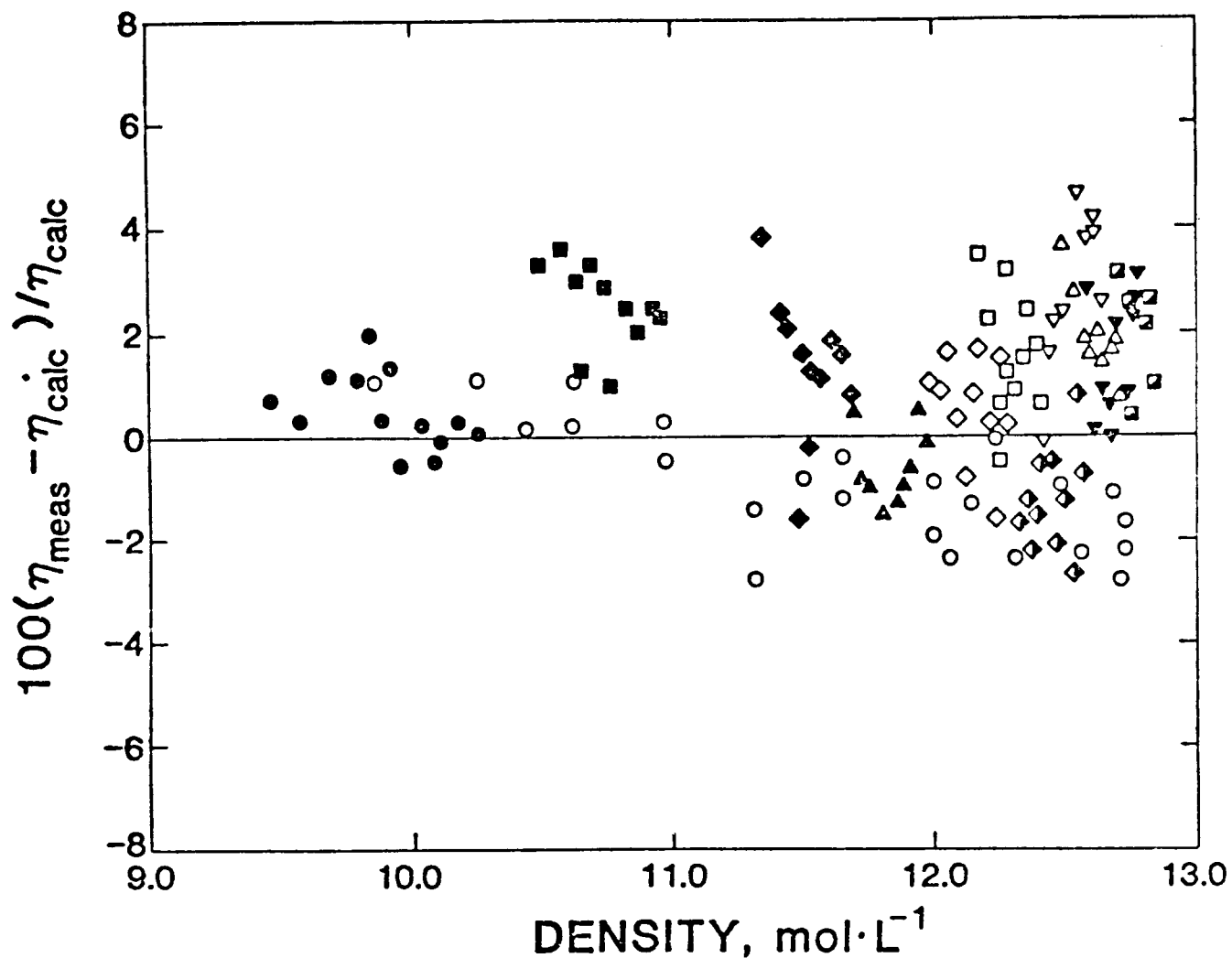150 K; ◆ , 140 K. ☉, saturated liquid.

Fig. III 21   Percentage departures of the viscosity of isobutane
from a Hildebrand-type correlating equation. ● ,
300 K; ▣, 250 K; ◆, 200 K; ▲, 180 K; ◊, 160 K; □,
150 K; ◈ , 140 K; ▽ , 135 K; △, 130 K; ▼ , 125 K;
◪ , 120 K. o, saturated liquid.